Weld World (2016) 60:415–457
DOI 10.1007/s40194-016-0317-9

RESEARCH PAPER

Trend and innovations in laser beam welding of wrought aluminum alloys

Ojo Olatunji Oladimeji[1,2] · **Emel Taban**[2]

Received: 21 July 2015 / Accepted: 16 February 2016 / Published online: 1 March 2016

Abstract The drive toward fulfilling weight reduction obligation, superior weld quality requirement, and industrial manufacturing rationale has sprung up considerable interest in applying laser welding technology on aluminum alloys. Nevertheless, porosity, solidification cracking, and surface reflectivity have been the major banes of laser welding of aluminum alloys. However, literature has shown that positive efforts have been accomplished in reducing these fundamental concerns by adopting careful selection of welding procedure, modification of pure laser welding techniques, and the use of appropriate filler metal. Albeit, there is still upbeat progression on the application and improvement of laser welding of aluminum alloys. At present, laser welding technology has the potential of fulfilling industrial requirements in joining lightweight aluminum alloys because of its capacity for automation and intrinsic flexibility, precision and repeatability, low general heat input, high welding speed, and low weld distortion. As a result, this report examines the available and current status of laser technologies in welding aluminum alloys. It further categorizes the laser technologies of aluminum alloys into four assemblages, namely, pure or single-beam laser welding, laser-arc hybrid welding, tailored heat source laser welding, and other innovative laser welding technologies, respectively. Mechanical, corrosion, and microstructural behaviors of laser welded aluminum alloys are also studied. Conversely, some of the research areas that need further investigations are proposed. Corrosion behavioral properties, influence of micropores on fatigue and quasi-static tensile strength, and toughness characterization of laser welded aluminum alloys are insufficient in literature.

Keywords (IIW Thesaurus) Laser welding · Aluminum alloys · Reviews · Weldability · Hybrid laser-arc welding · Microstructure · Porosity · Solidification cracking · Mechanical properties · Corrosion

Recommended for publication by Commission IV - Power Beam Processes

✉ Emel Taban
emelt@kocaeli.edu.tr

[1] The Federal University of Technology Akure, Akure, Ondo State, Nigeria

[2] Kocaeli University, Kocaeli, Turkey

1 Introduction

The continuous evolution in laser welding technology through proactive and problem-solving researches has undoubtedly opened up a unique pathway toward the actualization of high-productive industrial manufacturing in the transportation industries such as aerospace and aviation, automotive [1, 2], and high-speed train manufacturing. Consequently, weldability concerns in laser beam welding of aluminum alloys are gradually being subdued and substantial interest in welding of aluminum alloys with laser beam has been growing stronger. For instance, solidification cracking in laser beam welding of aluminum alloys has been significantly curtailed by the use of appropriate filler metals [3], the adoption of a dual-beam laser welding approach [4], and the use of double-pulse laser welding technology [5]. Likewise, porosities in laser welding of aluminum alloys have been reduced by pulse shaping and modulation at appropriate frequency to maintain a stable keyhole motion [6] during deep penetration welding process. Similarly, the use of twin-spot Nd:YAG laser welding approach to generate elongated weld pool for escape of gases [7] and hybridized laser-arc welding or plasma augmented laser welding [8] has equally inhibited pore formation in aluminum alloys. In fact, it was reported that no X-ray detectable

porosity was observed under sub-atmospheric pressure (10^{-1} Pa) laser welding of 5083 aluminum alloy sheet [9]. On the other hand, the use of a high quality parabolic focusing element (it increases power density) is expected to impede reflectivity problem during laser welding of aluminum alloys [10]. Also, superficial surface treatment of aluminum alloys is another proactive means of preventing reflection of laser beam during laser welding process of aluminum alloys. This form of surface treatment has demonstrated higher radiation absorption in 5083 aluminum alloy [11]. With the present state-of-the-art and progression in laser beam technology, laser beam welding of aluminum alloys is primed to fulfill industrial manufacturing dreams that have been envisaged by manufacturers.

The contemporary laser welding equipment offers desired industrial application attributes such as low and precise heat input [2, 12, 13], high production rate, controlled flexibility and repeatability, high localization ability leading to narrow heat affected zone [2, 9, 11–13], non-contact operation, and high weld quality. Therefore, laser welding technology has evolved to become an all-encompassing powerful industrial welding technology [8] that has seamless potential to weld thin metal sheets and to complete girth welds in engineering structures with significantly fewer numbers of welding passes [14], and it is similarly not restrained to welding of a definite cluster of materials but broad spectrum of materials such as other available metals and non-metals.

On the other hand, efforts toward enacting/enforcing weight reduction in modern facilities have consistently put aluminum alloys on the summit of weight reduction approaches. As a result, aluminum has become one of the most sought after structural engineering materials. Similarly, attributes of aluminum alloys such as low density and high strength-to-weight ratio [15–18], derived benefits from aluminum-based engineering systems such as fuel economy [19] and better performance, and government regulations on carbon emission have conveniently made aluminum alloys important choices in the transportation industries [20]. In fact, 7075 aluminum alloys have been reported to make lightweight fortified structural design and integrated protection systems possible [21]. Moreover, laser has the cutting edge to weld not only thin sheets of aluminum alloys but also complex structures of aluminum alloys. Sekhar and Bjorneklett [22] investigated 3.2 kW Nd:YAG laser welding of complex aluminum structures comprising of 3.0-mm-thick base/flat plate and 2.5–5.0-mm-thick extruded tubes of 6063-T5 aluminum alloy. The outcome of the weld was appreciably sound even though 4043 filler wire was utilized in the welding process [22]. Even, cellular metallic materials such as cellular aluminum (porous material formed by injecting gas into molten metal of aluminum) have been welded with 6 kW CO_2 laser and 4 kW Nd: YAG laser, and their resultant welds have been found to be acceptable [23]. Equally, high strength aluminum alloys are essentially the preferred choices for thin gauge frame structures [10] in aerospace, automotive, and other major industries, and laser welding technology has performed remarkably well in fabricating their acceptable welds. In actual fact, it has been reported that aluminum laser welding has the prospect of fabricating body in white assembly panels and components of automobile, fuselage, and wing skin panels of aircraft and panel structures of ships [10].

Thus, this article examines the available laser beam welding technologies that have been applied in welding of aluminum alloys, and it methodologically classifies them as single-beam laser welding, laser-arc hybrid welding, tailored heat source laser welding and other innovative laser welding technologies, respectively. Mechanical properties of laser welded aluminum alloys such as tensile strength, hardness, and fatigue are examined; while the nature of microstructures obtained under some available laser welding conditions is also made available. Lastly, recommendations on areas that are still insufficient in literature are suggested. Areas such as effect of micropores on fatigue strength and toughness and corrosion properties of laser welded aluminum alloys are some of the noteworthy areas that need to be further expounded.

2 Aluminum alloys

Aluminum naturally exists in the earth crust in a combined state due to its activeness [2]. It reacts with oxygen to form a very hard tenacious aluminum oxide film or stable oxide layer [2, 24–30] with a melting point of 2052 °C [31]. This unique oxide film on the surface of aluminum provides its excellent corrosion resistance [26, 32]. Table 1 shows some relevant properties of aluminum while its other properties can be found in different literature [2, 34–36].

Aluminum alloys are non-ferrous light weight materials for structural applications in many of today's industries. It has low melting point and low density [32, 37, 38] when compared to

Table 1 Properties of aluminum [2, 24–31, 33]

Properties of aluminum	Values
Symbol	Al
Periodic table (category)	Boron group
Atomic number	13
Atomic weight	27
Density at 293 K	2.702 g/cm^3
Melting point	660.37 °C
Boiling point	2467.0 °C
Number of energy levels	3
Color (appearance)	Silvery
Crystal structure	Faced centered cubic
Major ore	Bauxite
Commercial extraction process	Electrolytic reduction process

steel. Furthermore, it has high thermal expansion [27] and contraction ratio, tenacious surface oxide, excellent corrosion resistance [39], lifelong durability, high thermal and electrical conductivity [32, 40–42], high strength-to-weight ratio [16–18, 43], high strength and stiffness, energy absorption capacity [44] and good formability [45], and machinability [46] or workability nature [29, 30, 44, 47]. From economic efficiency and recycling standpoint, aluminum exhibits excellent attributes as compared to other non-metallic and metallic materials [48]. At liquid state, its thermal conductivity is higher than those of liquid steel. However, the viscosity and surface tension of liquid aluminum alloys are lower than that of steel [49].

The yield strength of pure aluminum is about 10 MPa; in applications where higher strength is required, pure aluminum needs to be alloyed and strengthened either via solid solution strengthening (to increase stress field acting on dislocations) or precipitation hardening [44]. Some of the major alloying elements of aluminum include copper, manganese, silicon, magnesium, and zinc. Advanced metallurgical technology has generated high strength aluminum alloys with higher strength-to-weight ratio [50] and appreciable corrosion resistance [15]. However, aluminum alloys are generally grouped into two distinctive categories; namely, cast aluminum alloys and wrought aluminum alloys with each of these categories being further subdivided into heat treatable and non-heat treatable alloys. However, this report focuses on wrought aluminum alloys; therefore, an overview of wrought aluminum alloys is considered. Non-heat treatable wrought aluminum alloys are strengthened by solid solution strengthening or via strain hardening, and the initial strength of this category of alloys primarily depends on the hardening effect of alloying elements like silicon, manganese, and magnesium [51]. 1xxx, 3xxx, 4xxx, and 5xxx series aluminum alloys are the available non-heat treatable wrought aluminum alloys. On the other hand, heat treatable wrought aluminum alloys are strengthened by solution heat treatment whereby the alloy to be strengthened is subjected to solution heat treating (the alloy is maintained at elevated temperature), quenched in a medium, and subsequently aged either naturally or artificially. This phenomenon is often referred to as precipitation hardening. 2xxx, 6xxx, and 7xxx series aluminum alloys are classified into this category. More detailed reports on aluminum alloys, their classification and strengthening mechanisms are available in literature [2, 34–36, 52–58].

Conversely, the drives toward low weight, energy efficient, and improved performance [16, 19, 43, 59–64], and deleterious mitigation of environmental hazardous emission such as CO_2 pollution [16, 23, 47, 65], have made aluminum alloys an important alloys among metals [31]. Based on traditional automotive designs, theoretical estimations show that 40 % weight reduction in the body weight of automobiles can invariably increase fuel economy or efficiency by 7 % or more [15]. Likewise, increasing regulatory pressure on automobile manufacturers to improve the overall fleet mileage of their products [16, 28] has increased the use of aluminum alloys in manufacturing both interior and external panels of automobiles. For instance, 5754 and 5182 aluminum alloys have been extensively adopted for structural components while 6111 for the fabrication of outer panels [28]. In general, aluminum is recognized as one of the most versatile engineering and structural material in modern day manufacturing [48]. Aluminum alloys have become efficient substitute materials for steel in modern manufacturing industries [15]. In fact, aluminum alloys have been adopted as superb engineering and structural materials in high speed train manufacturing, shipbuilding, aviation and aerospace [66], automobile manufacturing [26, 31, 48, 67, 68], cryogenic applications, nuclear, chemical, architectural and construction applications [16], packaging such as beverage cans and household foil [42], and other engineering constructions [31]. For instance, Al-Li alloys have high specific strength and high specific modulus [69], and these features have even made them extremely suitable for weight-dependent applications [69] such as aircraft and other airships. Secondly, safety components such as bumper beams and crash boxes are being fabricated using aluminum alloys [44], while various body panels, interior and external parts of modern vehicles are made from wrought aluminum alloys [16]. In fact, works have emerged toward producing fully maximized aluminum-based engines and entire body structures [42].

However, the conventional or fusion welding of aluminum alloys reduces the mechanical properties of aluminum welds and also causes weld defects such as porosity, evaporation of alloying elements, oxide inclusions, hot cracking, and solidification cracking [40, 51, 70, 71]. The choice of welding method affects the quality of aluminum weld. For instance, copper segregation in the fusion zone of 2219 aluminum alloy inhibits its possibility for natural aging during traditional fusion welding processes. However, high cooling rate-welding processes, such as laser beam welding, have been suggested for the welding of 2219 aluminum alloys, because these processes will help to decrease copper segregation in the resultant weld structure. Therefore, there will be availability of more copper in solution for natural aging and improved weld ductility through grain size reduction owing to high cooling rates [72]. Conversely, the most efficient methods of welding aluminum alloys include laser beam welding, electron beam welding, friction stir welding methods, etc. These methods produce appreciable weld quality compared to the traditional fusion welding methods.

3 Laser beam welding

LASER stands for Light Amplification by Stimulated Emission of Radiation [4, 73]. A laser beam is a collimated

and coherent light energy [30] or a concentrated coherent light beam [73]. A laser beam is also referred to as a single phase (coherent) light of a single wavelength (monochromatic) [73]. It is referred to as a high power density heat source [74] with a very low beam divergence attribute. A pulsed ruby laser was the first recognized laser [30, 75]. Laser processing technique has become an indispensable technology in this twenty-first century [30] due to its unique attributes such as high power density and high speed of operation, superlative potentials, and contribution to contemporary manufacturing. Laser technology is efficient for joining, cutting, and drilling of engineering materials and surface modification treatments such as laser peening and cladding. Actually, it is also reported that laser technology support system can produce transformation hardening of material surface [30, 75–80], and it can also be used for repairing materials [11]. Laser power densities within the range of 10^3–10^4 W/cm^2 are employed for surface hardening and chemical vapor deposition while densities of 10^5–10^6 W/cm^2 are usually employed for surface alloying and cladding. However, the laser power densities for melting and welding usually range from 10^5 to 10^7 W/cm^2 while above 10^7 W/cm^2 power densities are employed for drilling and ablation [81]

Laser technology as a joining medium can efficiently perform welding, soldering, and brazing [30]. Laser welding employs a laser beam consisting of high power, high energy density, or localized energy [10, 29, 30, 75, 77, 82–84] and non-contact process [10] in joining metallic and non-metallic materials such as steels, aluminum, magnesium, titanium, carbon steels, stainless steel, high strength low alloy steels [40, 73, 76], plastic, carbon, and glass fiber reinforced polymers [65] and composites. Varying thicknesses of the aforementioned materials can be laser welded. Also, laser beam welding also offers the environment to weld both similar and dissimilar metals together. The power density of a laser beam is higher than that of arc or plasma welding processes but it is almost or equivalent to that of an electron beam [30]. The extremely powerful laser beam has made laser welding an extremely productive tool for industrial joining of metals [8]. Laser welding offers high welding speed capacity usually ranging from 10 to 50 mm/s when compared to 3–25 mm/s of tungsten inert gas welding [13]. The available welding lasers use active mediums which are usually in the form of a solid or a gas. As a result, they are referred to as solid-state lasers and gas lasers [77]. At first, ruby, neodymium glass, and the neodymium yttrium aluminum garnet (Nd: YAG) lasers were the three classes of solid-state laser that existed. However, Nd:YAG laser has apparently replaced the other two because of its suitability for high production welding and its potential for higher powers for longer periods without jeopardizing its performance [77], as compared to the other two. The output wavelength of Nd:YAG laser is 1.06 μm [85]. Nd:YAG lasers can be delivered through an optical fiber delivery system [30]. Presently, CO_2 and Nd:YAG laser welding techniques are the two most common industrial lasers that have been employed in welding metals like aluminum alloys [14]. In fact, industrial application of laser welding has been found in offshore, aerospace (space shuttles and aircrafts) [86], shipbuilding, automotive [87, 88], and white goods industries [76]. Figure 1 shows the industrial application of laser and laser beam welding of a typical test sample.

Unlike electron beam welding technology, laser welding technology does not generate hazardous x-rays. Electromagnetic interference is also not an issue in laser welding; nonmagnetic (paramagnetic) behavior is exhibited by laser beam [42]. Localized or smaller footprint heating [10, 78, 91] and melting are achieved almost instantaneously during laser welding, and this unique attribute of laser welding facilitates high productivity or welding speed [78, 92–99]. All joint configurations can be fabricated with laser beam welding process [30]. Laser systems are usually automated and coupled with excellent precision positioning systems [42]; this exploit makes manipulation and repeatability of welding process to be easily achieved. Laser beam welding offers great deal of flexibility [91, 93, 96, 97, 100, 101] because a laser beam can be easily modulated or regulated, shaped, reflected, aligned, redirected, divided, and focused by either optical or optomechanical elements [42]. Also, it offers high weld aspect ratio (large depth to width ratio), ease of automation, high

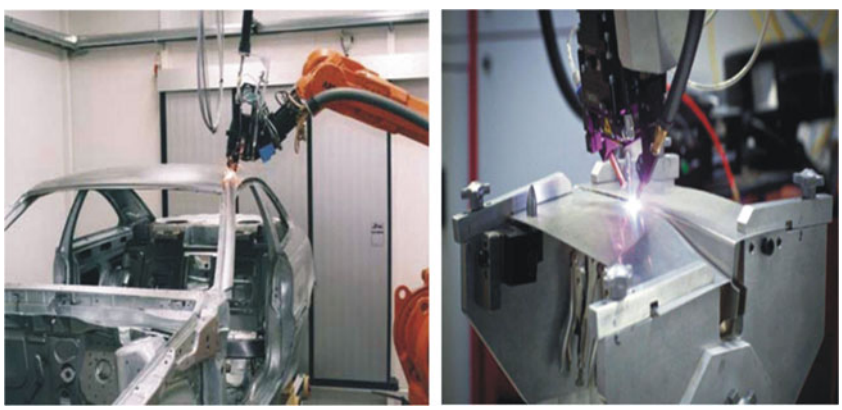

Fig. 1 Laser welding of the top of Volvo C70 [89]; fiber coupled diode laser welding of a test sample [90]

productivity, manufacturing flexibility [51, 102, 103] and superior controllability [23, 98, 99], little distortion, and small heat affected zones [9, 77]. Material thicknesses of 20 mm and beyond can be welded with laser technology. However, the success of weld depends greatly on the formation of stable keyhole [104].

With a laser welding technology, longitudinal and transverse shrinkage stress variations along material thickness are much lower during weld pool solidification, as compared to other fusion welding technologies. Consequently, this leads to a very low bending and buckling of work piece [49, 84]. Generally, provoked strain from metallurgical phase changes and local shrinkage (associated with uneven cooling rates) during other fusion welding processes induce residual stress [105] in weldments. Therefore, the narrow fusion or weld zone and heat affected zone in laser beam welding processes indicate that the level of residual stresses in laser beam welded aluminum alloys will be considerably lowered. Some of the unique and attractive properties of laser welding technologies include high welding speed; ease of automation, low heat input or low bulk heating of material [42, 94, 98, 99], low distortion and residual stresses, high reproducible joint quality and in most cases, there is no requirement for filler metals. With these numerous benefits of laser welding technology, there is reduced potential for post-weld heat treatment or strengthening [76]. A generalized summary of the benefits or contributions of laser welding technologies is highlighted in Table 2.

Traditional methods of creating dissimilar joints, such as mechanical joining (like riveting, adhesive bonding, and screwing) [2, 66, 67], are not as fast as laser beam welding, and they may also add to the overall weight of joints. Therefore, laser beam welding offers the potential of welding autogenous and dissimilar materials. In fact, it provides great prospect of welding metallurgically incompatible materials

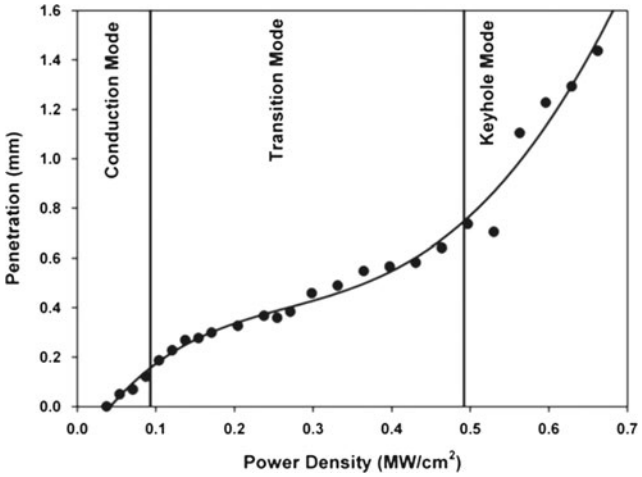

Fig. 2 A transition mode at 10-ms interaction time and 1.18-mm beam diameter [106]

because of its short processing time and one-sided access to joining area [67]. Scherm et al. [65] applied Nd:YAG laser welding in creating dissimilar weld of AZ31 magnesium alloy sheet and 5754 aluminum alloy sheet with the assistance of a ZnAl filler material. Obviously, welding of aluminum and magnesium has a high tendency of forming intermetallic phases like Mg_2Al_3 and $Mg_{17}Al_{12}$. As a result, the amount or layers of intermetallic compounds formed in the laser welding process of these metals (Al and Mg) were considerably minimal compared to other fusion welding processes [65]. Also, Laukant et al. [67] conducted Nd–YAG laser welding-brazing of zinc-coated steel and aluminum sheets. Kazuyoshi Saida et al. [26] applied diode laser brazing in joining 5052 aluminum alloy sheet to interstitial free steel (type 304 stainless steel) using 4047 aluminum filler metal and Nocolock flux [26]. Without the invention of laser beam welding technology, welding of the aforementioned dissimilar metals will be extremely difficult (Fig. 2).

Table 2 Benefits of laser welding technology [2–9, 11–33, 37–50, 60–150]

Properties of laser beam	Weld related benefits	Laser economy
• Collimated and coherent beam	• Smaller footprint/focused diameter	• High productivity/performance
• High power density	• Narrow HAZ	• Material versatility
• Tight focusability	• Low structural distortion	• Automation/robotization
• High precision	• Low thermal and mechanical strain	• Good flexibility
• Low heat input	• Fine grain structure	• Reduced manpower
• High welding speed	• Welding of variety of joint configurations	• Excellent repeatability
• Non-contact welding process	• Full penetration	• Low post weld operation time
• Cleaner than arc or gas welding	• Thick work piece can be welded	• Systematization of production lines
• Large working distance is possible	• Accessibility for complicated structures	• No tool wear/change over time
• Not influenced by magnetism	• Gap bridgeability	• No tool wear/change over time
		• Single-pass welding
		• Single-sided accessibility

However, low absorptivity or high surface reflectivity at infrared wavelengths and extremely high thermal conductivity are some of the major concerns in welding alloys such as aluminum and copper alloys [28, 42, 84] with the conventional laser welding technologies (single-laser beam welding approaches). Likewise, the other major shortcoming of laser beam welding includes high investment cost (costly equipment) and maintenance cost, likelihood of optical damage, and cracking in some weld metals as a result of rapid cooling rate [73]. For instance, the volatile alloying elements in aluminum alloys are magnesium, zinc and lithium because they have higher equilibrium vapor pressure [32, 74]. Therefore, loss of these elements during laser welding process would cause loss of strength.

3.1 Laser welding regimes or mechanisms

Laser welding regime or mechanism is referred to as the mode or approach in which weld or joint is achieved when a laser beam is impinged on a material surface. In laser beam welding, there are two known laser welding mechanisms, namely keyhole/deep penetration and heat conduction/shallow weld mechanisms or regimes [29, 30, 77, 106, 107]. These mechanisms are applicable to pure or single-beam laser welding and other modifications to laser beam welding such as hybrid laser welding [108] or pulsed laser welding. However, the type of welding regime depends on power density of the laser and the absorbed laser energy by the work piece [109]. Also, depending on the type of laser welding technology, there are other factors or parameters that may influence or alter laser welding regimes. It has been reported that as the welding current of CO_2 laser-TIG hybrid welding increases, the energy absorption or defocusing of laser also increases. As a result, the welding mechanism or regime will equally change from keyhole mode to heat conduction welding mode and there will be quick decrease in weld penetration [108]. The physics of laser beam welding is almost equivalent to other fusion welding process. In laser beam welding, a generated high power density beam is responsible for fusion welding operation. It is a rapid process that involves a high power density beam impinging on the material to be welded and the material's atomic constituents at the point of focus of the beam undergo rapid excitement and haphazard movements. As a result, temperature rise is swiftly initiated, melting of the focused position speedily occurs, and intense evaporation originates at a very high speed within a few microseconds.

3.1.1 Keyhole

Keyhole welding is synonymous to deeper weld penetration, and it is usually employed for thick work pieces. In fact, it is adjudged to be the most used in industries because of its capability to produce narrow heat affected zones and high aspect ratios [11]. Keyhole welding in laser welding of aluminum alloys requires a threshold laser power density [22, 110]. The power density required to produce keyhole mechanism in welding is stated to be higher than 10^6 W/cm^2 [11, 108, 111] or 5×10^6 W/m^2 [81]. Also, the required energy transfer efficiency for the production of a keyhole must be higher than the energy absorptivity of the work piece [74]. In this case, absorptivity of the laser beam is greatly increased and the absorption of laser power by the work piece material is approximately 100 % [42, 112]. This process is achieved when the surface temperature of the molten metal exceeds its vaporization temperature. The established metallic vapor exacts pressure on liquid surface and a depression or deformation of the surface occurs. As a result, weld penetration is formed in such a way that the penetration depth of weld is many times higher than the narrow weld width. However, the energy needed to melt and vaporize the base metal depends on the material's physical properties such as the absorption coefficient, the surface properties of the material, and the wavelength of the laser [81]. Reduction of defocusing of the laser beam helps in achieving deep penetration and improved laser energy density [108].

Keyhole welding regime involves focusing of a laser beam on a small spot of a work piece and as the laser beam impinges on the material, the temperature rises and melting occur almost instantaneously giving rise to the formation of weld pool. The vapor pressure and surface tension of the molten metal exact a downward force on the surface of the weld and displace the molten metal; thereby, creating a cavity or deep penetration in the material or work piece [23] [27]. In clear terms, during deep penetration welding, surface tension and hydrostatic pressure act on the melted aluminum alloy fluid; these forces tend to close the keyhole while the generated vapor pressure and recoil pressure within the hole tend to open the keyhole. Therefore, there is a general force balance acting on the keyhole wall which should be maintained in order to avoid keyhole collapse. Though, high speed imaging of keyhole has shown that it fluctuates in radial direction during deep penetration welding process as a result of intense beam-molten metal interaction. Actually, an unstable keyhole is established when its length is greater than its circumference due to Rayleigh instability [113]. In a keyhole welding regime, the effects of hydrodynamics pressure, surface tension, and recoil force due to evaporation and convection in the liquid metal cause keyhole instability [109, 113]. Figure 3 shows a typical keyhole formation mechanism.

High vapor pressure alloying elements such as magnesium, zinc, and lithium [48] increase the pressure in the keyhole and also reduce the surface tension of the molten alloys. Though, the addition of surface active elements and the degree of surface cleanliness significantly affects surface tension of a weld pool

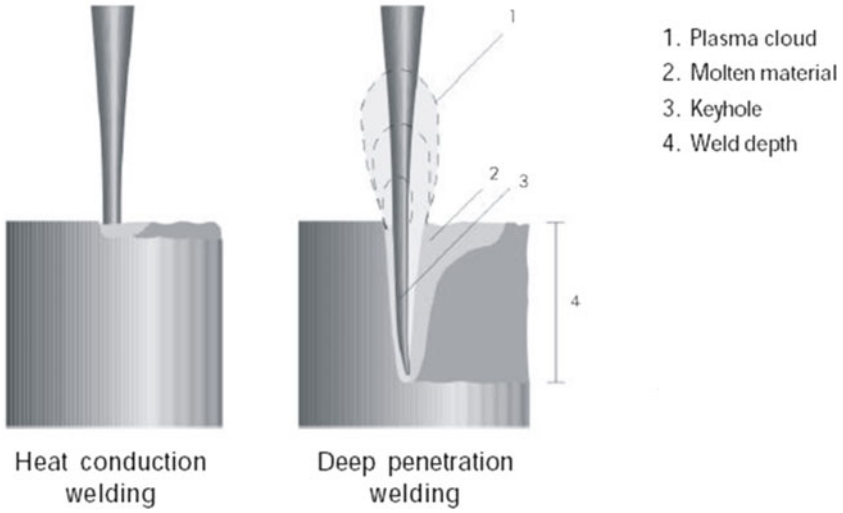

Fig. 3 Conduction and keyhole welding regimes [120]

[114]. During deep penetration laser welding of metals, plasma is generated above the work piece. The formed plasma unavoidably affects the efficiency of laser welding processes and the stability of keyhole. The induced plasma causes a shielding effect and instability in the keyhole; as a result, deep weld penetration is inhibited and porosity defects are strengthened [9]. Keyhole welding regimes have the propensity to create some issues or concerns during laser welding. The known keyhole issues are instability [13], keyhole oscillation, and keyhole collapse or intermittent closure of keyhole. This anomalous tendency within the keyhole during laser welding generally creates porosity because of gas entrapment [11]. During dual-beam laser welding of aluminum alloys (Al-Mg alloys), magnesium elements in the alloys create higher vaporization rates and pressures in the keyhole. Consequently, keyhole instabilities, porosity, and rough under-bead surfaces ensue. It was reported that good welds were only obtained when the power of the leading beam was higher than the lagging beam during double-beam laser welding of aluminum alloy [27].

Full penetration laser welding was achieved with a 3 kW single-beam Nd:YAG laser at speeds up to 15 m/min on 1.6-mm-thick 5182 aluminum alloy sheets. However, spikey under bead surface geometry was observed owing to high vapor pressure of magnesium in the alloy [20]. Keyhole instability was attributed to the formation of occluded porosity within the weld borderline and partial weld penetration [20]. Penetration depth of welds is greatly dependent on parameters such as the material to be welded, the laser type, atmospheric pressure, etc. The penetration depth of material under laser welding condition increases with decreasing ambient pressure [115]. Under deep penetration welding conditions, sub-atmospheric pressure laser welding has greatly improved keyhole stability and weld quality. Penetration depth increases with decreasing ambient pressure due to low metal vapor pressure, and also the refractive angle of laser is also stabilized as the ambient pressure is reduced [9, 115].

Variation in penetration depth of weld is highly sensitive to vaporization tendency of alloying elements in aluminum work pieces. Relatively higher vaporization pressures of elements such as zinc and magnesium bring about deeper weld penetration depth; although, crack propensity may be higher as a result of gaseous vaporization. 6 N01-T6 aluminum alloy showed a lower weld depth as compared to 5083-O and 7 N01-T6 alloys because of the presence of silicon as its major element (silicon is more difficult to vaporize as compared to zinc, magnesium, and even aluminum). The penetration depths of 5083-O and 7 N01-T6 alloys were stated to be approximately twice the depth of 6 N01-T6 aluminum alloy [48].

3.1.2 Transition mode

A transition welding regime or mode has been reported to exist between conduction and keyhole modes. Assuncao et al. [106] affirms that transition mode occurs within a range of power densities (not at a single density value), and it is equally dependent on beam diameter and interaction time [106]. A typical illustration diagram showing the existence of transition mode between conduction mode and keyhole mode is shown in Fig. 2.

3.1.3 Heat conduction

The power density necessary to establish conduction regime in laser welding has to be less than 10^6 W/cm^2 [11]. This is a process whereby a molten weld pool is created by conduction of heat. However, the irradiation of material is cut off before vaporization of the material surface is attained. As a result, the resultant weld is often wide and not deep; in this case, it can be stated that the penetration depth is less than the weld width. The convection of liquid metal during laser welding exerts strong effects on weld pool and eventually affects the shape

of the weld pool [116]. Conduction laser welding occurs at lower power densities or at higher welding speeds. The absorbed laser energy is transferred into the volume of the base metal by heat conduction. At the end, a broad and shallow molten pool is produced. As compared to keyhole welding regime, conduction welding regime has been adjudged to be a more stable process because vaporization of metal takes place at a lower level with respect to that of keyhole welding regime [11]. Laser conduction welding regime has been described as the alternative approach of welding difficult materials like aluminum, magnesium, and titanium alloys [11].

Heat conduction regime occurs during laser welding when laser energy heats up the surface of the base or parent metal. As a result, there will be high thermal conductivity of the material and heat transfer into deeper sections of the work piece [23]. Therefore, the material commences to melt when the intensity of the laser is sufficiently high. It should be noted here that the material-specific threshold intensity must not be exceeded [23] in order to establish conduction regime, otherwise, keyhole regime will emanate as a result of vaporization of the molten metal. Also, the ratio of absorbed energy by the irradiated aluminum material to the laser output energy is referred to as energy transfer efficiency of the laser welding system [112]. Zhao et al. [74] reported that the absorption of laser energy greatly depended on conductive absorption of laser energy by free electrons and the nature of metal surface influenced the absorptivity. As a result, the energy transfer efficiency during conduction regime is adjudged to be equivalent to the absorptivity of the metal or aluminum work piece [74].

3.2 Interaction effects in aluminum laser welding

Plasma or plume is formed when high power laser beam interacts with metal vapor inside the keyhole or above it. This interaction influences welding behavior by affecting the absorption, refraction, and scattering of laser beam [113]. The formed plasma usually has high temperature field that also affects reaction between molten metal and atmospheric gas [113]. Laser-induced plasma is also referred to as laser generated hot spot because it has higher temperature and greater electron density than the adjoining regions. As a result, this region presents least resistance or lowest potential drop [117]. High-speed video camera is generally used to investigate the relationship between laser beam and arc in hybrid welding. Tsukamoto [113] reported the application of monochromatic imaging technique for the assessment of plasma state and analysis of atomic or ionic species (metal or gas) [113] during welding. The intensity of the laser, arc, and plasma radiations needs to be reduced with the aid of optical filters while additional source of illumination such as the use of halogen lamp maybe necessary in order to obtain clean and clearer image [40]. The integration of laser beam to arc ensures that unstable electric arc can be stabilized by laser beam. Plasma arc stabilization can be achieved in laser-arc hybrid welding with a low power laser beam of about 100 W in a current range up to 100 A [101]. Under argon shielding condition, induced plasma during high power CO_2 welding reduces weld penetration [118].

Chen et al. [119] investigated the effect of laser-induced metal vapor on arc plasma during bead on plate laser-arc double-sided welding (LADSW) of 4-mm-thick 5A06 wrought aluminum alloy plates. Emission spectroscopy technique was used to assess the laser-induced metal vapor effect on the arc plasma, and the outcome of 5A06 aluminum laser welding was compared with that of the conventional gas tungsten arc welding [119]. The emission spectroscopic analysis revealed that the amount of metal vapor in arc plasma during LADSW was larger than that of gas tungsten arc welding (GTAW). As a result, the electron temperature of the established arc plasma during LADSW was lower than that of the GTAW. In this process, the established laser-induced metal vapor during LADSW of 5A06 aluminum alloy changed the composition of the arc plasma. As a result, the major observable difference between LADSW and traditional GTAW was the changing composition of the arc plasma [119].

The effective temperature of a weld pool is often estimated from the vapor composition of a laser welding process. He et al. [121] estimated the effective temperature of a laser spot welding process from the vapor composition or laser plume near the weld pool. It was revealed that the estimated temperature was close to the numerically calculated peak temperature of the weld pool's surface. The authors employed an open-ended quartz tube to condense a portion of the vapor on the inner surface of the tube. However, the condensation procedure showed that the concentrations or compositions in the vapor or laser plume were slightly varying with increasing power density of the laser [121].

4 Innovations in aluminum laser beam welding

Earlier efforts in laser welding of aluminum alloys have shown difficulties or weldability concerns such as laser beam reflectivity, evaporation of alloying element [20], weld metal porosity susceptibility, and cracking [4, 70, 71]. Also, unique properties of aluminum alloys such as tenacious oxide layer, high thermal conductivities, high thermal coefficients, and low melting temperatures [27] have posed significant challenges to the massive application of laser welding technology on aluminum alloys. Therefore, attempts to overcome some of these fundamental concerns in laser welding of aluminum alloys have brought about a few innovations into laser welding technologies. These innovations basically involve careful selection of welding procedures or modification of

pure laser welding techniques and the use of filler metal [22]. The available laser welding technologies of aluminum alloys in literature are examined under this section. In order to have a logical assessment and arrangement of the innovations in laser welding of aluminum alloys, classification of the utilized laser technologies was carried out based on the nature of heat source. Laser wave characteristics such as continuous wave and pulsed wave were not utilized in classifying the available laser welding technologies because literature-based laser technologies were solely considered. Nevertheless, the technology in laser beam welding of aluminum alloy is classified into four assemblages, namely single-beam or pure laser welding, laser-arc hybrid welding, tailored heat source-laser welding, and other innovative laser welding technologies as shown in Fig. 4.

4.1 Pure laser welding/single-beam laser

Pure laser or single-beam laser has a single laser heat source and no other form of weld-influencing gadget like electromagnetic field inducing device or vibration inducing appliance is attached to the welding system. Conventional lasers such as CO_2, Nd:YAG, pumped diode, fiber, and disk lasers belong to this category. They apply laser beams generated from different sources (solid or gas) to weld aluminum alloys.

4.1.1 CO_2 laser welding

CO_2 laser welding applies laser beam generated from carbon dioxide in welding aluminum alloys. Carbon dioxide (CO_2) lasers have output wavelengths of 10.6 μm and maximum laser power of about 50 kW [30]. They are more efficient and generate higher power when compared to Nd:YAG lasers [77]. Carbon monoxide (CO) laser with a shorter wavelength of 5.3 μm is available but they have not been investigated in welding aluminum alloys. However, one of the major inconveniences of high power CO_2 laser is that it must be delivered by mirrors and not by optical fibers [14]. Therefore, the optical system of CO_2 laser beams includes mirrors and ZnSe lenses [81]. Likewise, the formation of argon plasma which reduces weld penetration depth occurs during CO_2 laser welding as a result of argon shielding [30]. In addition, due to the higher wavelength of CO_2 laser, it exhibits more or high surface reflectivity when its beam is impinged on the surface of aluminum alloys. The energy transfer efficiency of CO_2 laser beam to the base metal is capable of reaching 0.8 [81]. Very few researchers have applied CO_2 laser beam in welding aluminum alloys. Ramasamy et al. [16] examined the continuous wave 5 kW CO_2 laser beam welding on 1.6-mm-thick 5754-O aluminum alloy sheets, but joint configuration was employed for their experimentation.

4.1.2 Nd:YAG laser welding

Nd:YAG laser generates its laser beam from a solid crystal of neodymium-doped yttrium aluminum garnet (Nd_3+:$Y_3Al_5O_{12}$ garnet solid) [30]. Optical lenses and fiber optics [81] are some of the noteworthy laser delivery systems used for Nd:YAG laser. There is usually good coupling of Nd:YAG laser to aluminum alloys owing to the distinctive low wavelength (1.06 μm) of Nd:YAG laser beam, unlike CO_2 laser with higher wavelength of 10.6 μm [30]. As a result, aluminum alloys absorb Nd:YAG laser beam more efficiently [66]. The thickness of materials that can be welded with Nd:YAG laser is restricted due to its lower power as compared to higher power of CO_2 lasers. However, TWI combined up to three Nd:YAG lasers to create solitary laser beam capable of generating 8.9 kW laser power, and the resultant beam was

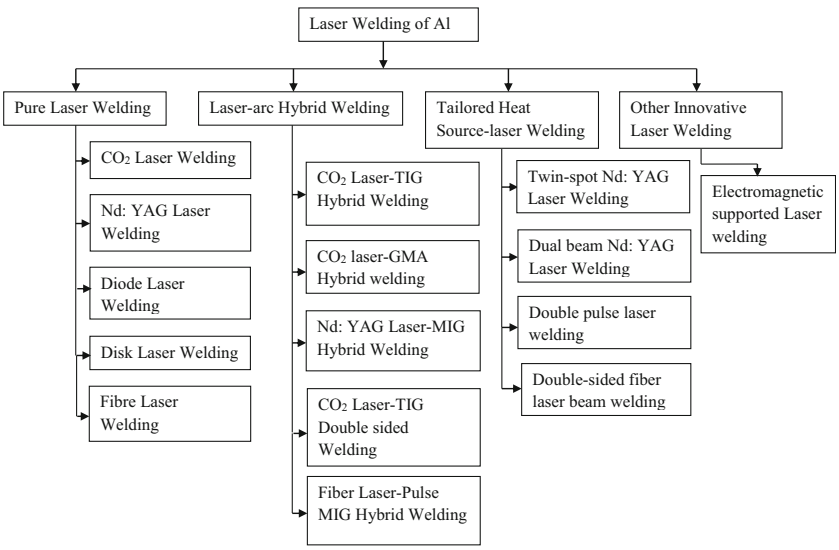

Fig. 4 Innovations in laser welding of aluminium alloys

transmitted through a 1.0-mm diameter optical fiber [14]. Beam absorption of aluminum alloy at 1.06 micron is about three times much more than that of the CO_2 laser [51]. Several authors have worked on the application of single-beam Nd:YAG laser on aluminum alloys. Deutsch et al. [20] applied a single-beam Nd:YAG laser in welding 1.6-mm-thick 5182 aluminum alloy sheets. Bead on plate welds was produced with laser powers ranging between 2.5 and 6 kW. Continuous wave 3 kW Nd:YAG laser welding of 1.6-mm-thick 5754-O aluminum alloy was examined by Ramasamy and co-authors [16]. Mujibur Rahman et al. [122] applied 3.5 kW continuous Nd:YAG laser in welding 2-mm-thick 6061 aluminum alloy sheets using 4043 filler wire [122]. Simone Mattei and co-authors investigated a 6 kW continuous wave Nd:YAG laser welding of 4-mm-thick 2024-T4 aluminum alloys using a 1-mm diameter 4047 alloy filler wire [123]. Haboudou and co-authors conducted 4 kW continuous wave Nd:YAG laser autogenous welding of 4-mm-thick 5083-O and 356-T6 aluminum alloy plates [124].

Pulsed Nd:YAG laser welding of 6082 aluminum alloy has been examined with the aid of high-speed cameras. These cameras facilitated the capturing of visible and infrared radiation [46]. Pulse lasers are usually employed when precise and low heat input [46] is required in welds. There is usually heat dissipation between each laser pulse in order to minimize or reduce thermal stresses in areas near the fusion zone. As a result, distortion is considerably reduced in this type of welding approach [46]. Peter Stritt et al. [125] reported a new technique in establishing a homogenized weld pool mixture through modulation of pulse shape during dissimilar welding of copper and aluminum by using a pulsed dual wavelength of 532 and 1064 nm. At the applied frequency, the modulation of the pulse shape transferred appreciable oscillations into the melt pool and homogeneous weld pool was achieved [125].

4.1.3 High power diode laser

Diode laser obtains its laser beam from a high brightness semiconductor or diode. This category of lasers uses a wavelength in the near infra-red region of spectrum usually in nanometer like 808 nm [81] [126]. It has higher absorption coefficient on metallic materials. It is a successful innovation over the CO_2 and Nd:YAG lasers because of its unique broad wavelength spectrum usually from 450 to 2200 nm [127]. Sanchez-Amaya et al. [11] investigated laser welding of 5-mm-thick 5083 aluminum alloys using a 2.8 kW high power diode laser to create bead on plate. The welding was conducted in continuous mode and at a relatively high value of power [11]. A 2.8 kW maximum powered diode laser was also employed in welding 3-mm-thick 5083 and 4-mm-thick 6082 aluminum alloy sheets using conduction welding regime [11]. Diode pumped Nd:YAG laser is much more expensive but efficient. However, its high cost has hindered it general acceptance in the industry [51].

4.1.4 Disk laser welding

Disk laser is also an innovative advancement in solid-state laser welding. It has a wavelength of 1.03 μm, and it equally has high brightness and high efficiency (15–25 %) [30]. Coniglio et al. [4] examined the weldability of 3.2-mm-thick 6060-T6 aluminum alloy plates using a 1030 nm, 10 kW Yb:YAG disk laser beam. High power fiber laser and disk laser have shown tremendous advantages over the common yttrium aluminum garnet (YAG) laser and carbon dioxide (CO_2) laser. They have superior beam quality and offer flexible fiber delivery because of their wavelengths of about 1 μm [118].

4.1.5 Fiber laser

Fiber laser has excellent beam quality [99] with a wavelength of 1.07 μm and high efficiency ranging from 20 to 30 % [30]. Fiber lasers are classified as high power lasers because of their features such as high power with low beam divergence, high efficiency, and compact size [128]. In fact, the productivity and high welding speed of high power fiber lasers are unmatched with most of other traditional or single-beam laser sources [99]. Wang et al. [129] examined the solidification cracking behavior in 10 kW fiber laser welding of 2.5-mm-thick 6013-T6 aluminum alloy plates. The solidification cracking initiation site and propagation were examined using a high-speed camera system and through metallurgical examination. It was revealed that the solidification cracking initiated near the fusion line and propagated through the weld center [129]. Also, Oliveira and co-authors employed a 2 kW high power Yb-fiber laser in welding of 1.6-mm-thick 6013-T4 aluminum alloy in overlapped and T-shaped geometries [130]. Banglong Fu and co-authors investigated the microstructure and mechanical properties of 2-mm-thick 2A97-T4 aluminum-lithium alloy using a fiber laser with powers ranging between 2.8 and 4.1 kW [131]. Paleocrassas et al. [132] examined the inherent instability in 300 W ytterbium, single-mode fiber laser (1075 nm) welding of aluminum [132].

4.2 Hybridized laser-arc welding/laser-arc hybrid welding

Laser-arc hybrid welding merges two different heat sources (laser beam and arc heat sources) together to obtain a unified process zone (fusion zone) and to obtain synergetic benefits of the two heat sources. In the early 1980s, Steen first recommended and realized the idea of combining laser beam with an electric arc to facilitate efficient material processing such as cutting. CO_2 laser beam source was the first class of laser that was integrated into an electric arc welding process [101].

Overtime, the successful synergy of laser beam and arc led to the development of more efficient and high power laser-arc hybrid welding approaches [14, 29, 30, 117, 133–136].

A single-weld pool is created in this class of welding. An electric arc welding (MIG, MAG, or plasma) process is integrated into laser beam welding technology in order to compensate for non-consistent fit-up between parts to be welded [22] and to equally improve the effectiveness of laser beam welding of aluminum alloys [8]. The major outcomes of this technique of welding are the creation of a wider weld pool and retention of penetration depth capacity [22] [133]. Synergetic benefits of laser and arc welding technologies are the gains of this class of aluminum welding. Some of the advantages of this class of welding include good weld bridge-ability [137], higher welding speed, higher process stability, improved depth penetration and metallurgical properties [40, 138], and improved gap and misalignment tolerances [29, 30, 38, 123, 139, 140]. Greater tolerance toward poor joint fit up and toward lateral misalignment of energy source to the joint line, suppressed zinc exposure during welding of coated material, smoother blend between thicker and thinner material, and high consistency and repeatability of weld quality have been highlighted as some other contributions of this class of laser welding [8, 136]. Laser-arc hybrid welding assists in reducing metallurgical defects and it helps in improving joint strength because of laser-arc synergetic effects. Single-beam or pure laser welding of aluminum alloys is highly susceptible to high reflectivity of laser beams but laser-arc hybrid welding of aluminum helps in reducing the surface reflectivity of laser beam [141]. Plasma arc stabilization can be achieved in laser-arc hybrid welding with a low power laser beam of about 100 W in a current range up to 100 A [101].

In literature, there are two major adaptations of hybrid laser-arc welding: the first is the application of both laser and arc sources directly onto the same side of the work piece while the second has the respective heat sources directed on the opposite sides of the work piece. The adaptation of laser and arc heat sources on the opposite sides of 0.2-mm-thick mild steel at a current of 25 A has been reported to increase the welding speed by a wholesome value of 300 %. However, when both heat sources are applied on the same side of 0.8-mm-thick titanium and also on 2-mm-thick mild steel, 100 % increase in welding speed has been realized [8]. Liu et al. [142] reported that melting efficiency of about 20 % was achieved with laser-TIG hybrid welding mode while a fluctuating efficiency with maximum value of 53.14 % was attained at arc current of 120 A in TIG-laser hybrid welding mode [142].

Hybrid approach/manner in laser-arc hybrid welding may be coaxial, paraxial, multi-electrode, or autogenous laser hybrid in nature. Chen et al. [108] reported on a coaxial hybrid welding (CO_2 laser-TIG hybrid welding) having a concentric hollow tungsten electrode with the laser beam [108]. Coaxial hybrid welding has been demonstrated to effectively inhibit energy absorption or defocusing of laser (deeper weld penetration in return) as compared to CO_2 laser-TIG paraxial hybrid welding. Other authors have reported that the coaxial hybrid welding is difficult to realize due to the limitation in preparing hollow electrode (tungsten electrode), as compared to the paraxial hybrid welding. Paraxial hybrid welding is easy to realize. In fact, it is reported that welding quality is independent of welding direction in coaxial hybrid welding because of the symmetry of the welding heat source's distribution. On the other hand, welding quality is affected by welding direction in paraxial hybrid welding [142].

Some of the major disadvantages of hybridized laser-arc welding include limited orientation of torch over which an arc can be maintained [8] and vulnerability of exposed tungsten electrode (in case of hybridized laser-GTA welding) to metal vapor, ejected material, and other contaminants [8]. Page et al. [8] highlighted in their works that the major issues with hybridized laser-GTA welding could be effectively overcome by substituting plasma arc for gas tungsten arc in the hybrid welding system. Since, plasma arc system has its electrode enclosed behind the nozzle, and it offers stable and directional arc column that permits welding operation at an increased standoff distance [8]. However, hybridized laser-plasma arc welding has been sparingly utilized in the literature.

4.2.1 CO_2 laser-TIG/GTA hybrid welding

The two type of heat sources here are CO_2 laser and gas tungsten heat sources. Hybridized laser-TIG welding process can be controlled with ease when compared to hybridized laser-MIG laser welding process because it does not have droplet transitions [108]. Hybridized laser-GTA welding has been reported to provide combined greater thermal effects together with high welding speed capability and penetration improvement [8]. Laser radiation in a laser-TIG hybrid system aids arc stabilization and improves process efficiency [117, 134]. Some of the advantages of hybridized CO_2 laser-TIG welding as reported by Chen et al. [108] include stable arc and deep weld penetration, improved weld appearance, high efficiency and economy, high gap bridging capability with permissible tolerance, and high welding speed [108]. It is also affirmed that hybridized laser-TIG welding process in comparison to pure laser welding offers a further 20 % increase in penetration depth and welding speed under a definite arc current of 100 A [108]. Chen et al. [119] report that there is an inevitable reduction in laser energy during hybridized laser welding because of the transfer of laser beam through the arc plasma before reaching the surface of materials to be welded. As a result, the authors investigated a new laser welding approach aimed at preventing laser energy loss [119].

4.2.2 CO_2 laser-GMA Hybrid welding

This hybrid welding system combines CO_2 laser and gas metal arc heat sources to form a solitary welding system. It equally has the synergetic benefits of the two heat sources. Alessandro Ascari and co-authors utilized a 3 kW continuous wave CO_2 laser-GMA hybrid welding of 8-mm-thick 6082 aluminum alloy to investigate the porosity formation [140]. Jun Yan et al. [143] assessed the performance of 5 kW CO_2 laser-MIG hybrid welding on 8-mm-thick 2A12 aluminum alloy by using 4043 and 2319 welding wires [143]. Casalino [144] employed a 3 kW CO_2 laser-MIG hybrid welding in joining 3-mm-thick 5005 aluminum alloy plates with a 1.2-mm diameter filler wire of 5356 alloy. It was observed that laser power and focuses' height had direct dependence on weld penetration while an indirect relationship existed between inclinations of the MIG torch and weld penetration [144].

4.2.3 Nd:YAG Laser-MIG/MAG/GMA hybrid welding

Nd:YAG laser and gas metal arc heat sources are combined together to aid the welding of aluminum alloys. Thicker plates with deeper weld penetration can be welded with the application of laser MIG hybrid welding. In addition, laser-assisted alternating current (AC) pulsed MIG welding has been suggested for joining thin aluminum alloys at high welding speed. It was reported that 1.2- and 1.5-mm-thick aluminum alloys can be reasonably lap welded at a high speed of 4 m/mm by using laser alternating current pulsed MIG welding technique [108]. Kim et al. [40] investigated continuous wave 3.5 kW Nd:YAG laser-MIG hybrid welding of 5-mm-thick marine grade 5083 and 5356 aluminum alloy sheets using a 1.6-mm diameter 5356 alloy as filler material [40]. A high speed video was employed to examine the relationship between laser beam and bead formation, as well as arc and molten wire droplets. The revelations from high-speed images during the Nd:YAG laser-MIG hybrid welding of 5083 aluminum alloy plates revealed that the heat input delivered to the plate was dependent on the nature of the leading heat source and joint condition employed in hybrid setup [40]. The authors reported that the maximization of the synergetic benefits from the combination of laser and arc heat sources was attained when the laser beam was located between the arc center and droplet impact point [40]. Also, other authors have equally examined the application of Nd:YAG laser-MIG hybrid welding on aluminum alloys. Zhang et al. [145] examined the application of Nd:YAG laser-GMA hybrid welding on 2-mm-thick 6061-T6 aluminum alloy sheets using 4043 filler [145]. Nd:YAG laser-MIG hybrid welding of 4-mm-thick 2024-T4 aluminum alloy sheets was performed by Mattei eta al. [123] using filler metal of 1-mm diameter 4047 alloy and wire speed of 4 m/min [123]. He et al. [146] also examined the influence of Nd:YAG laser-MIG hybrid welding on 2-mm-thick 1A80 aluminum plates using 4043 filler wires and argon shielding environment [146]. Ola and Doern investigated Nd:YAG laser-GMA hybrid welding of 6.3-mm-thick 7075-T651 with a spool of 0.89-mm diameter 4043 welding wire [147]. Hu and Richardson [18] conducted Nd:YAG laser-GMA hybrid autogenous welding of 2-mm-thick 7075-T6 alloy and 1-mm-thick 2024-T3 alloy [18].

Kim et al. [38] utilized the grey relational analysis to determine the optimum Nd:YAG laser-GMA hybrid welding parameters of 1-mm-thick 6 K21-T4 aluminum alloy sheets in butt configuration. The optimization criteria chosen for their works included ultimate tensile stress of weld, penetration depth, and bead width [38]. In non-aluminum metals, improvement of weld toughness has been demonstrated in Nd:YAG laser-MAG hybrid welding system [14]. Tong et al. [148] also investigated the laser-alternating current pulsed metal inert gas hybrid welding process on 1.5-mm-thick 5052 aluminum alloy using a 1.2-mm diameter welding wire made from 5356 alloy [148].

4.2.4 CO_2 Laser-TIG double-sided welding (LTDSW) /laser-arc double-sided welding

Laser-arc double-sided welding was first utilized by Chen et al. [119] during the welding of 5A06 aluminum alloy. Laser-arc double-sided welding combines a laser beam together with an arc welding source which are vertically positioned or located on the opposite sides of the work pieces to be welded. The major aim of laser-arc double-sided welding is to prevent laser energy loss through arc plasma (since there is usually loss in laser energy when laser beam passes through the established arc plasma during hybrid laser welding or when there is overlapping of laser induced plasma plume with the arc). In the works of Chen et al. [119], a CO_2 laser beam and a gas GTAW torch were positioned vertically on the opposite sides of 4-mm-thick 5A06 wrought aluminum alloy plates with a major reason of preventing laser energy loss via arc plasma. In LADSW process, there is compression and stabilization of the GTAW arc on the arc side, and this phenomenon leads to a higher arc current density and more stable welding process. Interactions between the laser and the arc plasma also take place in the arc side of the welding arrangement. The physical process of LADSW is different from the traditional hybridized laser-arc welding process because the interaction between the laser-induced metal vapor and the arc plasma only take places at a definite threshold of laser power [119]. The interaction effect between the induced metal vapor and arc plasma was studied by Chen et al. [119] using electron spectroscopy in examining electron temperature and density (Fig. 5).

Liu et al. [142] investigated the influence of relative location of laser beam and TIG arc in different hybrid welding

modes (laser leading mode and arc leading mode). Laser leading hybrid welding mode is designated with laser-TIG hybrid welding while TIG leading hybrid welding mode is represented with TIG-laser hybrid welding [142]. With laser-arc hybrid welding, high quality appearance, and stable welding process can be easily obtained in aluminum welding. The arc voltage in laser-TIG double-sided welding is lower than the conventional TIG welding process [117]. Also, Yan-Bin and co-authors investigated the 3.0 kW CO_2 laser-TIG double-sided welding of 4-mm-thick 5A06 aluminum alloy plates [149].

4.2.5 Fiber laser-pulse MIG/GMA hybrid welding

The application of fiber laser heat source together with pulsed gas metal arc heat source is grouped under this category. Zhang and co-authors employed a 6 kW continuous fiber laser-pulse MIG hybrid welding in the welding of 6-mm-thick 2219-T87 aluminum alloy sheets with the aid of two types of filler wires, namely 5087 and 2325 [141]. Wu et al. [150] also employed fiber-laser-pulsed GMA hybrid welding on 2-mm-thick 7075-T6 aluminum alloy sheets with the aid of 5356 filler wire with a 1.2 mm diameter.

4.3 Tailored heat source-laser welding

Tailored heat source-laser welding approach makes use of two laser beams simultaneously in order to control the weld pool geometry, stability of keyhole, and weld bead shape. Also, this setup is desirable to create sufficient surface area and longer time for the escape of porosity forming gases [22]. The difference between tailored heat source-laser welding category and laser-arc hybrid welding is that it applies laser heat sources alone in welding, unlike laser-arc hybrid welding that employs a laser beam source and an arc heat source in welding (two different heat sources). This category of laser welding of aluminum alloys applies two or twin/double-laser heat sources that are systematically positioned either side by side or overlapped with one beam leading and the other as a lagging beam.

4.3.1 Twin-spot Nd:YAG laser welding

This is a laser welding process that creates two focused beam spots on work pieces, usually with a definite spot separation distance. The application of twin-spot laser welding creates elongated weld pool and due to this phenomenon, porosity level in aluminum weld metal is considerably reduced. Verhaeghe and Hilton [7] applied continuous wave twin-spot laser welding with a spot separation distance of 0.27 mm and focus diameter of 0.45 mm on a 3.2-mm-thick 2024 aerospace aluminum alloy. The experiment was investigated under square-edge butt weld configuration, and a 1.2-mm diameter 2319 filler wire was positioned at the leading edge of the weld pool during the welding operation. The authors established that the application of this class of laser welding technology helped to effectively eliminate coarse porosity in 3.2-m-thick 2024 wrought aluminum alloy [7].

4.3.2 Dual-beam Nd:YAG laser

Owing to the restriction in maximum power of Nd:YAG laser welding systems to about 3 kW, dual-beam Nd:YAG laser welding system has been made available with higher laser power up to about 8.9 kW [27]. Dual-beam laser welding technology assists in suppressing vapor plume fluctuation, and it assists in establishing a stable process and improved weld quality [9]. This type of laser welding system systematically combines the individual power of two independent lasers to increase the total available laser power required for welding. The first laser beam acts as the leading laser beam while the second acts as the lagging laser beam. Therefore, lead-lag beam power ratio of the dual-beam Nd:YAG laser welding system can be varied as a changing parameter [27].

Punkari et al. [27] investigated the application of dual-beam laser welding on 1100, 5182, and 5784 aluminum alloys in order to examine the influence of magnesium on the resultant welds. In their works, the lead laser power ranged from 3 to 6 kW while the lag beam power levels ranged from 0 to 3 kW. The second laser beam was responsible for improved keyhole stability and improved under-bead geometry of 5182 aluminum alloy sheets [27]. Deutsch et al. [20] applied 2.5–6 kW dual-beam laser in welding 1.6-mm-thick 5182 aluminum alloy sheets. Lead/lag laser beam power ratios ranging from 2:3 to 3:2 and speeds between 4 and 15 m/min were utilized in their works. The authors also affirmed that the lagging laser beam of a dual-beam Nd:YAG laser welding system influenced the stability of keyhole, the escape of high vapor pressure magnesium gas from the keyhole, and the efficient solidification of under bead weld metal [20].

4.3.3 Double-pulse laser welding

This involves the application of two pulsed laser heat sources with definite delay times. von Witzendorff et al. [5] studied the application of a double-pulse laser welding approach in welding 0.5-mm-thick 6082 aluminum alloy sheets. At a definite temporal delay period, Nd:YAG and diode laser pulses were superimposed and synchronized with two diachronic mirrors. Here, the aim of the application of double-pulsed laser welding was to reduce hot cracking in the aforementioned aluminum alloy. After the application of the first pulsed laser (Nd:YAG), the second pulsed laser (diode) power was needed to eliminate hot cracking susceptibility in the weld. The author reported that the delay or timing of the subsequent pulsed diode laser was the principal parameter in eliminating

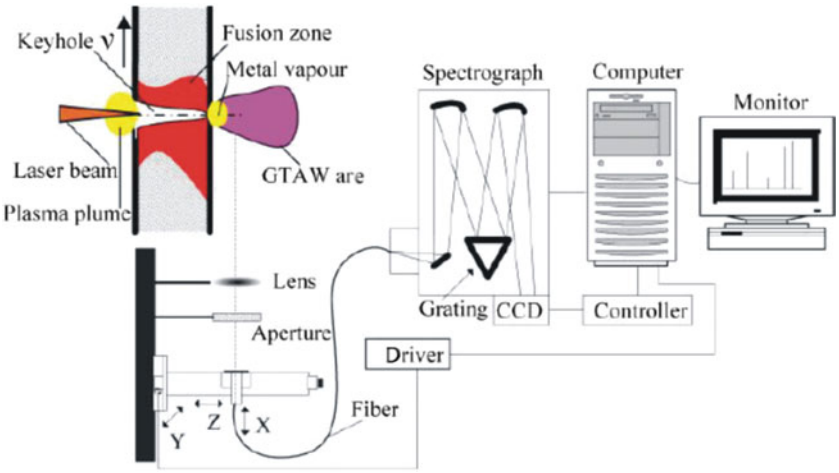

Fig. 5 Schematic diagram of laser-arc double-sided welding with spectroscopy analysis [119]

hot cracking in 6082 aluminum alloy because the second laser beam assisted in compensating for internal strains during the welding process [5]. Representations of the pulse shaping and timing, as well as the schematic arrangement for a double-pulse laser welding are shown in Fig. 6.

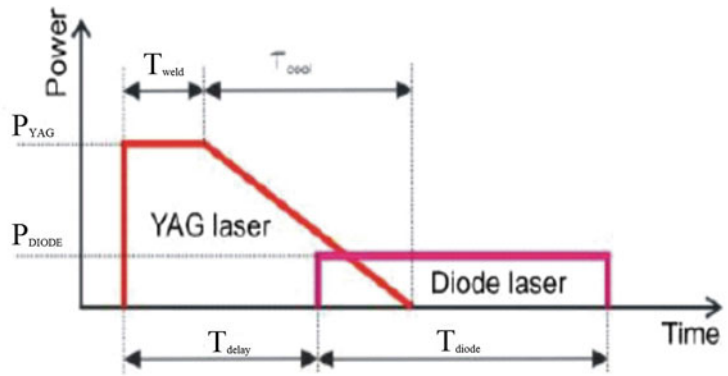

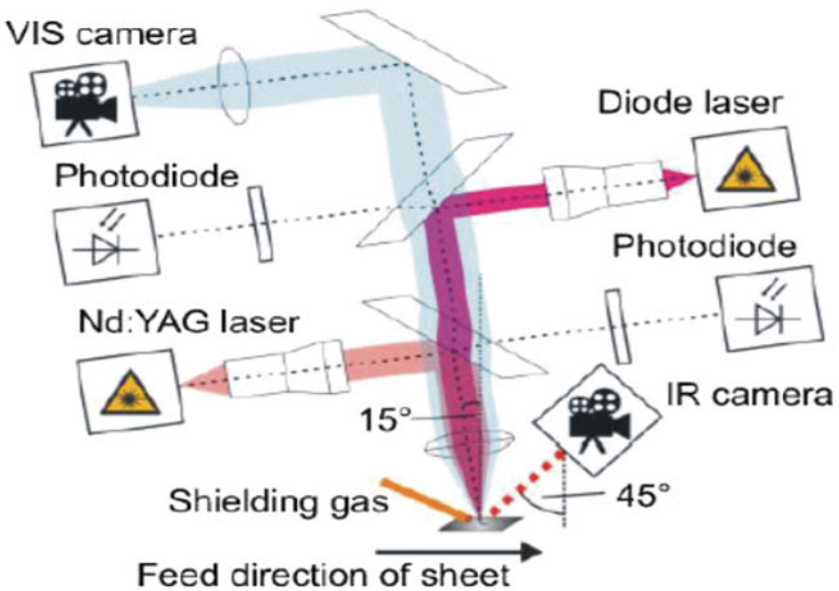

Fig. 6 Pulse shaping and timing in double-pulse laser welding; experimental set-up of double-pulse laser welding [5]

4.3.4 Double-sided fiber laser beam welding

Double-sided fiber laser beam welding is a typical exception because it employs two different laser beams and two gas metal arc sources in welding. It is classified under tailored

heat-source laser welding because of the presence of two laser beams; otherwise, it can be easily classified as laser-arc hybrid welding (Fig. 7).

This is a special case that is particularly suited for T-joint configurations in which the lower skin panel and the upper stringer of a work piece arrangement are welded simultaneously from both sides of the stringer. It involves the application or focusing of two separate laser beams symmetrically onto the opposite sides or positions along the stringer of a T-joint. Equally, two wire feeders controlled robotically are applied in both sides of the configuration to achieve a common molten pool. Wang Tao and co-authors employed this kind of laser welding procedure in welding 1.8-mm-thick 6156-T6 alloy (skin) to 1.8-mm-thick 6056-T4 alloy (stringer). The 10 kW continuous wave fiber lasers and 4047 filler wires having diameters of 1.2 mm were used in the welding process [133].

Yang et al. [151] also investigated the double-sided CO_2 laser welding of 1.8-mm-thick 6156-T6/6056-T4 aluminum alloys using 4047 alloy as filler wires. Penetration depth was revealed to be dependent on the incident beam angle. As the beam angle increases, the penetration depth also increases [151].

4.4 Other innovative laser welding technologies

Other innovative laser welding technologies are welding technologies with deviation from any of the aforementioned classes above. Here, there is an addition of a support device to a single-beam laser welding technology in order to improve the quality of aluminum welds. For instance, the integration of electromagnetic inducing appliance into a single-beam laser welding system is classified under this category.

4.4.1 Electromagnetic supported laser welding

This class of welding integrates electromagnetic field into a single-beam laser welding in order to improve the weld quality. Avilov et al. [49] investigated the full penetration of 15 kW Yb fiber laser welding up to 30-mm-thick 5754 aluminum alloy plates by using an electromagnetic weld pool support. The authors utilized a contactless inductive electromagnetic weld pool support system to prevent gravity dropout of melt. The electromagnetic weld pool support system made use of 460-Hz frequency and about 200 W ac power to prevent melt outflow (from depth up to 30 mm and weld width of about 25 mm). The assistance of electromagnetic field in welding was responsible for the creation of full penetration depth in 30-mm-thick 5754 aluminum alloy plates. Oscillating-induced magnetic field was able to suppress Marangoni convection in the lower section of the weld pool. The established electromagnetic force helps in refining the melt and stabilization of the weld pool. However, the authors employed electromagnetic field in preventing gravity dropout of the melt.

The results revealed that partial penetration was obtained in welding 40-mm-thick 5754 plates without electromagnetic support. Similarly, the weld centerline and bottom region of the welds had clusters of small pores and irregular weld surfaces as a result of intensive Marangoni convection. However, the assistance of electromagnetic support in welding the aforementioned aluminum alloy helped in overcoming the major issues of conventional laser welding [49].

Schneider et al. [152] also investigated the application of electromagnetic field on Nd:YAG rod laser welding of 6-mm-thick 5754 plates. It was revealed that the oscillating magnetic field favored pore out-gassing and welds' pore reduction of about 80 % was attained. Thus, at high frequencies of oscillation of the magnetic field, small penetration depth and stabilization of weld surface were observed [152]. Gatzen et al. [153] examined the influence of electromagnetic stirring on the element distribution during laser beam welding of aluminum alloy with filler wire via numerical modeling. It was affirmed that the frequency of the magnetic field and the flux density had an influence on the filler material distribution and the concentration of the alloying elements in the weld seam [153].

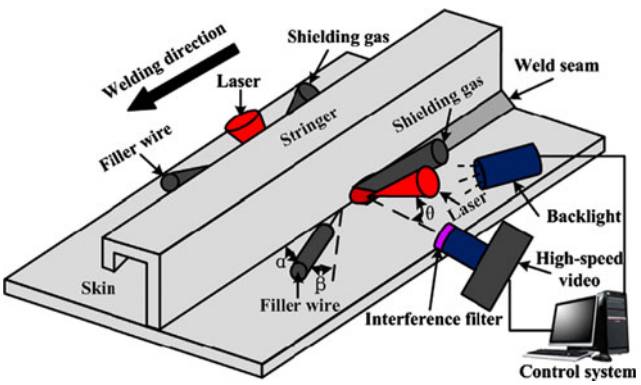

Fig. 7 Schematic setup for a typical double-sided fiber laser welding with filler wires [133]

4.5 Laser weldable aluminum alloys

Laser beam technology has been employed in welding quite a number of aluminum alloys; heat treatable and non-heat treatable wrought aluminum alloys are weldable with laser technology. Although, the application of laser welding technology on cast aluminum alloys is still very limited in literature. One of the noteworthy laser-welding of cast aluminum alloys was conducted by Haboudou and coauthors in 2003. The authors examined the application of Nd:YAG laser welding technology on 4-mm-thick 356-T6 cast aluminum alloy [124]. Nevertheless, since the laser-welding of cast aluminum alloys is sparingly available in literature, the available wrought aluminum alloys are considered. The application of the aforementioned laser welding technologies on different categories of aluminum alloys is summarized in

Tables 3 and 4. However, the chemical compositions of these alloys are given in Appendix Tables 14 and 15, respectively, while Appendix Table 16 shows the chemical compositions of the few cast aluminum alloys that have been welded with laser beam welding technology. Likewise, the chemical compositions of the filler materials that have been used in laser welding of aluminum alloys are reported in Appendix Table 17.

5 Laser beam parameters

The success of a typical laser beam welding of aluminum alloy strongly depends on the composition of the alloy, process gases, filler materials, material preparation technique, and process parameters [3]. For instance, the incident laser beam that is absorbed during welding is greatly dependent on aluminum material and its surface properties. The amount of power needed to produce a melted zone depends on the heat capacity of the material [81]. Welding parameters influence the quality of welded aluminum joints and performance level of the resultant weldment. Depending on the nature of waves (continuous or pulsed wave), there are quite a lot of laser welding parameters available. However, some of the most critical processing or welding parameters during laser welding include laser power or power density (ratio of power to beam size), welding speed, type of shielding gas, beam shape on work piece, position of focal plane of the beam, etc. In case of pulsed laser welding, additional parameters such as pure duration, pulse shape, pulse energy, and average peak power density have to be considered.

5.1 Composition of alloys

The composition of aluminum alloy or the addition of a typical alloying element through the use of filler material affects weld quality of laser welded aluminum joints. Punkari et al. [27] investigated the influence of magnesium content on 1.6-mm-thick 1100-O (0.008 wt% Mg), 5754-O (3.2 wt% Mg), and 5182-O (4.6 wt% Mg) aluminum alloy sheets using a dual beam Nd:YAG laser welding technology [27]. Good welds were produced under the application of a dual-beam Nd:YAG welding technique in joining aluminum-magnesium alloys when lead/lag laser beam power was greater or equal to 1 [27]. Excellent full weld

Table 3 Non-heat treatable alloys available in literature

S/N	Laser type	Material	Thickness	Filler material	filler diameter	Weld type	Shield gas	Ref
1	Dual-beam Nd:YAG	1100	1.6 mm			Bead-on-plate	Ar	[27]
2	Nd:YAG laser-MIG	1A80	2 mm	4043		Butt	Ar	[146]
3	CO_2 laser-GTA	5A06	4 mm			Bead on plate	Ar	[119]
4	Single-beam Nd:YAG	5182	1.6 mm			Bead on plate		[20]
5	Dual-beam Nd:YAG	5182	1.6 mm			Bead on plate		[20]
6	Dual-beam Nd:YAG	5754	1.6 mm			Bead on plate	Ar	[27]
7	Dual-beam Nd:YAG	5182	1.6 mm			Bead on plate	Ar	[27]
8	High power diode laser	5083				Bead on plate		[11]
9	Pulsed YAG laser	5083-O	5 mm				Ar	[109]
10	CO_2 laser	5083	4 mm					[154]
11	CO_2 laser	5083	3 mm				He	[155]
12	CO_2 laser-MIG hybrid	5005	3 mm	5356	1.2 mm			[144]
13	Nd:YAG laser	5A90-T8	3 mm					[156]
14	Nd:YAG laser	5083-O	4 mm				He	[124]
15	Fiber delivered Nd:YAG	5083	10 mm				Ar	[9]
16	CO_2 laser	5083					He	[6]
17	Yb fiber laser welding + EM	5754	up to 30 mm			Butt		[49]
18	Nd:YAG laser	5A90	3 mm				Ar	[91]
19	Nd:YAG laser	5754-O	1.6 mm			Butt		[16]
20	CO_2 laser	5754-O	1.6 mm			Butt		[16]
21	Nd:YAG laser	5182	1.0 mm				He	[157]
22	Nd:YAG laser	5754	1.47 mm				He	[157]
23	High power diode laser	5083	3 mm			Bead on plate	N	[11]
24	Laser-GMA hybrid	5182	1.1 & 2.1 mm	AA5356		spot weld		[95]
25	CO_2 laser-TIG double side	5A06	4 mm			double side		[149]

Note: EM connotes electromagnetic field

Table 4 Heat treatable alloys available in literature

S/N	Laser type	Material	Thickness	Filler material	filler diameter	Weld type	Shield gas	Ref
1	Nd:YAG laser	2024	3.2 mm	2319	1.2 mm	Butt	He	[7]
2	CO_2 laser-MIG hybrid	2A12	8 mm	4043 & 2319				[143]
3	Fiber laser	2A97-T4	2 mm				Ar	[131]
4	Nd:YAG laser-GMA	2024-T3	1 mm					[18]
5	Nd:YAG laser	2024-O	2 mm				Ar	[158]
6	Nd:YAG laser	2024-T4	4 mm	4047	1 mm	T-joint		[123]
7	Nd:YAG laser-MIG	2024-T4	4 mm	4047	1 mm	T-joint		[123]
8	Nd:YAG laser	2024-T4	2 mm			Single spot		[12]
9	Nd:YAG laser	2024-T4	2 mm			Overlapped spot	Ar	[12]
10	CO_2 laser	2090	1.6 mm					[13]
11	Fiber laser + MIG	2219–T87	6 mm	2325 & 5087	1.6 mm			[141]
12	Nd:YAG laser-GMA	6 K21-T4	1 mm	5356		Butt	He	[38]
13	Nd:YAG laser	6063-T5	2.5–5.0 mm	4043	1.2 mm			[22]
14	Fiber laser	6013-T6	2.5 mm				Ar	[129]
15	High power Yb-fiber laser	6013-T4	1.6 mm			Overlapped & T-joint	Ar; He	[130]
16	Double-pulse laser welding	6082	0.5 mm			bead on plate	Ar	[5]
17	Fiber laser	6013	1.6 mm			T-joint		[159]
18	Nd:YAG laser	6082					Ar	[46]
19	High power diode laser	6082	4 mm			Bead on plate	N	[160]
20	Nd:YAG laser	6061	2 mm	4043				[122]
21	Nd:YAG laser-GMA	6061-T6	2 mm	4043				[145]
22	CO_2 laser-GMA	6082	8 mm			Bead on plate		[140]
23	Double-sided fiber laser	6156-T6/6056-T4	1.8 mm	4047	1.2 mm	T-joint		[133]
24	Nd:YAG laser-GMA	6056-T4	2.5 mm	4047	1 mm		Ar	[161]
25	Nd:YAG laser	6156-T4	3.6 mm	4047				[162]
26	Nd:YAG laser-GMA	7075-T6	2 mm	5754 & 2319				[163]
27	Nd:YAG laser-GMA	7075-T6	2 mm					[18]
28	Nd:YAG laser-GMA	7075-T651	6.3 mm				Ar; He	[147]
29	Fiber laser-GMA	7075-T6	2 mm	5356	1.2 mm	Butt		[150]

penetration of a 1.6-mm-thick 1100-O aluminum alloy was produced. Meanwhile, rough, undercut, and spiky under beads with drop-through were observed in 5754-O and 5182-O aluminum alloys. This was attributed to the presence of volatile magnesium constituents in them [27]. Weld penetration and welding speed were recorded to increase with magnesium content under keyhole welding process of aluminum-magnesium alloys. This phenomenon was attributed to the influence of magnesium on vapor pressure within the keyhole and surface tension of the alloys [27]. Zhao et al. [45] investigated the influence of silicon content on laser welding performance of Al-Mn-Mg aluminum alloy sheets. It was revealed that laser welding cracking susceptibility changed with the amount of silicon in aluminum welds. When the amount of silicon in the weld pool was below 0.34 %, no cracking was observed. However, cracking in Al-Mn-Mg alloy increased as the amount of silicon increased to 0.47 %. This phenomenon (Si content inducing cracking) was attributed to different morphologies of eutectic phases at the grain boundary [45].

5.1.1 Laser power

Laser power can also influence the quality of welds. The adjustments of laser power and welding speed affect the penetration depth of welds [148]. Variation of laser power during laser-TIG double-sided welding of aluminum alloy resulted in the formation of three arc shapes, namely arc column convergence, arc expansion, and arc root constriction [117]. Figure 8 shows the influence of laser power on weld penetration depth in 5083 and 6082 aluminum alloys, respectively.

5.1.2 Focal position/laser focus position

Laser focus position plays a significant role in laser beam welding of aluminum alloys. A laser beam can be focused onto the surface or beneath the surface (keyhole) of the material to be welded. The effect of focal position on weld quality

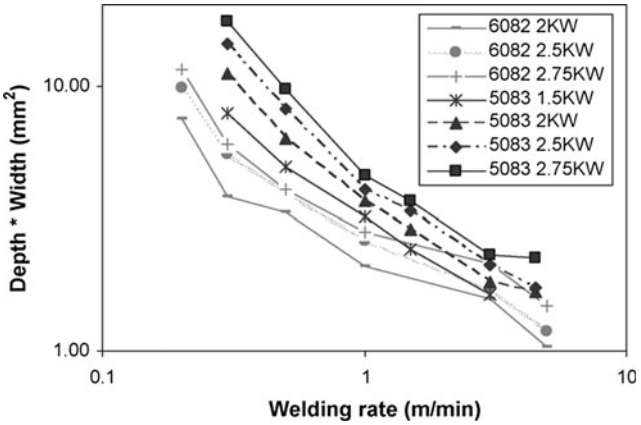

Fig. 8 Dependence of weld depth and width on laser power and welding rate/speed in 5083 and 6082 aluminum alloys [160]

was investigated with the aid of a single-beam laser and a dual-beam Nd:YAG laser welding on 1.6-mm-thick 5182 aluminum alloy. However, the formation of unacceptable spikey under bead geometry was reported not to be affected by changes in focal position in each of the laser systems [20].

5.1.3 Welding speed/Traveling speed

Laser welding speed greatly influences the penetration depth of weld as shown in Fig. 9. At a given laser power, the penetration depth increases as the welding speed is reduced; equally, an increase in weld pool's width also ensues [49]. With increasing thickness of aluminum alloy, the welding speed requires for a full penetration weld decreases [8].

5.1.4 Shielding gas

The major function of a shielding gas is to protect the weld's molten pool from environmental gas interference. Shielding gas affects the penetration depth of aluminum alloys during laser beam welding process. Penetration depth of joints shielded with helium gas is higher than that of nitrogen or argon shielding [9]. Also, contamination of shielding gas is

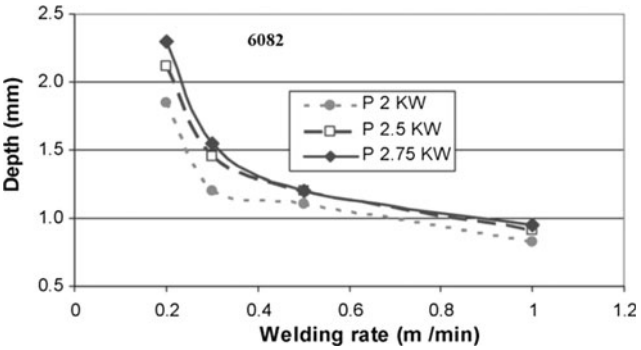

Fig. 9 Influence of welding rate/speed on weld depth during laser welding of 6082 Al alloy [160]

a likely source of porosity in keyhole welds [69]. Nitrogen causes more severe porosity in 2195 aluminum-lithium alloys than either hydrogen or oxygen. Therefore, shielding of its weld pool from atmospheric air is highly imperative [69]. The influence of shielding gas on single- and dual-beam Nd:YAG laser welded 5182 aluminum alloy sheets was investigated. The parameters of the shielding gas were observed not to influence the undesirable spikey under bead geometry formed as a result of high vapor pressure of magnesium [20]. The type of shielding gas (chemical composition of the gas), the nozzle parameters, and the flow rate or geometry of the shielding gas are important factors that affect the size of plasma plume and resultant quality of laser welded aluminum joints. Teresa Sibillano et al. [164] investigated the influence of shielding gas on laser welding of 5083 aluminum alloy sheets. It was revealed that shielding gas significantly influenced the losses of alloying elements [164]. Ancona and coauthors applied continuous wave CO_2 laser welding on 4-mm-thick 5083 aluminum alloy plates by using two different nozzle configurations (two-pipe configuration and coaxial nozzle). It was revealed that gas flow rate and nozzle standoff distance had a slight influence on weld penetration depth. However, the most efficient gas delivery system was affirmed to be two-pipe delivery system because welds with lower width, deeper penetration, and larger melted areas were obtained as compared to that of coaxial nozzle delivery system [154].

5.1.5 Filler metal/wire and wire feed-rate

Filler metal is a typical auxiliary material for gap filling or bridging during laser welding. It offers the opportunity of controlling the metallurgy of welds [51] and ensuring good weld quality. The filler wires used in laser welding basically assist in replenishing the evaporated alloying elements, and they equally prevent solidification cracking in welds. It also offers the possibility of controlling the properties of the fusion zone of welds. Filler metals are necessary in establishing deep penetration welding process [8]. Similarly, filler wire plays an important role in improving the strength of welds. Zhang et al. [141] examined the influence of 1.6-mm diameter 5087 and 2325 wires on the tensile strength of laser-MIG hybrid welded 6-mm-thick 2219 aluminum alloy sheets. The tensile strength of joint produced from 5087 was about 313 MPa, which was 20 % higher than that of the 2325 wire [141]. The reasons for strength improvement in the weld metals produced from 5087 wire were attributed to the formation of large amount of fine S–Al_2CuMg precipitates and also pinning effect of precipitates on dislocations [141]. Bernard Johan Aalderink et al. [95] reported that the use of 5356 filler wire was completely indispensable in order to increase the gap tolerance during single-spot laser, twin-spot laser, and laser-GMA hybrid welding of 1.1- and 2.1-mm-thick 5182 aluminum alloy

sheets. Though, the level of gap that could be bridged was reported to vary from one laser welding method to another. However, in case of laser spot welding, a proper alignment of filler wire with the laser spots is very crucial [95]. Kah and co-authors revealed that the application of 4043 and 5356 alloy filler metals in welding 10-mm-thick 6005-T5 and 6082-T6 heat treatable aluminum alloys prevented solidification cracking [168]. In laser-arc hybrid welding of aluminum alloys, it was revealed that wire feeding position, feeding direction, and feeding angle would influence the melting behavior of wire and the process stability of the welding process. Tao et al. [133] reported that an increased in wire feeding angle during double-sided fiber laser welding of 1.8-mm-thick 6156-T6 and 6056-T4 aluminum alloys prevented gas escape from the molten pool of welds [133].

5.1.6 Joint configuration

Gap presence in a laser butt joint configuration changes heat transfer efficiency and electrical circuit condition [40]. For joints with gaps larger than the laser beam diameter, metal inert gas leading hybrid welding process (MIG-laser hybrid welding) has been adjudged to be more suitable [40]. Weld bead shape is dependent on gap condition (in case of gap bridging or butt welding), motion, or movement of molten wire in the gap, leading heat source and preheating effects [40].

5.1.7 Current

During a low- or medium-current welding operation of a laser-arc hybrid system such as laser-TIG hybrid welding, the laser induced plasma could stabilize and compress the electric arc. As a result, an increase in current density and penetration depth of welds would be achieved. On the other hand, when current level is increased up to a critical value, the arc will not be compressed. Therefore, defocusing of the laser energy may ensue (reduction of energy density) and shallow keyhole will be produced [117]. Current intensities have corresponding effects on arc resistance and the number of carriers of electric current in a hybridized laser-arc welding system. Low current intensities bring about a reduced arc resistance and an equivalent increase in the number of carriers of electric current [108]. Transition from laser-induced keyhole (deep penetration depth) to heat conduction welding may occur in hybridized laser-arc welding process when an arc current is increased to reach a critical value (arc expansion takes place and conduction mode of welding is created) [108].

5.1.8 Pulse duration and arc shape

Changes in arc shape or behavior greatly affect the arc current density and its stability [117]. Arc shape is greatly affected by interaction time between laser beam and arc during hybrid welding. The influence or variation in arc shape will in turn affect the weld penetration depth and transition of hybrid welding mechanisms [108].

Laser pulse duration greatly influence arc shapes; short pulse duration may not be sufficient to complete the compression and stabilization of arc while long pulse duration may expand the arc by increasing absorption or defocusing of laser [108].

Pulse laser can effectively reduce the interaction time between laser beam and arc in laser-TIG hybrid welding by preventing the growth of plasma and decreasing absorption or defocusing of laser energy [108].

6 Microstructural properties

Microstructure of laser welded aluminum alloy sheets is usually examined with the aids of scanning electron microscopy (SEM), energy dispersive spectrometry (EDS), transmission electron microscopy (TEM), electron backscattering diffraction, or X-ray diffraction analysis (XRD). The microstructural properties in the fusion zones of welded aluminum alloys are greatly influenced by the nature of welding technology, process parameters, and the composition of base metal [169]. Optimum selection of process parameters during laser welding of aluminum alloys can help limit the amount of pores in welded joint of aluminum [169]. During laser beam welding of aluminum alloys, variations in fusion zone morphologies and microstructures are chiefly influenced by heat flow which is largely controlled by laser power, travel speed, and focus diameter [170]. Weld zones obtained during laser beam welding of aluminum alloys are often classified into fusion zone, heat affected zone, and at times, partially melted zone. The high power density and low heat input of a laser beam welding system coupled with high cooling rates influence the microstructure of laser welded joints. As result, a narrow heat affected zone and fine grained weld zone (microstructures) are often obtained in laser welding of aluminum alloys.

Fiber laser welded 2-mm-thick 2A97-T4 aluminum-lithium alloy showed four distinctive weld zones (apart from that of base metal). Heat affected zone, partially melted zone, non-dendritic equiaxed zone, and fusion zone were observed. The amount of constitutional super cooling was described to affect crystal morphologies in the fusion zone. Slight traces of liquation was seen in the partially melted zone while the formation of equiaxed zone was attributed to heterogeneous nucleation involving the effects of lithium (Li) and Zirconium (Zr) [131].

Li Cui and co-authors examined the influence of Nd:YAG laser welding on the microstructure of 3-mm-thick 5A90-T8 aluminum alloy. It was observed that a narrow band of equiaxed grain structure existed along the fusion boundary

while a predominantly equiaxed dendritic structure existed in the weld fusion zone. The formation of predominantly equiaxed dendritic structure in the fusion zone was attributed to heterogeneous nucleation mechanism that was assisted by equilibrium A13Zr phases and dendrite fragmentation or grain detachment as a result of laser welding processes [156].

During the solidification process of weld metals, temperature gradient of the molten pool decreases and heterogeneous nucleation of equiaxed dendrites can be initiated by the presence of nucleating particles in the center of the fusion zone. As temperature gradient decreases, the formation of equiaxed dendrites increases. Therefore, a decrease in the peak power density of the laser will reduce the temperature gradient in the fusion zone and the formation of equiaxed dendrite will be favored [12]. Thermal gradient (G_L) and growth rate (R) influence the macroscopic grain structure of weld metal and quite a number of authors have worked on this. Norman et al. [13] investigated the application of thermal modeling on CO_2 laser beam welding of 1.6-mm-thick Al-Li-Cu-Mg-Zr aluminum alloy. It was predicted that columnar grain structures would occur at low welding speed (high G_L/R ratio or ratio of thermal gradient to growth rate) while equiaxed grain structures would be formed at high welding speeds (low G_L/R ratio). It was also stated that dendrite arm detachment was caused by turbulent melt flow while other particles present in the weld pool acted as nuclei for the growth of grains in the equiaxed structure [13].

Similarly, the microstructure of laser welded 5754-O aluminum alloys revealed cellular dendritic structure in the fusion zone. Also, the weld center or fusion revealed predominantly equiaxed grain structure. The percentage or amount of equiaxed grains in the weld center was observed to decrease with increasing traveling speed [16]. In addition, microstructural investigation of high power diode laser welded 5083 aluminum alloy sheets was investigated by Sanchez-Amaya et al. [11]. The inner part of the weld bead had fine equiaxed grain microstructure. Thus, fine precipitation of the second phases in a solid solution matrix of magnesium was observed in the microstructure of the weld bead [11]. Regions of the bead close to the base metal were characterized by dendritic growth, which was attributed to higher solidification rates. In these zones, intermetallic compounds were not completely dissolved compared to the fusion zone that demonstrated complete dissolution of intermetallic compounds to form fine microstructure during the laser welding processing of 5083 aluminum alloy [11]. Also, fine recrystallized grain structure was observed in the fusion zone of Nd:YAG laser-GMA hybrid welded 2-mm-thick 6061-T6 aluminum alloy sheets using 4043 filler wire. Likewise, the evolution of increased precipitate phases was observed in the heat affect zone of the welds [145]. For instance, the pictorial representation of micrographs (weld zones) for Nd:YAG laser welded 6156-T6 aluminum are shown in Fig. 10.

Nd:YAG laser welded 2024-T4 aluminum alloy sheets revealed equiaxed dendrites in the fusion zone but columnar zone was also observed around the equiaxed dendrites [12]. The microstructural investigation of laser-MIG hybrid welded 2219-T87 aluminum alloy sheets revealed the presence of large percentage of fine S-Al_2CuMg precipitates in the grains of the weld metal. This precipitate was attributed to the supply

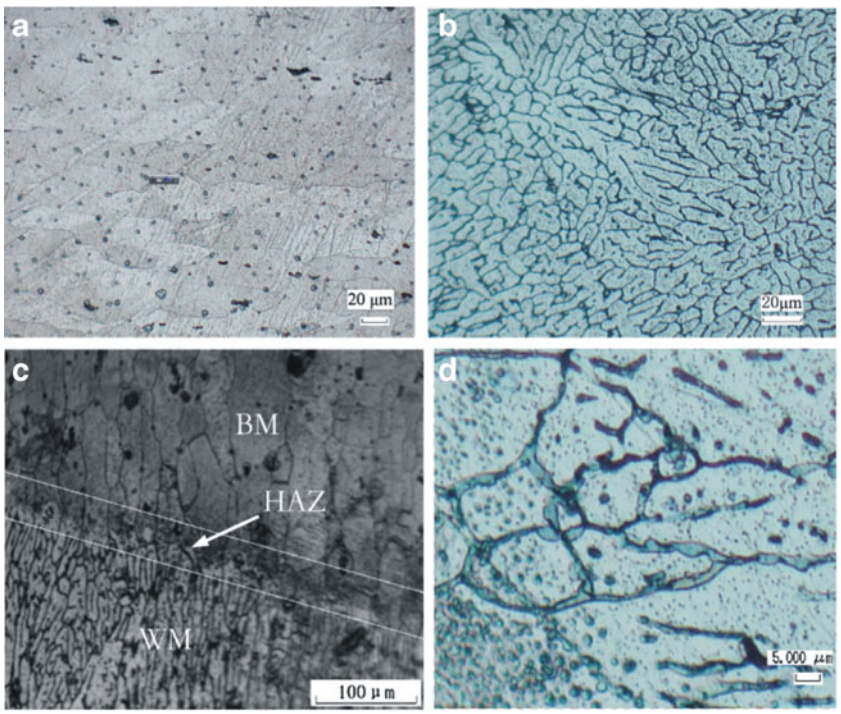

Fig. 10 Micrographs of Nd:YAG laser welded 6156-T4 aluminum alloy with 4047 filler wire: **a** base metal (BM); **b** weld metal (WM); **c** heat-affected zone (HAZ); **d** grain boundary liquation zone [162]

of magnesium elements from 5087 filler wire. As a result, the strength of the welds was improved due to the presence of large amount of the aforementioned precipitates. In fact, it was reported that the addition of magnesium (Mg) from 5087 wire to the molten weld puddle established an Al-Cu-Mg ternary system. Based on this ternary system, it is obvious that θ-Al_2Cu and S-Al_2CuMg phases are the likely precipitates that maybe formed. However, the authors concluded that the lower Gibbs formation energy (ΔG) and higher cohesive energy of S-Al_2CuMg phase ensured that it precipitated first and its precipitates restrained the formation of θ-Al_2Cu phase because most of the copper (Cu) element of the weld pool was consumed (there was no enough copper to form θ-Al_2Cu phase) [141].

Fine equiaxed zone or chill zone is considered to be formed in Al-Li alloys during solidification process, under a high under cooling condition [171]. Badini et al. [66] conducted continuous wave Nd:YAG laser welding of 3.2-mm-thick 2139-T3 alloy to extruded 2.5-mm-thick 7xxx-T4 aluminum alloy with the assistance of 4047 filler wire having a diameter of 1 mm. A mixture of helium and argon was utilized by the authors. The authors revealed that the microstructural analysis of 2139-T3 alloy showed large grains with relatively low aspect ratio and that of 7xxx-T4 alloy revealed characteristic texture caused by extrusion. However, after welding and upon solidification of the weld puddle, fine, and equiaxed grains were revealed in the fusion zone while the partially melted zones showed dendritic structure with elongated grains. Remarkable contents of alloying elements such as Si, Zn, Cu, and Mg were present in the resultant welds prior to post-weld thermal treatments (artificial aging at 175 °C for 8 h and at 120 °C for 24 h). The aging performed at 120 °C showed a certain increase in hardening precipitates in the section of 2139 alloys, and the resultant microstructure of the weld was not affected by heat treatment compared to the as-welded alloys. However, post-weld aging at 175 °C for 8 h revealed further precipitation of strengthening phases in the weld metal [66].

Cui et al. [91] studied the microtexture of 4.5 kW Nd:YAG laser welded 3-mm-thick 5A90 aluminum-lithium alloy using electron backscattered diffraction analysis. A change in component and intensity of texture was observed in the weld metal and heat affected zone of the welded aluminum joints. Though, the weld metal was predominantly composed of equiaxed grains with a random microtexture [91]. A very narrow heat affected zone was obtained due to the low heat input and high cooling rate. However, the fusion boundary of the weld was majorly composed of narrow band of non-dendritic equiaxed grains [91]. The microtexture of 5A90 aluminum-lithium sheets revealed cold rolling microtexture with strong intensity. However, the texture's characteristic of the heat affected zone was similar to that of the base metal except that it had a lower intensity while that of the weld metal had a random texture [91]. Sanchez-Amaya et al. [160] employed high power diode laser welding in autogenous welding of 3-mm-thick 5083 and 4-mm-thick 6082 aluminum alloy sheets. The microstructural analyses revealed dendritic grain growth in areas with higher solidification rates (that is external zone or part of the welds). Thus, the inner parts of the fusion zones were predominated by fine precipitation of the second phases in the solid solution matrixes of the aluminum alloy [160].

7 Defects/imperfections and solutions

Like other fusion welding technologies, laser beam welding of aluminum alloy also has its own shortcomings. Porosities, cracking as a result of solidification shrinkage and thermal stresses, weld inclusions, and evaporation of alloying elements [66] are some noteworthy defects in laser beam welding of aluminum alloys. Equally, geometrical defects such as misalignment and undercut could impair the quality of laser welded aluminum joints. Thus, precise joint fit-up and placement of filler materials are vital in eliminating geometrical defects in laser welding processes. Besides, rapid and complex flow in the molten puddle of aluminum alloys during laser beam welding process coupled with the high cooling rate of aluminum weld metal induces gas entrapment or porosity in laser welded aluminum joints [24]. Also, low absorption coefficient of laser energy is a concern during laser welding process of aluminum alloys. In fact, it has been emphasized that the absorption coefficient of laser beam or radiation is a function of laser wavelength [157]; there is an inverse relationship between the wavelength of a laser beam and the absorption coefficient of laser radiation. A laser with a shorter wavelength, such as high power diode laser (having a wavelength of about 808 nm), will demonstrate a higher laser absorption coefficient than other lasers with higher wavelength such as CO_2 laser (10.6 μm) or Nd:YAG laser (1.06 μm).

Nevertheless, the main defects of laser beam welding of aluminum alloys as reported in open literature are directly discussed in this section. These include porosity due to dissolved hydrogen and other alloying elements, solidification cracking, and surface reflectivity. Meanwhile, other defects such as stress corrosion cracking in certain alloy, loss of alloying elements [51], loss of precipitation hardening due to thermal cycling, softening due to grain growth [8], and poor weld bead geometry [3] are to some extent referred to under corrosion behavioral, microstructural, and mechanical sections, respectively.

7.1 Porosity

Porosities are internal or external small pores or large irregular voids (gas blowholes) formed in weld metals of aluminum

alloys during fusion welding process or during the solidification phase of molten weld pool. External hydrogen sources (from welding supplements), keyhole instability as a result of flow turbulence [42] or collapse of keyhole [51, 124], and metal vapors (evaporation of volatile alloying elements such as magnesium) are some manners in which porosity is formed during laser welding of aluminum alloys. During laser welding process of aluminum alloys, diffusion or floatation of gases such as hydrogen is impeded [51] because of the weld's high cooling rate and narrow weld zone. Therefore, hydrogen gas is entrapped in the solidifying aluminum weld metal; numerous small pores of varying sizes are consequently left in the resultant joint. In fact, after laser welding of aluminum-magnesium alloy, grey powder is normally left on the surface of the alloy's weld area, which directly signifies the evidence of loss of magnesium alloying element [27]. A typical morphology of porosity in the fusion zone of laser beam welded aluminum joint is shown in Fig. 11.

On the other hand, evaporation of alloying elements during laser welding of aluminum alloy has a beneficial contribution to deep penetration welding process because of the recoil pressure of vaporization needed to create deep penetration weld. However, this strong and dynamic pressure action creates keyhole and weld pool instabilities during laser welding process. The unstable state of the keyhole will eventually bring about entrapment of gases within weld metals, and it will consequently form gas pores in the fusion zone of laser welded joints [6].

The classification of porosity in aluminum alloys has been carried out by a few researchers such as Geert Verhaeghe and Hilton [7] and Matsunawa [6]. Verhaeghe and Hilton [7] classified porosity into fine and coarse porosities. Fine porosity is referred to as a distribution of fine spherical pores in weld bead, and it is understood to originate from hydrogen entrapment or from the rejection of shielding gases during solidification process. Coarse porosity has detrimental influence on mechanical performance of welds, and it is referred to as random distribution of large irregularly shaped voids in weld bead. This is usually observed in penetrating welds and in keyhole instability caused by low boiling point constituents [7]. However, the most distinctive porosity is formed in deep penetration or keyhole laser welding of aluminum alloys. Matsunawa [6] reports that keyhole porosity majorly consists of large spherical and elongated cavities around the upper and middle sections of aluminum weld metal [6]. Nevertheless, other porosities attributed to laser beam welding of aluminum alloys existing in open literature are summarized in Table 5.

7.1.1 Porosity preventive measures

Porosity in laser beam welding of aluminum alloys can be reduced through two basic manners, namely, laser innovative approach and conventional approach as depicted in Table 6. Based on the existing literature, the laser innovative approaches for reducing the formation of porosity in aluminum welds can be classified into five groups which include laser pulse shaping and modulation, sub-atmospheric laser welding, application of oscillating magnetic field, application of twin-spot laser welding, and welding with dual beam laser.

7.1.2 Laser pulse shaping and modulation

In an attempt to stabilize keyhole during laser welding process, laser pulse shaping and modulation were investigated by Matsunawa [6] in 2001. He examined porosity formation dynamics and solutions in CO_2 laser welding of 5083 aluminum alloy under a helium shielding environment via an X-ray technique [6]. Thus, his result affirms that pulse shaping and pulse modulation with appropriate duty cycle and frequency are efficient in reducing porosity. The shaping and modulation of the laser beam assist in maintaining a stable keyhole motion by forced oscillation of the keyhole [6].

7.1.3 Sub-atmospheric pressure laser welding

Porosity defects have been effectively eliminated under sub-atmospheric pressure Nd:YAG laser welding of 10-mm-thick 5083 aluminum alloy sheet. Weld beads without any porosity

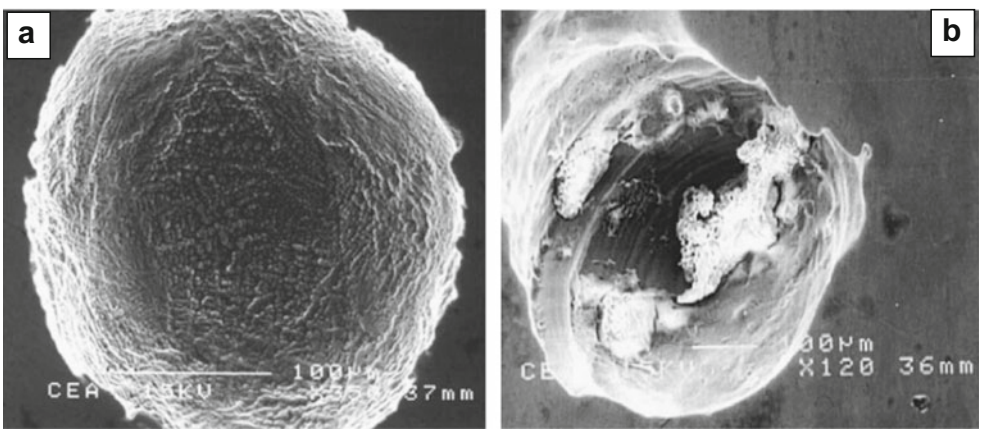

Fig. 11 Typical SEM analyses of porosity in fusion zone of laser welded 5083 alloy **a** 0.2 mm spherical porosity; **b** magnesium oxide enriched walls of 0.6 mm macroporosity [124]

Table 5 Reported causes and nature of porosity in literature

Type of laser	Alloy (filler metal)	Shielding gas (flow rate)	Nature of Pores	Reported causes of porosity	Max. Diameter of pore (μm)	Ref
Hybrid fiber laser- pulsed GMA	7075-T6 (5356)	– (1.25 m^3/h^2)	Near spherical pore	Hydrogen induced	150–280	[150]
Nd:YAG laser	5083	Atmospheric and sub-atmospheric conditions	Irregularly shaped pores; micro-pores	Hydrogen induced; keyhole fluctuation; entrapped gas bubbles	25–80 (sub-atmospheric condition)	[9]
Dual beam Nd:YAG laser	5754-O	Ar (9.4 L/min)	Occluded vapor porosity or blowholes	Mg induced; keyhole instability	–	[27]
Dual beam Nd:YAG laser	5182-O	Ar (9.4 L/min)	Occluded vapor porosity or blowholes	Mg induced; higher vaporization rate and pressure in keyholes	–	[27]
CO_2 laser	5083	–	–	Loss of Mg induced; insufficient incident power to keep the keyhole steadily open	–	[155]
Nd:YAG laser	5784	He (5.66 m^3/h)	–	Keyhole instability; high cooling rate	–	[157]
Nd:YAG laser	5182	He (5.66 m^3/h)	–	Keyhole instability; high cooling rate	–	[157]

were produced under sub-atmospheric pressure or ambient pressures of 10^{-1} Pa as shown in Fig. 12. Plasma shielding effect is suppressed under sub-atmospheric pressure, and it is utterly eliminated under 10^{-3} Pa ambient pressure as seen in Fig. 13. Thus, effective laser power deposition inside the keyhole is achieved and porosity is also extremely reduced. This achievement was attributed to keyhole stability and change in liquid flow (upwards movement along the rear wall of the keyhole) [9].

7.1.4 Application of oscillating magnetic field

The instability in laser weld pool can be efficiency reduced through the application of oscillating magnetic field. Avilov and co-authors employed an AC magnet in inducing oscillating magnet field in the weld pool of 4.4 kW Nd:YAG laser welding of 5754 aluminum alloy sheets. It was reported that the induced magnetic field reduced the surface roughness of welds and the x-ray image analysis revealed that weld porosity was also greatly reduced. In fact, the electromagnetic field performs electromagnetic rectification on the aluminum melts [172].

7.1.5 Twin-spot laser welding

The application of twin-spot laser welding approach on aluminum alloy has shown its effectiveness in eliminating coarse or large and irregular pores in weld metal of aluminum alloy. Twin-spot laser welding creates elongated weld pool during the welding process of aluminum. As a result, this offers more room for the escape of gases that are likely going to be trapped when a single-beam laser welding process is used. However, evidence of the reduction of micro-pores with twin-spot laser is still missing in literature. It was reported that the application of a twin-spot Nd:YAG laser welding with a spot separation (distance) of 0.27 mm effectively eliminated coarse porosity in 3.2-mm-thick 2024 aerospace aluminum alloy, but it was ineffective on pores smaller than 0.4–0.5 mm diameter [7].

7.1.6 Dual-beam laser welding

Dual beam laser welding approach can effectively reduce porosity level in full penetration welds by paying attentions to laser beam power ratio of the welding system. It has been reported that an efficient porosity reduction can be attained in dual beam laser welding of aluminum alloy by constraining the lead/lag laser beam ratio to be greater than or equal unity (lead/lag laser power ratio is ≥1) [27]. Punkari et al. [27] investigated the effects of dual-beam Nd:YAG laser welding on 1.6-mm-thick 1100, 5754, and 5182 aluminum alloys, respectively. No evidence of porosity was affirmed in full penetration welds of 5754 and 5182 alloys when the leading and

Table 6 Generalized causes of porosity and their preventive measures in aluminum welds

Types of weld porosities	Causes	Preventive measures through innovative laser modifications	Conventional preventive measures
Fine porosities or spherical micro-pores [6, 7]	Hydrogen contamination of welding materials	Laser pulse shaping and modulation with appropriate frequency [6]	Pre-cleaning of aluminum alloys and other welding supplements [7, 22]
Coarse porosities or large irregularly shaped voids [7]	Keyhole instability due to flow turbulence [42, 157]	Sub-atmospheric pressure laser welding [9]	Use of low dew-point research grade shielding gas [7]
–	Entrapment of gas bubbles [6]	Application of oscillating magnetic field [172]	Temperature controlled storage of aluminum specimens, filler metals and shielding gas
–	Evaporation of alloying elements [6]	Twin-spot laser welding to induce weld pool elongation [7]	Reduced or lower welding speed [51]
–	High cooling rate of deep welds [157]	Dual beam laser welding suitable for full penetration weld (when the lead/lag laser beam power ratio is ≥1) [27]	Aluminum oxide removal through chemical etching, machining, etc. [7]
–	High welding speed [6]	–	–

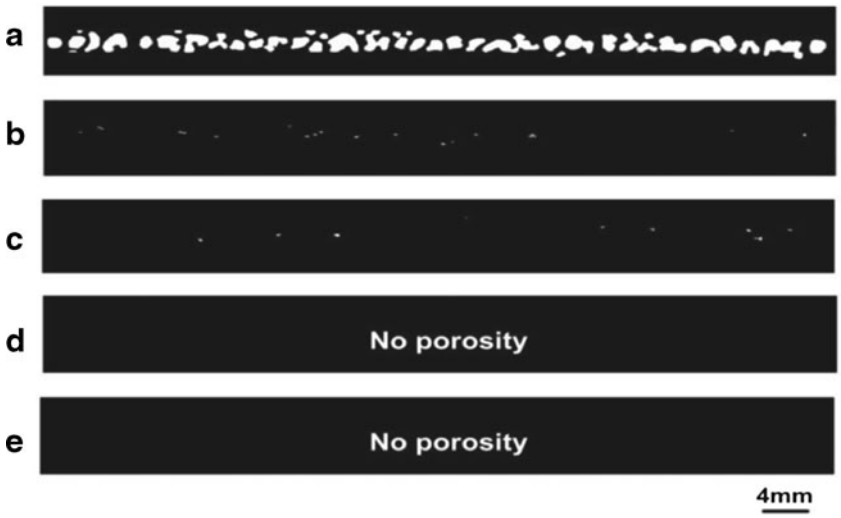

Fig. 12 Weld porosity levels under varying ambient conditions: **a** atmospheric pressure; **b** 10^3 Pa; **c** 10^1 Pa; **d** 10^{-1}Pa; **e** 10^{-3}Pa [9]

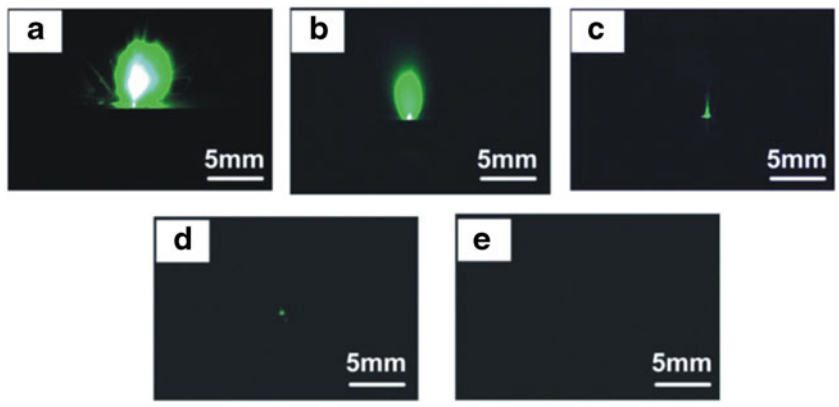

Fig. 13 Nature of plasma plume under varying ambient pressures: **a** atmospheric pressure; **b** 10^3 Pa; **c** 10^1 Pa; **d** 10^{-1}Pa; **e** 10^{-3}Pa [9]

lagging beams had equal powers (lead/lag = 1) and when the leading beam had higher power (lead/lag > 1).

7.1.7 Conventional approach

The conventional approach of reducing porosity is referred to as any approach suitable for removing or reducing external hydrogen content from welding supplements and aluminum work-piece prior to actual laser welding process. This includes surface preparation or cleaning of welding supplements and work-pieces [3, 66, 124]. Thus, porosity in weld metal of aluminum alloys can be reduced by performing filler wire cleaning (through chemical etching, etc.), using of low dew-point research grade helium shielding gas (high purity) and removing aluminum oxide layer (linishing, scraping, machining, or chemical etching). After the removal of oxide layer, the recommended time prior to welding must be less than 24 h in order to avoid atmospheric pick up [7]. Sekhar et al. [22] recommended in their works that pre-cleaning of aluminum alloys' surfaces, temperature controlled storage of aluminum specimens and filler wires, and use of helium as processing gas could prospectively reduce porosity levels in aluminum weld metal. Also, steel wool scraping of the filler metal and mechanical scrapping or linishing of aluminum base metal need to be carried out before degreasing and welding [22].

7.2 Solidification cracking

Solidification cracking is extremely detrimental to the integrity of aluminum welds. Cracks are regions of high stress concentration sites and weld failures often commence from these regions. Solidification cracking in laser welded aluminum alloys is majorly attributed to the properties of aluminum alloys such as high coefficient of thermal expansion, high thermal conductivity, and high solidification shrinkage. During solidification process, the induced (or restrained) contraction of the weld causes tensile-compressive stresses in the weld zones and this may eventually cause cracking. Though, there are two major categories of cracking in aluminum alloy's weldments which are solidification cracking (it occurs in the weld's fusion zone) and liquation cracking (it occurs in the narrow partially melted zone due to tearing of liquate) [51, 158]. It has also been reported that pulsing of laser power increases the susceptibility of cracking in aluminum alloys owing to high cooling rates and rapid solidification [12] of the fusion zone. Also, aspect ratio (depth/width) affects the degree of cracking in fusion zone of aluminum alloys. An increase in aspect ratio increases the tendency of cracking in the fusion zone [48]. However, other reported causes of solidification cracking in laser beam welding of aluminum alloys are highlighted in Table 7.

Solidification cracking has been reported to occur during or immediately after solidification of weld metal, when the alloy being welded passes through a temperature range where ductility is incredibly low. At this unique temperature range, cracking commences and the thermal tensile strains of the weld exceed its endurance strain limit [12]. As a result, cracking occurs in weld when the accumulated strain exceeds the ductility limit represented by characteristic ductility curves of specific alloys [4]. When a weld metal is solidifying, there is thermally induced deformation as a result of thermal contraction and shrinkage from phase transformation. These conditions (residual stress or strain) open up connected dendritic arms in the mushy zone and eventually if there is an insufficient amount of liquid flow back to fill or heal up the existing opening, solidification cracking will occur [129].

The 2024 aluminum alloy is one of the most vulnerable aluminum alloys to solidification cracking during laser welding [12]. Likewise, 6xxx series alloys are also highly susceptible to solidification cracking [4]. Welding parameters and the resultant weld's microstructure influence the severity of cracking in aluminum alloys. Consequently, crack morphology greatly depends on microstructure of the weld metal and overlapping factor [12]. Wang and coauthors investigated solidification cracking behavior with the application of a 10 kW fiber laser in welding 2.5-mm-thick 6013-T6 aluminum alloy plate. The solidification cracking initiation site and propagation were examined using a high-speed camera system and through metallurgical examination. It was revealed

Table 7 Causes of cracking and their preventive measures in aluminum welds

Types of Cracking	Causes	Thermal approach	Metallurgical Approach
Weld metal solidification cracking [51, 158]	Increase in aspect ratio (depth/width) [48]	Dual beam laser welding [4]	Use of appropriate filler metal to compensate for evaporated alloying elements [3]
Liquation cracking [51, 158]	Residual stress or strain [129]	Double-pulse laser welding [5]	Microstructural change attributed to thermal influence [12, 129]
	Welding parameters like power density, overlapping factor [9, 12]	Modification of cooling rate [147]	
	High cooling rate [12]	Decrease in peak power density of laser [12]	
	Resultant weld microstructure [12]		

that the solidification cracking initiated near the fusion line and propagated through the weld center [129]. Typical morphologies of solidification cracking (longitudinal and transverse cracks) in laser beam welded joints of aluminum alloys are represented in Fig. 14.

Sheikhi et al. [12] examined the effect of power density and overlapping factor on cracking behavior during single-spot welding and overlap spot welding modes by using 2-mm-thick 2024-T4 aluminum alloy. Cracking severity was characterized by estimating the mean crack length of the welds and the severity index of crack (crack length divided by surface area of fusion zone). The authors revealed that equiaxed dendrites and columnar dendrites existed in the fusion zone of welds. However, the ratio of equiaxed zone to fusion zone increased with decreasing the peak power density of the laser. It was concluded that the mechanism of cracking in columnar zone was based on shrinkage brittleness theory while the mechanism of cracking in equiaxed zone was based on strain theory [12].

7.2.1 Prevention of solidification cracking

Prevention of solidification cracking in aluminum alloys revolves round thermal and metallurgical factors as illustrated in Table 7. The thermal approach of preventing solidification cracking is employed to minimize induced thermal strains in welds, while the metallurgical approach is utilized to balance the composition of weld metal and to equally prevent alloy segregation. In actual fact, the thermal approach includes the application of dual-beam laser and double-pulse laser welding methods on aluminum alloys. On the other hand, the metallurgical approach includes the use of filler metals during laser beam welding of aluminum alloys.

7.2.2 Metallurgical approach (filler material)

Solidification cracking in laser welding of aluminum alloys can be eliminated by using appropriate filler metal. The major aim of appropriate filler material is to minimize the solidification temperature interval and to equally compensate for loss of alloying elements as a result of evaporation [3]. According to the report of Ion [3], Al-Cu and Al-Si filler wires are popular choices for 2000 and 6000 series alloys, respectively. Several authors have applied different filler materials during laser welding of aluminum alloys but only a few has reported on the role of filler materials on solidification cracking. A compilation of aluminum alloys welded with the application of filler materials is highlighted in Table 8 while their chemical

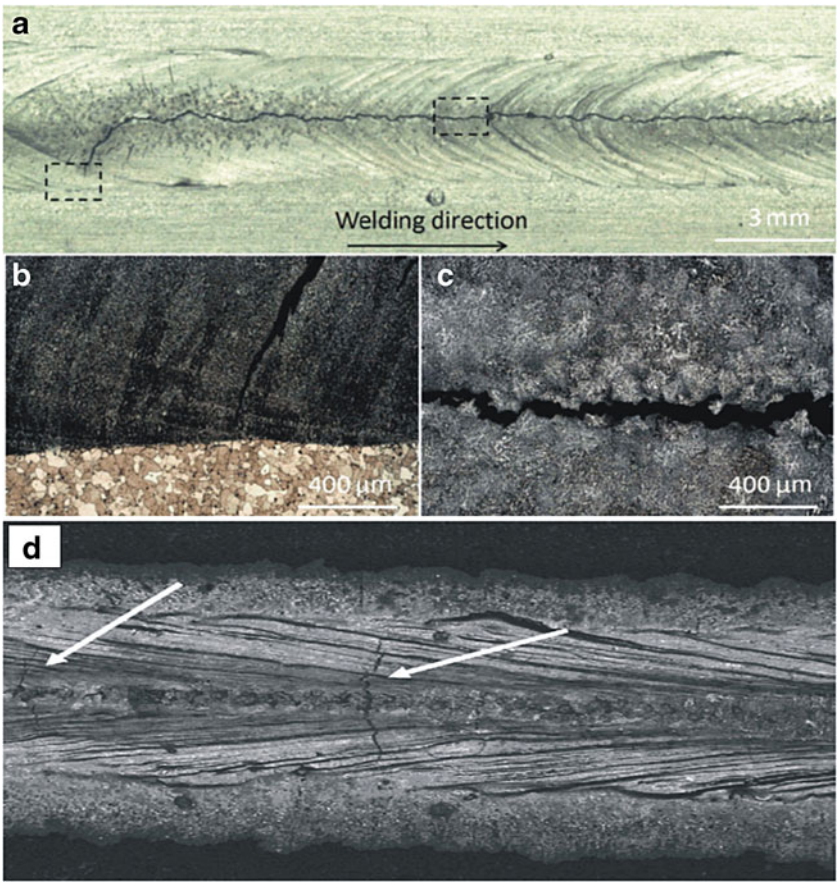

Fig. 14 Morphology of solidification cracking: **a** Crack initiation and propagation; **b** magnification of crack initiation zone; **c** magnification of crack propagation zone [129]; **d** Transverse cracks in 7075 weld samples [18]

Table 8 Aluminum alloys welded with filler materials

Alloy	Filler materials	SC	Mechanical Properties	Microstructural properties	Corrosion properties	Ref
2219	2319	–	H; TS	YES	–	[72]
6063-T5	4043	–	TS	YES	–	[22]
6061	4043	–	–	YES	YES	[122]
2A12	4043 & 2319	–	TS; EL	YES		[143]
5005	5356	–	–	–	–	[144]
5083	5356	–	–	YES	–	[40]
6061-T6	4043	–	–	YES	YES	[145]
2024-T4	4047	–	–	–	–	[123]
1A80	4043	–	H; TS; F	YES	–	[146]
7075-T651	4043	YES	H;	YES	–	[147]
6 K21-T4	5356	–	TS	–	–	[38]
5052	5356	–		YES	–	[148]
2219-T87	2325 & 5087	–	H; TS	YES	–	[141]
7075-T6	5356	–	F	–	–	[150]
2024	2319	–	TS	YES	–	[9]
6056-T4	4047	–	–	YES	–	[133]
6156-T6	4047	–	–	YES	–	[133]
5182	5356	–	TS	YES	–	[95]
6056-T4	4047	–	TS	YES	–	[161]
6056-T4	4047	–	TS	YES	–	[151]
6156-T6	4047	–	TS	YES	–	[151]
6156-T4	4047	–	H; F	YES	–	[162]
7075-T6	2319 & 5754	–	H; TS	YES	–	[163]
7xxx-T4	4047	–	H	YES	–	[66]

SC solidification cracking, *H* micro-hardness, *TS* tensile strength, *EL* % elongation, *F* fatigue

compositions are given in appendix Tables 14, 15, and 17, respectively. Equally, the nature of microstructure of the weld zone affects cracking susceptibility. Crack severity or susceptibility is reported to be minimal in fully equiaxed microstructure while it is more sensitive in columnar part of the fusion zone [12]. Lower interdendritic spacing and finer equiaxed dendritic grained microstructure are suggested to reduce hot cracking susceptibility in aluminum weld metal. In fact, microstructures with longer growing primary dendrites are also adjudged to curtail solidification cracking susceptibility [129].

7.2.3 Thermal approach (welding method)

Likewise, solidification cracking can be efficiently arrested by welding with a dual-beam laser welding technology (additional pulsed laser beam trails the weld pool created with the first laser beam) [4]. Thus, the thermal strains established by the leading beam are reduced by the lagging beam. Double-pulse laser welding (Nd:YAG pulsed laser-diode pulsed laser) was applied on 0.5-mm-thick 6082 aluminum alloy sheets. It was reported that it effectively prevented solidification cracking because of the second laser's (diode) effects on the weld zone; the laser assisted in compensating for internal strains created by the first laser (Nd:YAG) [5] as illustrated in Fig. 15. Also, the power density of a laser beam affects the microstructure of welds; while the microstructure influences the susceptibility to solidification cracking. For instance, a decrease in the peak power density of a single-spot laser beam was reported to increase the percentage of equiaxed zone in the fusion zone of 2024 aluminum joints. As a result, susceptibility to solidification cracking was reduced in the laser weldment of 2024 alloy [12].

Modification of the cooling rate of weld is also classified as a thermal approach. Modifying the cooling rate of laser welded aluminum alloy reduces the susceptibility of welds to cracking. For instance, intergranular liquation cracking was observed in the heat affected zone of 7075-T651 alloy welded with a 4043 filler metal, and this crack was minimized by modifying the cooling rate within the heat affected zone of the joint [147].

7.3 Surface reflectivity

During laser beam welding of aluminum alloy, little fraction of the incident laser radiation maybe absorbed due to high surface reflectivity. Also, laser plume formed just above the weld zone could also reduce the absorption of the incident

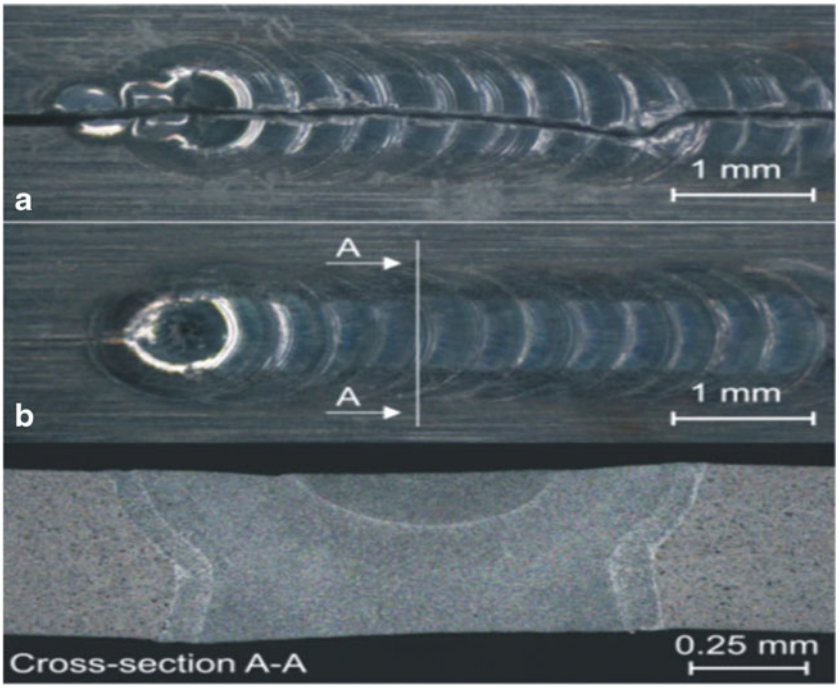

Fig. 15 Effect of superposition of laser beams on weld **a** no laser superposition; **b** double-pulse laser welding [5]

beam during laser welding [8]. As a result, there would be a need to increase the incident laser power (energy) required for welding purpose. In fact, depending on purity of the alloy, surface reflectivity of aluminum alloys can be as high as 80 % or even higher [11]. In case of high reflectivity of the laser beam, much laser energy would be wasted or dissipated out of the focused position.

The danger of optical feedback during laser welding of aluminum alloys is another major problem attributed to high surface reflectivity. However, this has been prevented by conducting and positioning laser beam at an angle to the work-piece material. Cai et al. [9] prevented optical feedback in their works (Nd:YAG laser welding of 5083 alloy) by employing a laser beam having an incident angle of 50° along the welding direction. In order to avoid optical damage of lens, the laser incident beam was positioned at 10° to the vertical direction while the arc torch was at 60° to the surface of the work piece by Zhang et al. [141]. In the works of Avilov and co-authors, the incident angle of 15 kW Yb fiber laser beam was about 8° to the vertical in order to prevent optical feedback [49]. Pastor et al. [157] positioned their laser focusing head at an angle of 75° to the aluminum plates in order to prevent optical damage of lens due to any possibility of laser reflection.

Meanwhile, the preventive approaches that have been employed to reduce surface reflectivity and its associated risk during laser welding of aluminum alloys are summarized in Table 9. The reflectivity problem in laser welding of aluminum alloys is expected to be overcome or positively affected by using a high quality parabolic focusing element. A parabolic focusing lens increases the power density of the laser beam at focus, compared to when a spherical focusing optics is used. As a result, the increase in laser power density is expected to influence the reflectivity problem of aluminum alloy surfaces [10].

Table 9 Causes of surface reflectivity and their preventive measures during aluminum welding

Causes	Preventive measures	Demerits of surface reflectivity
Aluminum alloys are reflective materials	Use of a definite beam incident angle to aluminum plate [9]	Danger of optical feedback or damage to optical lens [9, 157]
Reflection of laser beam is dependent on wavelength or laser type	Use of a high parabolic focusing element [10]	More laser energy will be needed for welding or waste of laser energy [11]
	Use of oxide activating flux but a poor weld appearance ensues due to slag removal [167]	
	Superficial treatment of the surface of aluminum alloys with black coating [11]	
	Use of lasers having shorter wavelengths	

Qin Guo-liang et al. [167] investigated the effect of activating flux on CO_2 laser welding process of 1.8 mm thick 6013 aluminum alloy. The result showed that oxide activating flux assisted in improving the absorption of CO_2 laser energy as compared to fluoride activating flux. However, slag detachability was affirmed to be poor and caused bad weld appearance [167].

It has been reported that high reflectivity of aluminum alloys are not affected by grounding or polishing of the surfaces of aluminum alloy; laser radiation demonstrates higher reflectivity under these conditions. As a result, different superficial treatments have been examined on aluminum alloys to improve laser radiation absorption during high power diode welding of 5083 aluminum alloy sheets. It was revealed that superficial treatments with the incorporation of black marker layer caused higher radiation absorption in 5083 alloy and larger values of weld penetration depth and width ensued [11].

8 Mechanical properties and corrosion behavior

Mechanical properties of aluminum alloys such as tensile strength and ductility, fatigue and hardness can be impaired by weld porosity, surface appearance of work piece and other factors like the type of welding mechanism, etc. [48]. Also, loss of strengthening alloys such as magnesium during laser welding of aluminum alloys invariably degrades mechanical properties of joints [131, 149]. As a matter of fact, the presence of weld defects or imperfections and loss of strengthening precipitates (solid solution or precipitation hardening phases) in laser welded aluminum alloy are some of the principal means through which mechanical quality of welds are being impaired [131].

8.1 Tensile strength

Some of the reported tensile properties of laser welded aluminum alloys in literature are highlighted in Table 10. The application of filler metals, the choice of laser welding method and porosity levels in welds affect the tensile strength of laser welded aluminum joints. Improved tensile strength and hardness of laser welded 5A90 aluminum-lithium alloy sheets have been attributed to fine microstructure of the weld metal or fusion zone and narrow heat affected zone [91]. Also, most reports have shown that tensile strength of pure laser welding method reduces weld strength. However, the use of appropriate filler metal in laser welding of aluminum has greatly improved weld strengths. Likewise, the strength of laser welded aluminum alloys is considered to be better when compared to other traditional fusion welding methods. Zhao et al. [165] compared laser-arc double-sided welding of a 6-mm-thick 5A06 aluminum alloy with that of double-sided arc welding. It was observed that the strength of laser-arc double-sided welded alloy was about 91.7 % of the base metal as compared to 82.3 % of the double-sided arc welding [165].

Also, decrease in ambient pressure influences the tensile strength of laser welded aluminum alloys. In fact, up to 87.7 % joint efficiency has been reported and attributed to the contribution of sub-atmospheric pressure effect. Cai et al. [9] affirmed that the tensile strength of 10-mm-thick 5083 aluminum alloy increased up to 300.2 MPa at a critical ambient pressure of 10^1 Pa compared to that of atmospheric pressure (254.4 MPa). However, beyond the critical ambient pressure, the resultant weld strength was reported to remain the same [9].

Likewise, the fabricated joint of 2219-T87 aluminum alloy sheets with 2325 wire showed the presence of θ-Al_2Cu precipitates in the microstructure of the weld. These precipitates were few and coarser; consequently, it affected the tensile

Table 10 Some tensile properties of laser welded aluminum alloys

Type of laser	Alloy (filler metal)	Joint	UTS	Comment	Ref
Laser-arc double-sided welding	5A06	–	91.7 % of BM	Due to finer grain size of the FZ	[165]
CO_2 laser	5083	Butt	Lesser than 70 % of BM	Due to high Porosity level	[155]
CO_2 laser	5083	Butt	More than 90 % of BM	Due to less than 3 % porosity level	[155]
Fiber laser	2A97-T4	Butt	83.4 % of BM	loss of precipitation hardened structure weakens UTS	[131]
Hybrid fiber laser + pulse MIG	2219–T87 (5087 & 2325)	Butt	UTS of joints produced with 5087 was 20 % higher than 2325	Due to formation of large amount of S–Al_2CuMg precipitates in 5087 & pinning effect of precipitates	[141]
Nd:YAG laser	5083		85.7 % of BM under ambient pressure	Due to plasma plume suppression and reduced porosity	[9]
Hybrid CO_2 laser + MIG welding	2A12 (4043)		69 % of BM	Presence of Si and Cu at the dendritic boundaries	[143]
Hybrid CO_2 laser + MIG welding	2A12 (2319)	–	78 % of BM	Only Cu was concentrated at the dendritic boundaries	[143]

UTS ultimate tensile strength, *BM* base metal, *FZ* fusion zone

strength of the weld [141]. Jun Yan et al. [143] utilized 5 kW CO_2 laser-MIG hybrid approach in welding 8-mm-thick 2A12 aluminum alloy using welding wires of 4043 and 2319, respectively. It was revealed that joint efficiency of 2319 and 4043 wires reached 78 % (316 MPa) and 69 % (280 MPa) of the base metal [143]. Zhang et al. [141] examined the strength improving the mechanism of laser-arc hybrid (laser-MIG) welding of 6-mm-thick 2219-T87 aluminum alloy using 5087 wire. The presence of fine S–Al_2CuMg precipitates in the weld metal and pinning effect of precipitates on dislocations strengthened the resultant welds. In fact, the collision of adjacent dendrites during the solidification process of laser-MIG hybrid welding of 2219-T87 alloy with 5087 wire induced dislocations in the joints. As a result, the interaction of moving dislocations and precipitates caused pinning effect of precipitates on the dislocation. This attribute was reported to also improve the tensile strength of the welds [141].

The influence of heat treatment on tensile stress or strength and ductility of laser welded aluminum alloys was investigated by Rafael Humberto Mota de Siqueira et al. [159]. About 1.5 kW average powered fiber laser was employed in welding 1.6-mm-thick 6013 aluminum alloy sheets in T-joint configuration. The result of their hoop tensile strength revealed an increase in tensile strength (76 MPa) and a decrease of about 4 % in strain when post weld heat treatment was performed at 190 °C for 4 h. However, at 205 °C for 2 h, the strain decrease by 5 % and there was an increase in strength as well. Conversely, the result of T-pull tensile tests was not affected or influenced by post weld heat treatment [159].

Cicala et al. [173] examined the influence of operational laser parameters on the tensile strength of 6xxx series alloy by using continuous wave Nd:YAG laser. The authors reported that welding speed, wire parameters like wire feed rate and position, and fastening system had great influences on the tensile strength of the fabricated welds. However, low welding speeds and uniform compression fastening system are recommenced in order to obtain optimum weld strength [173]. Also, the influence of laser heat input on tensile strength is revealed in Fig. 16b while Fig. 16a shows the effect of varying laser power on engineering stress–strain properties of 2A97 aluminum joints.

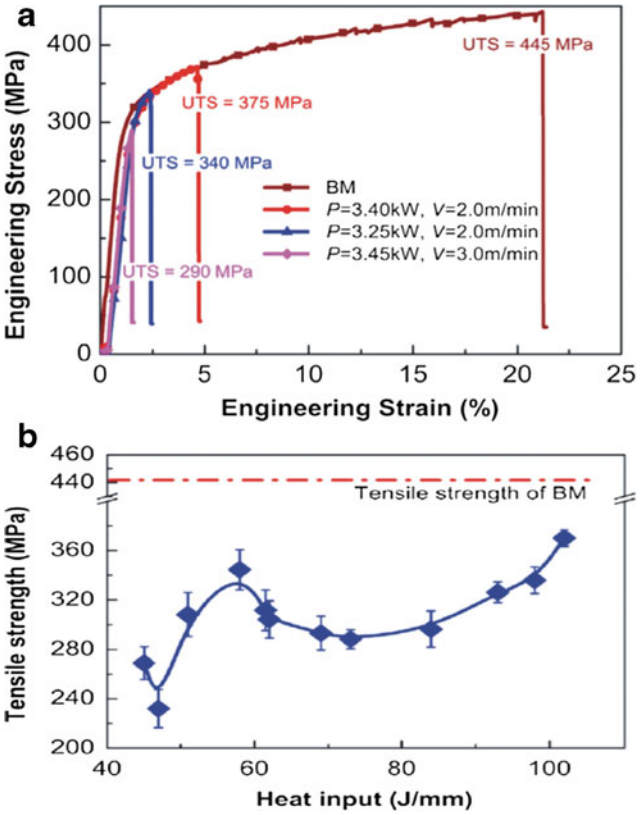

Fig. 16 Welding parameters influences on laser welded 2A97 alloy **a** stress–strain curve; **b** tensile strength-heat input curve [131]

8.2 Hardness

Microstructural changes and the formation of precipitates in laser welded aluminum alloys greatly influence the hardness values of aluminum alloys' weld metal [81]. Table 11 shows some of the hardness properties of laser welded aluminum alloys that are available in literature. For instance, a gradual increase in hardness profile was observed in dual beam Nd:YAG laser welded 5754 and 5182 aluminum alloys. The hardness values increased from the base metal of the alloys through the heat affected zone to a maximum value in the weld metal adjacent the fusion boundary. This hardness measurement increase was attributed to the presence of precipitates such as Mg_2Al_3 or metastable Mg_2Al_3 in heat affected zone and the weld zone [27].

Meanwhile, magnesium element plays a dominant role in strengthening. The results of laser welding of 5182 and 5754 aluminum alloys revealed that the hardness values of the weld metal and the base metal of 5182 alloy were higher than that of 5754. This was attributed to higher magnesium content in 5182 alloy [27]. Loss of magnesium element from the weld metal produces an equivalent drop in hardness value and a reduced solid solution strengthening in aluminum-magnesium alloy [27].

The application of high power diode laser in welding 5083 aluminum alloy sheets showed no evidence of heat affected zone between the weld bead and the base metal. It was reported that hardness measurements of the weld beads were slightly higher than those of the base metal. This major increase in weld bead's hardness values was attributed to microstructural changes provoked by laser heat treatment and refinement of grain structure [11]. Also, Sanchez-Amaya et al. [160] accessed micro hardness measurements of high power diode laser welded 3-mm-thick 5083 and 4-mm-thick 6082 aluminum alloy sheets. It was reported that the micro hardness values of the alloys' fusion zones were slightly higher by values between 5 and 10 HV, than those of their respective

Table 11 Some hardness properties of laser welded aluminum alloys

Type of laser	Alloy (filler metal)	Joint	Hardness	Comment	Ref
Dual beam Nd:YAG	1100-O, 5754-O, 5182-O	–	presence of Mg_2Al_3 precipitates in the HAZ increases hardness in 5754 and 5182	Good welds were produced when the lead/lag laser beam power ratio ≥ 1	[27]
High power diode laser	5083	Bead on plate	Micro hardness value of FZ is slightly higher than that of BM	Refinement of microstructure in FZ	[11]
Nd:YAG laser + MIG hybrid welding	1A08 (4043)		Micro hardness value in FZ is higher than that of HAZ and BM	Due to the presence of brittleness phase (Mg_2Si) in FZ	[146]
Hybrid Nd:YAG Laser-GMA welding	7075-T6 (2319)	Butt	Micro hardness value of the FZ is about 70 % of BM	due to redistribution or segregation of alloying elements	[163]
Nd:YAG laser	5A90	–	Micro hardness value of FZ was lesser than that of BM	Due to decrease in the quantity of precipitate in the FZ	[156]
CO_2 laser	5083	Butt	Micro hardness value of the FZ is higher than BM.	Due to fine solidification structure caused by steeper temperature gradient	[155]
Hybrid fiber laser + pulse MIG	2219–T87 (5087 & 2325)	Butt	5087 produces (81 HV) higher hardness than 2325 (63 HV)	Due to formation of large amount of S–Al_2CuMg precipitates in 5087	[141]

HAZ heat affected zone, *FZ* fusion zone, *BM* base metal

base metals. This micro hardness variation was attributed to microstructural changes within the welds. In the same manner, He et al. [146] examined the hardness profile of Nd:YAG laser-MIG hybrid welded 2-mm-thick 1A08 aluminum alloy using a Vickers indenter with a load of 0.98 N, dwell time of 15 s and spacing of 0.25 mm. It was revealed that micro-hardness value in the fusion zone was higher than that of the heat affected zone and the base metal due to the presence brittleness phase (Mg_2Si) of high hardness [146].

However, in the Nd:YAG laser-GMA hybrid welding of 7075-T6, dendritic structure was formed in the fusion zone of the weld and this resulted in the segregation of alloying elements. As a result, the hardness values of the fusion zone were greatly impaired [163]. Cui et al. [156] examined the influence of Nd:YAG laser welding on the hardness profile of 3-mm-thick 5A90-T8 aluminum alloy. Lower micro-hardness values were obtained in the fusion zone as compared to that of the base metal. This was attributed to the decrease in the amount of strengthening precipitates in the fusion zone [156]. Typical hardness characterizations performed on Nd:YAG laser-GMA welded 7075-T6 alloy are shown in Fig. 17.

8.3 Fatigue

Metallurgical defects such as microstructural flaws significantly influence initiation and propagation of fatigue cracks or fatigue failure. Laser welded aluminum alloys having micropores are at risk of rapid failure during cyclic or monotonic loading conditions [150]. Porosity is easily induced in laser welding of aluminum alloys and pores are stress concentration sites which aid crack initiation and propagation. Therefore, it

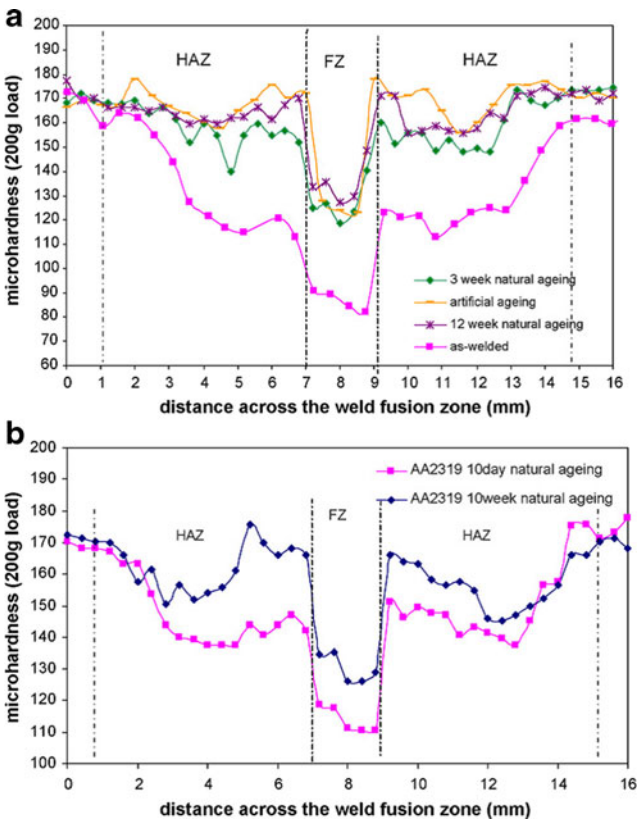

Fig. 17 Nd:YAG laser-GMA welded 7075-T6 alloy **a** produced with 5754 filler wire at 80 mm/s **b** produced with 2319 filler wire at 60 mm/s [163]

is of high importance to determine the correlation between fatigue damage and induced weld pores in welded aluminum alloys. Some authors reported that porosities in welded aluminum alloys such as 7075-T6 greatly influenced fatigue crack initiation and propagation. Under fatigue cyclic loading conditions, it was observed that weld micropores grew until they were distorted and in due course, resulted in fatigue cracks [150]. Eibl et al. [166] revealed that the cyclic properties of 6005A-T6, 361-T6, and 5083 aluminum alloys were governed by porosity. As a matter of fact, fatigue strength was restrained to about one half of that of the base metal due to the presence of weld micropores [166].

The available number, size, and morphology of pores [150] present in laser welded aluminum alloy sheets have been reported to greatly impair fatigue resistance. Also, fatigue failure or crack initiation may commence from the surface pores or pores within the resultant aluminum weld metal [150]. In fact, it has been reported that interaction occurs between fatigue cracks and pores during cyclic loading; and in some instances, this interaction can lower fatigue crack growth rate. Likewise, when there is fatigue crack advancement into adjacent pores, fatigue crack growth may be hindered due to notch blunting effect [150]. Some of the available fatigue properties of laser beam welded aluminum alloys are summarized in Table 12.

Also, Wu et al. [150] examined porosity-induced fatigue damage on fiber laser-pulsed GMA welded 2-mm-thick 7075-T6 aluminum alloy joints using a high resolution synchrotron radiation X-ray microtomography. The authors investigated the spatial distribution and growth behavior of pores [150]. Irregularities in the size and location of pores or micropores in the hybrid welds were observed. It was concluded that the largest micropore was generally not responsible (not the preferential site) for fatigue crack initiation. However, fatigue cracks were prone to be initiated and propagated into pores with effective diameters within the range of 10 to 100 μm [150]. Secondly, fatigue crack initiation sites were frequently observed to commence from pores situated near the surface of the weld while the interior pores were regarded to be relatively safe [150]. The general morphology of fatigue cracks was observed to be non-planar and nonlinear due to the complex microstructural interactions between weld pores, primary, and secondary cracks (or fatigue cracks) respectively [150].

Liu and co-authors investigated the fatigue crack growth behavior of Nd:YAG laser welded 3.6-mm-thick 6156-T4 aluminum alloy plates using a welding wire of 4047 Al-Si alloy. It was revealed that the base metal of the aforementioned alloy demonstrated superior fatigue resistance compared to its weld metal (lowest crack growth resistance) and heat affected zone. However, this variation in fatigue crack resistance was attributed to microstructural changes, dissolution of second phase particle, and grain boundary liquation in the fusion line [162].

The fatigue analysis of fiber laser welded 6013 aluminum alloy sheets in T-joint configuration revealed that the number of cycles to failure for the tested welds reduced. Equally, post weld heat treatment did not affect the fatigue properties of the alloy when subjected to 190 °C thermal treatment for 4 h and equally, at 205 °C for 2 h, respectively [159]. He et al. [146] investigated the fatigue behavior of Nd:YAG laser-MIG hybrid welded 2-mm-thick 1A08 aluminum alloy plates using a stress ratio of 0.1 and frequency of 50 Hz. It was revealed that the accumulated plastic strain or deformation continuously increased in the heat affected zone of the alloy during cyclic loading. However, no plastic deformation was observed in the fusion and base metal of the alloy [146].

8.4 Corrosion

Corrosion behavior of laser beam welded aluminum alloys is summarized in Table 13 while images of corroded laser welded 6061 alloy are shown in Fig. 18. High power diode laser welding of 5083 aluminum alloys with superficial surface treatments showed clear improvement in corrosion behavior due to microstructural refinement. The corrosion behavior of the weld zones was investigated by means of electrochemical techniques. Among the three superficial treatments (black marker layer coated samples, chemical treatment with black marker layer samples, and corindon blasted

Table 12 Some fatigue properties of laser beam welded aluminum alloys

Type of laser	Alloy (filler metal)	Test conditions	Fatigue cracks	General comments	Ref
Hybrid fiber laser + pulsed GMA welding	7075-T6 (ER5356)	$R = 0.1$; f = 10Hz	Complex non-planar and non-linear morphological characteristics	Interaction of gas pores with other pores influenced the fatigue crack mode	[150]
CO_2 laser	6005A-T6; 5083; 361-T6	$R = 0$ & −0.1; f = 25–35 s^{-1}	–	Presence of pores reduced fatigue strength to about one half of base metal	[166]
Nd:YAG	6156-T4 (ER4047)	$R = -1$, 0.06 & 0.5; f = 10 Hz	Quasi-cleavage fracture with river pattern and plastic tearing	WM had the lowest fatigue resistance due to microstructural changes	[162]
Fiber laser	6013-T4 (4047)	$R = 0.1$; f = 20 Hz	Mixed mode of failure (dimples and cleavage)	Heat treatment had no influence on comparative fatigue behaviour	[159]
Nd:YAG laser + MIG welding	1A80 (4043)	$R = 0.1$	Initiation and propagation of fatigue crack along slip bands in the HAZ	At lower cyclic loading, fatigue crack was controlled by the size of gas pore	[146]

Table 13 Summary of corrosion behaviors of laser beam welded aluminum alloys

Type of laser	Alloy (filler metal)	Joint type	Corrosion test		Weld bead	Base metal	Comment	Ref
High power diode laser	5083	Bead on plate	Polarisation or electrochemical tests		Cathode behaviour	Anode behaviour	Corrosion improvement of the weld bead is as a result of microstructural refinement during laser treatment	[11]
Nd:YAG + GMA hybrid	6061 (4043)	–	Weight loss corrosion test & electrochemical measurement		Severe pitting corrosion of the fusion zone	–	Increased precipitation phase enhanced corrosion in the weld metal	[145]
Nd:YAG laser	6061 (4043)	Bead on plate	Galvanic potential measurement and potentiodynamic polarization measurement		The most cathodic region	The most anodic region	Porous nature of the surface film layer and build up of intermetallic phases increased galvanic corrosion	[122]

samples), corindon blasted samples demonstrated the best corrosion behavior on (bead on plate) welds. This behavior was attributed to the effect of blasting superficial surface treatment on magnesium evaporation; blasting process was reported to minimize magnesium evaporation [11].

In the Nd:YAG laser-GMA hybrid welding of 2-mm-thick 6061-T6 alloy with 4043 filler metal, galvanic corrosion of the weld fusion zone was reported; this was attributed to increase precipitate phase in the zone. As a result, aggravation of pitting and cracking (severe pitting and cracks) occurred in the weld fusion zone of the alloy [145]. Also, in the works of Mujibur Rahman and co-authors, Nd:YAG laser welded 6061 aluminum alloy sheets with 4043 filler metal demonstrated galvanic corrosion in the weld fusion zone. This was attributed to either increase in intermetallic phases in the surface layer or significant increase in the surface area of the weld fusion zone. Also, it was reported that a local increase in pH of the weld fusion zone as a result of cathodic process of the zone caused the dissolution of the surface film or layer; conversely, loss of aluminum to solution and an increase of intermetallic phases occurred [122]. Typical corrosion potential changes across the weld zones of laser welded 6061 aluminum alloy are shown in Fig. 19. It reveals that the most cathodic region is the weld fusion zone while the base metal is the most anodic region.

9 Outlook

The ultimate goal of welding is to obtain high quality welds capable of meeting expected performance or service conditions. Therefore, a full understanding of laser welding phenomena during the welding process and solidification stage will influence defect control and improvement of weld quality in laser welding of aluminum alloys. As a rapid and complex process, laser welding process causes intermittent or continuous melting of aluminum base metal, generates fluid flow behavior or dynamics, originates atomic or ionic distribution of gases and metals, induces the formation of plasma or plume (interaction of laser beam with metal vapor), and establishes heat transfer through mechanisms or modes like conduction. The characterization of laser welding phenomena in literature has majorly been on pure or single-beam laser welding and with a few observatories or numerical modeling and simulation on hybridized laser welding. Limited resources on aluminum laser welding phenomena of tailored heat source-laser welding technologies such as double-pulse laser welding, double-sided laser beam welding, and dual-beam Nd:YAG laser are available in literature. Also, limited number of literatures is available on other innovative technologies like the integration of electromagnetic field into laser welding of aluminum alloys.

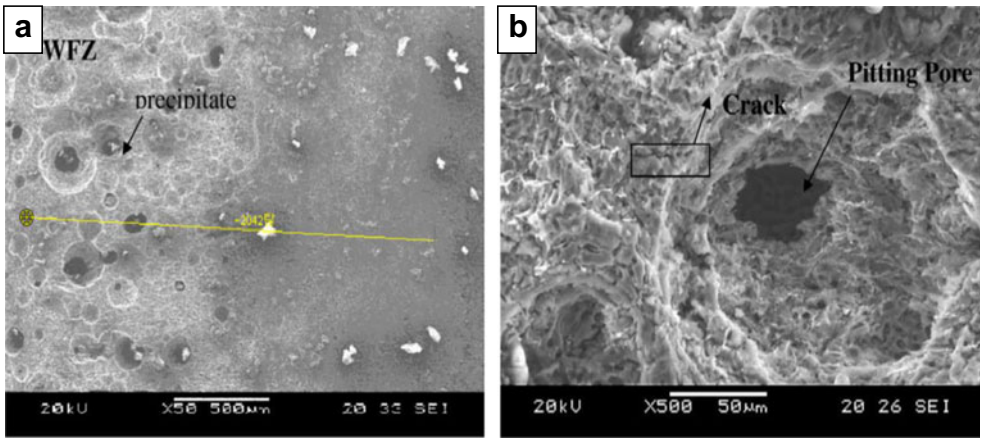

Fig. 18 SEM Images of corroded Nd:YAG laser-GMA welded joints of 6061 alloy **a** corroded weld surface; **b** pit in fusion zone [145]

Likewise, information on precise identification of the type and location of interior or inner weld defects during aluminum laser welding is still insufficient in literature. At present, defects on weld seams are predominantly examined with off-line investigational measure; this will eventually add up to manufacturing cost. An alternative means known as on-line or real-time monitoring of welds can help in locating and classifying of defects during laser welding process of aluminum alloys and it will consequently reduce manufacturing cost. Together with this, on-the-job information about molten pool, keyhole and metallic vapor can also be obtained from real time monitoring of laser welding of aluminum alloys. You et al. [1] reported that non-contacting optical sensing such as photodiode sensor has been proposed to be an ideal real time monitoring technology for laser welding process, owning to its low cost, simple structure, rich information on high frequency features, and industrial manufacturing adaptability [1]. Though, in situ X-ray transmission technique and other high-speed powerful imaging techniques are available but few aluminum laser welded joints have been investigated with these technologies.

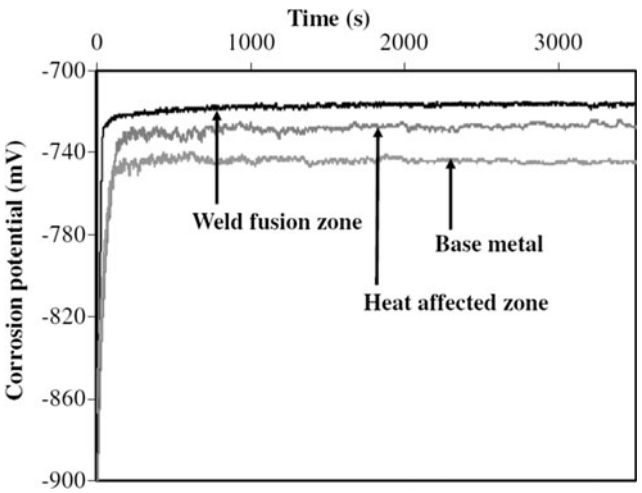

Fig. 19 Corrosion potential plots of fusion zone, base metal and heat affected zone of Nd:YAG laser welded 6061 alloy [122]

As an evolving technology, laser beam welded aluminum alloys need full mechanical, microstructural, and corrosion characterizations, in order to avoid catastrophic failure of aluminum weldment when placed in service. Currently, a host of articles is available on microstructure, tensile, and hardness properties of laser welded aluminum alloys. However, there are important aspects that are still insufficient in literature; areas such as fatigue behavior, fracture toughness, and corrosion sensitivity of laser welded aluminum joints are limited in literature. Other areas like characterization of stress intensity factor of laser welded aluminum joints, interaction between weld defects like porosity and microstructural cracks or local crack inducing mechanism in laser welded aluminum joints are research areas that need further assessments.

10 Summary

The advancement in laser beam welding technology has evolved to be considerably suitable for virtually all materials including thin metal sheets of aluminum alloys, copper, magnesium, and stainless steels such as duplex and super duplex steels [174, 175]. With weight saving and performance enhancement focus, aluminum-based manufacturing has become one of the most logical and efficient approaches for weight reduction in the industries; it is at the summit of weight reduction measures. Diverse industries such as automotive, aviation and aerospace, shipbuilding, and high speed train manufacturing are seeking aluminum alloys for weight reduction of their products, in order to enjoy better performance and fuel efficiency or to meet compelling government regulations on carbon footprint. On the other hand, industrial justifications for the use of laser welding technology in welding aluminum alloys are enormous and these rationalizations have strongly impelled advancement or innovative development in aluminum laser welding. As a result, the fundamental concerns with the application of laser welding technology on aluminum alloys are progressively being cut back. The progressions in

laser beam welding of aluminum alloys have shown remarkable achievements such as mitigation of porosity, inhibition of solidification cracking, and improvement of laser energy efficiency (better coupling). Consequently, this report covers the present state-of-the-art and achievements of laser welding technology of aluminum alloys and it logically classifies the available aluminum laser technologies based on the number and type of heat source/input as pure or single-beam laser welding, laser-arc hybrid welding, tailored heat-source laser welding and other innovative laser welding technologies, respectively. Reviews of mechanical properties, microstructural behavior and corrosion sensitivity of laser welded aluminum alloys are also carefully scrutinized. The appraisal of literature shows some research areas that have not been fully expounded in the application of laser welding technology on aluminum alloys; these areas are reported under this article's outlook.

Acknowledgments Authors would like to acknowledge Prof. Dr. Erdinc Kaluc for valuable discussions and cooperation.

Appendix

Table 14 Chemical composition of laser welded non-heat treatable Al alloys

Alloy	Si	Fe	Cu	Mn	Mg	Zn	Cr	Ni	V	Ti	Pb	Ga	Others	Al	Ref
1A80	0.15	0.15	0.03	0.02	0.02	–	–	–	–	0.03	–	–	–	Bal	[146]
1100	0.13	0.53	0.079	0.016	0.008	–	–	–	–	–	–	–	–	99.2	[27]
5083	0.155	0.295	0.068	0.471	4.85	0.074	0.135	–	–	0.022	–	–	–	93.88	[11]
5182-O	**	**	**	**	4.5	**	**	**	**	**	**	**	**	**	[28]
5052	**	**	**	**	**	**	**	**	**	**	**	**	**	**	[26]
5182	0.065	0.2	–	0.34	4.65	–	–	–	–	–	–	–	–	Bal	[20]
5083-O	0.082	0.167	0.019	0.631	4.472	0.037	0.121	0.022	–	0.017	–	–	–	Bal	[48]
5A06	0.4	0.4	0.1	0.5–0.8	5.8–6.8	0.2	–	–	–	0.02–0.10		–	–	Bal.	[119]
5754-O	**	**	**	**	**	**	**	**	**	**	**	**	**	**	[16]
5083-O	0.5	–	0.1	0.5	4.5	–	–	–	–	0.15	–	–	–	Bal	[124]
5005	**	**	**	**	**	**	**	**	**	**	**	**	**	**	[144]
5083	0.4	0.4	0.1	0.40–1.0	4.0–4.9	0.25	0.05–0.25		–	0.15	–	–	0.15	Bal	[40]
5052	**	**	**	**	**	**	**	**	**	**	**	**	**	**	[148]
5A06	<0.4	<0.4	–	0.5–0.8	6.0–6.8	–	–	–	–	–	–	–	–	Bal	[149]
5754	**	**	**	**	**	**	**	**	**	**	**	**	**	**	[49]
5083-O	0.08	0.19	0.05	0.63	4.6	–	0.1	–	–	–	–	–	–	Bal	[109]
5083	**	**	**	**	**	**	**	**	**	**	**	**	**	**	[154]
5083	**	**	**	**	**	**	**	**	**	**	**	**	**	**	[155]
5A90-T8	**	**	**	**	**	**	**	**	**	**	**	**	**	**	[156]
5083	0.4	0.4	0.1	0.4	4.1	0.25	–	–	–	0.15	–	–	0.2	Bal	[9]
5083	**	**	**	**	**	**	**	**	**	**	**	**	**	**	[6]
5A90	**	**	**	**	**	**	**	**	**	**	**	**	**	**	[91]
5182	0.2	–	–	0	4.44	–	–	–	–	–	–	–	–	Bal	[157]
5754	0	–	–	9.45	2.82	0.02	–	–	–	–	–	–		Bal	[157]
5182	0.08		0.11	0.26	4.9	–	–	–	–	0.01	–	–	–	Bal	[95]
5182	0.065	0.2	0.04	0.34	4.65	–	–	–	–	–	–	–	–	94.66	[27]
5754	0.083	0.18	0.016	0.25	3.19	–	–	–	–	–	–	–	–	96.25	[27]
5083	**	**	**	**	**	**	**	**	**	**	**	**	**	**	[164]
5A06	0.4	0.4	0.1	0.5–0.8	5.8–6.8	0.2	–	–	–	0.02–0.10		–	–	Bal	[165]
5083	0.4	0.4	0.1	0.7	4.45	0.25	0.15	–	–	0.25	–	–	–	Bal	[166]
5083-T0	0.1	0.3	0.02	0.5	4.22	–	0.08	–	0.01	0.02	0.01	0.01	–	94.73	[160]

**Data not specified by the author; − indicates nil

Table 15 Chemical composition of laser welded heat treatable Al alloys

Alloy	Si	Fe	Cu	Mn	Mg	Zn	Ag	Zr	Li	Cr	Ni	V	Ti	Pb	Ga	Others	Al	Ref
2195	**	**	**	**	**	**	**	**	**	**	**	**	**	**	**	**	**	[69]
2139-T3	0.04	0.06	5.07	0.29	0.43	–	0.33	0.014	–	–	–	–	510 (ppm)	–	–	–	Bal	[66]
2A12	0.5	0.5	3.8–4.9	0.3–0.9	1.2–1.8	0.25	–	–	–	–	–	–	0.15	–	–	–	Bal	[143]
2219	0.05	0.1	5.95	0.27	–	–	–	0.1	–	–	–	0.09	0.06	–	–	–	Bal	[72]
2A97-T4	–	0.12	3.9	0.3	0.42	0.44	0.24	0.15	1.4								Bal	[131]
2024-O	0.16	–	4.52	0.61	1.4	0.08	–	–	–	–	–	–	0.05	–	–	–	Bal	[158]
2024-T4	0.16	–	4.52	0.61	1.4	0.08	–	–	–	–	–	–	0.05	–	–	–	Bal	[12]
2090	–	–	1.41	0.26	2.87	–	–	0.1	1.53	–	–	–	–	–	–	–	Bal	[13]
2024	**	**	**	**	**	**	**	**	**	**	**	**	**	**	**	**	**	[7]
2219-T87	0.05	0.1	6.5	0.32	0.02	0.04	–	0.11	–	–	–	–	0.04	–	–	–	Bal	[141]
2024-T4	**	**	**	**	**	**	**	**	**	**	**	**	**	**	**	**	**	[123]
2024-T3	**	**	**	**	**	**	**	**	**	**	**	**	**	**	**	**	**	[18]
6063-T5	**	**	**	**	**	**	**	**	**	**	**	**	**	**	**	**	**	[22]
6 N01-T6	0.615	0.189	0.277	0.022	1.021	0.034	–	–	–	0.259	–	–	0.022	–	–	–	Bal	[48]
6061	0.4–0.8	0.7	0.15–0.4	–	0.8–1.2	–	–	–	–	0.04–0.35		–	–	–	–	0.7	95.85–97.21	[122]
6 K21-T4	1	0.16	0.01	0.07	0.55	0.01	–	–	–	0.02	–	–	0.01	–	–	–	Bal	[38]
6061-T6	0.4–0.8	0.7	0.15–0.40	0.15	0.8–1.2	0.25	–	–	–	0.04–0.35	–	–	–	–	–	–	Bal	[145]
6082	**	**	**	**	**	**	**	**	**	**	**	**	**	**	**	**	**	[140]
6082	**	**	**	**	**	**	**	**	**	**	**	**	**	**	**	**	**	[46]
6060-T6	**	**	**	**	**	**	**	**	**	**	**	**	**	**	**	**	**	[4]
6013-T6	0.6–1.0	≤0.5	0.6–1.1	0.2–0.8	0.8–1.2	≤0.25	–	–	–	<0.1	–	–	–	–	–	–	Bal	[129]
6013-T4	0.62 ± 0.02	0.20 ± 0.01	0.82 ± 0.02	0.27 ± 0.04	0.94 ± 0.05	–	–	–	–	–	–	–	–	–	–	0.06 ± 0.01	Bal	[130]
6013	0.62 ± 0.02	0.20 ± 0.01	0.82 ± 0.02	0.27 ± 0.04	0.94 ± 0.05	–	–	–	–	–	–	–	–	–	–	0.06 ± 0.01	Bal	[159]
6082-T6	1.03	0.34	0.06	0.57	0.87	0.01	–	–	–	0.01	–	–	0.03	0.01	0.01	–	97.04	[160]
6056-T4	0.87	0.07	0.67	0.62	0.71	0.18	–	–	–	–	–	–	–	–	–	–	Bal	[161]
6156-T4	0.7	0.084	1.04	0.43	0.82	0.15	–	–	–	<0.05	–	–	–	–	–	–	Bal	[162]
6005 A-T6	0.7	0.35	0.3	0.5	0.55	0.2	–	–	–	0.3	–	–	0.1	–	–	–	Bal	[166]
6013	**	**	**	**	**	**	**	**	**	**	**	**	**	**	**	**	**	[167]
6005-T5	**	**	**	**	**	**	**	**	**	**	**	**	**	**	**	**	**	[168]
6082-T6	**	**	**	**	**	**	**	**	**	**	**	**	**	**	**	**	**	[168]
6082-T6	0.7–1.3	max0.5	Max 0.1	0.4–1	0.6–1.2	Max0.2	–	–	–	Max0.25	–	–	Max0.1	–	–	–	Bal	[5]
6056-T4	1	–	0.8	0.6	0.9	0.4	–	–	–	–	–	–	–	–	–	–	Bal	[133]
6156-T6	1	–	0.9	0.6	0.9	–	–	–	–	–	–	–	–	–	–	–	Bal	[133]
6056-T4	1	–	0.8	0.6	0.9	0.4	–	–	–	–	–	–	–	–	–	–	Bal	[151]
6156-T6	1	–	0.9	0.6	0.9	–	–	–	–	–	–	–	–	–	–	–	Bal	[151]

Table 15 (continued)

Alloy	Si	Fe	Cu	Mn	Mg	Zn	Ag	Zr	Li	Cr	Ni	V	Ti	Pb	Ga	Others	Al	Ref
7xxx-T4	0.1	0.11	0.61	0.15	3.07	10.05		0.1		0.15	–	–	0.02	–	–	–	Bal	[66]
7075-T6	0.4	0.5	1.2–2.0	–	2.1–2.9	5.1–6.1	–	–	–	–	–	–	–	–	–	–	Bal	[163]
7 N01-T6	0.032	0.084	1.608	0.004	2.667	5.414	–	–	–	0.246	–	–	0.02	–	–	–	Bal	[48]
7075-T651	0.07	0.17	1.59	0.05	2.44	5.76	–	–	–	0.18	0.01		0.02	–	–	–	Bal	[147]
7075-T6	**	**	**	**	**	**	**	**	**	**	**	**	**	**	**	**	**	[18]
7075-T6	–	–	1.3	–	2.43	5.54	–	–	–	–	–	–	–	–	–	–	Bal	[150]

**Data not specified by the author; − indicates nil

Table 16 Chemical composition of laser welded cast Al alloys

Alloy	Si	Fe	Cu	Mn	Mg	Zn	Cr	Ni	V	Ti	Pb	Ga	Others	Al	Ref
356-T6	7	–	0.25	0.35	0.3	–	–	–	–	0.25	–	–	–	Bal	[124]
361-T6	9.62	0.26	0.07	0.13	0.28	0.06	–	–	–	0.11	–	–	–	Bal	[166]

– indicates nil

Table 17 Chemical composition of filler metals used in laser welding of Al alloys

Alloy	Si	Fe	Cu	Mn	Mg	Cr	Zn	Zr	Be	V	Ti	Others	Al	Ref
2319	0.04	0.1	6.1	0.29	–	–	–	0.15		0.1	0.15	–	Bal	[72]
2319	0.2	0.3	5.8–6.8	0.2–0.4	0.02	–	0.1	–	–	–	0.2	–	Bal	[143]
2319	**	**	**	**	**	**	**	**	**	**	**	**	**	[163]
2319	**	**	**	**	**	**	**	**	**	**	**	**	**	[7]
2325	0.2	0.3	6.8	0.2	0.02		0.1	0.1			0.1		Bal	[141]
4043	**	**	**	**	**	**	**	**	**	**	**	**	**	[22]
4043	4.5–6.0	0.8	0.3	–	0.1	–	–	–	–	–	–	0.5	93.80–92.30	[122]
4043	4.5–6.0	0.8	0.3	0.05	0.05	–	0.1	–	–	–	0.2	–	Bal	[143]
4043	4.5–6.0	0.8	0.3	0.05	0.05	–	0.1	–	–	–	0.2	–	Bal	[145]
4043	4.8	0.08	0.3	0.05	0.05	–	0.1	–	–	–	0.2	–	Bal	[146]
4043	5	0.8	0.3	0.05	0.05	–	0.1	–	–	–	0.2	–	Bal	[147]
4047	**	**	**	**	**	**	**	**	**	**	**	**	**	[161]
4047	**	**	**	**	**	**	**	**	**	**	**	**	**	[123]
4047	12	0.8	0.3	0.15	0.1	–	0.2	–	–	–	–	–	Bal	[66]
4047	11.52	0.2	<0.001	0.01	0.01	–	0.001	–	–	–	–	–	Bal	[162]
4047	11.52	0.2	<0.01	0.01	0.01	–	0.001	–	–	–	–	–	Bal	[133]
4047	11.52	0.2	<0.01	0.01	0.01	–	0.001	–	–	–	–	–	Bal	[151]
5087	0.04	0.14	0.01	0.75	4.76	–	0.01	0.11	–	–	0.08	–	Bal	[141]
5356	**	**	**	**	**	**	**	**	**	**	**	**	**	[144]
5356	0.25	0.4	0.1	0.05–0.20	4.5–5.5	0.05–0.20	0.1	–	0.0008	–	0.06–0.20	0.15	Bal	[40]
5356	**	**	**	**	**	**	**	**	**	**	**	**	**	[38]
5356	**	**	**	**	**	**	**	**	**	**	**	**	**	[148]
5356	**	**	**	**	**	**	**	**	**	**	**	**	**	[150]
5356	–	–	–	0.1–0.5	4.5–5.5	<0.3	–	–	–	–	<0.15	–	Bal	[95]

**Data not specified by the author;

– indicates nil

References

1. You DY, Gao XD, Katayama S (2014) Review of laser welding monitoring. Sci Technol Weld Join 19(3):181–201. doi:10.1179/1362171813y.0000000180
2. Gene Mathers: The welding of aluminium and its alloys, Woodhead Publishing Limited (2002) ISBN 1 85573 567 9, Pg. 1–31, DOI: 10.1533/9781855737631
3. Ion JC (2000) Laser beam welding of wrought aluminum alloys. Sci Technol Weld Join 5(5):265–275. doi:10.1179/136217100101538308
4. Coniglio N, Patry M (2013) Measuring laser weldability of aluminum alloys using controlled restraint weldability test. Sci Technol Weld Join 18(7):573–580. doi:10.1179/1362171813y.0000000137
5. von Witzendorff P, Hermsdorf J, Kaierle S, Suttmann O, Overmeyer L (2015) Science and technology of welding and joining. Double pulse laser welding of 6082 aluminum alloys, 2015, Vol. 20, No. 1, pp. 42–47; doi: 10.1179/1362171814Y.0000000255
6. Matsunawa A (2001) Problems and solutions in deep penetration laser welding. Sci Technol Weld Join 6(6):351–354. doi:10.1179/stw.2001.6.6.351
7. Verhaeghe G and Hilton P (2004) Laser Welding of Low-Porosity Aerospace Aluminum Alloy, 34th International MATADOR Conference, 7th - 9th July 2004, UMIST, Manchester, UK, pp. 241 to 246; doi: 10.1007/978-1-4471-0647-0_36
8. Page CJ, Devermann T, Biffin J, Blundell N (2002) Plasma augmented laser welding and its applications. Sci Technol Weld Join 7(1):1–10. doi:10.1179/136217102225001313
9. Cai C, Peng GC, Li LQ, Chen YB, Qiao L (2014) Comparative study on laser welding characteristics of aluminum alloy under atmospheric and sub atmospheric pressures. Sci Technol Weld Join 19(7):547–553. doi:10.1179/1362171814y.0000000223
10. TWI: URL: http://www.twi-global.com/ accessed on 10th May, 2015
11. Sanchez-Amaya JM, Delgado T, De Damborenea JJ, Lopez V, Botana FJ (2009) Laser welding of AA 5083 samples by high power diode laser. Sci Technol Weld Join 14(1):78–86. doi:10.1179/136217108x347629
12. Sheikhi M, Malek Ghaini F, Torkamany MJ, Sabbaghzadeh J (2009) Characterization of solidification cracking in pulsed Nd:YAG laser welding of 2024 aluminum alloy. Sci Technol Weld Join 14(2):161–165. doi:10.1179/136217108x386554
13. Norman AF, Ducharme R, Mackwood A, Kapadia P, Prangnell PB (1998) Application of thermal modeling to laser beam welding of aluminum alloys. Sci Technol Weld Join 3(5):260–266. doi:10.1179/stw.1998.3.5.260
14. Moore PL, Howse DS, Wallach ER (2004) Microstructures and properties of laser/arc hybrid welds and autogenous laser welds in pipeline steels, 2004, Vol. 9, No. 4, pp. 314–322; DOI: 10.1179/136217104225021652

15. Long X, Khanna SK (2005) Residual stresses in spot welded new generation aluminum alloys Part B—finite element simulation of residual stresses in a spot weld in 5754 aluminum alloy. Sci Technol Weld Join 10(1):88–94. doi:10.1179/174329305x29483
16. Ramasamy S, Albright CE (2001) CO2 and Nd–YAG laser beam welding of 5754–O aluminum alloy for automotive applications, 2001, Vol. 6, No. 3, pp. 182–190 doi: 10.1179/136217101101538730
17. Rowe J (2012) Advanced materials in automotive engineering, Woodhead Publishing Limited, ISBN 978-1-84569-561-3 Pg. 6–14, doi: 10.1533/9780857095466
18. Hu B, Richardson IM (2006) Mechanism and possible solution for transverse solidification cracking in laser welding of high strength aluminum alloys. Mater Sci Eng A 429(2006):287–294. doi:10.1016/j.msea.2006.05.040
19. Babu SS, David SA, Vitek JM, Reed RW (2001) Solidification and microstructure modeling of welds in aluminum alloys 5754 and 611. Sci Technol Weld Join 6(1):31–40. doi:10.1179/136217101101538514
20. Deutsch MG, Punkari A, Weckman DC, Kerr HW (2003) Weldability of 1.6 mm thick aluminum alloy 5182 sheet by single and dual beam Nd:YAG laser welding. Sci Technol Weld Join 8(4):246–256. doi:10.1179/136217103225005499
21. Sudhakar I, Madhu V, Madhusudhan Reddy G, Srinivasa Rao K (2015) Enhancement of wear and ballistic resistance of armour grade AA7075 aluminium alloy using friction stir processing. Def Technol 11(1):10–17. doi:10.1016/j.dt.2014.08.003
22. Sekhar NC, Bjorneklett B (2002) Laser welding of complex aluminum structures. Sci Technol Weld Joining 7(1):19–25. doi:10.1179/136217102225002024
23. Haferkamp H, Bunte J, Herzog D, Ostendorf A (2004) Laser based welding of cellular aluminum. Sci Technol Weld Join 9(1):65–71. doi:10.1179/136217104225017170
24. AlShaer AW, Li L, Mistry A (2014) The effects of short pulse laser surface cleaning on porosity formation and reduction in laser welding of aluminum alloy for automotive component manufacture. Optics Laser Technol 64(2014):162–171. doi:10.1016/j.optlastec.2014.05.010
25. Cam G, Ventzke V, Dos Santos JF, Kocak M, Jennequin G, Gonthier-Maurin P (1999) Characterization of electron beam welded aluminum alloys. Sci Technol Weld Join 4(5):317–323. doi:10.1179/136217199101537941
26. Saida K, Song W, Nishimoto K (2005) Diode laser brazing of aluminum alloy to steels with aluminum filler metal. Sci Technol Weld Join 10(2):227–235. doi:10.1179/174329305x37060
27. Punkari A, Weckman DC, Kerr HW (2003) Effects of magnesium content on dual beam Nd:YAG laser welding of Al–Mg alloys. Sci Technol Weld Join 8(4):269–281. doi:10.1179/136217103225005516
28. Kwon Y, Weckman DC (2008) Double sided arc welding of AA5182 aluminum alloy sheet. Sci Technol Weld Join 13(6):485–495. doi:10.1179/174329308x271715
29. Olsen F O (2009) Hybrid laser–arc welding, Woodhead Publishing Limited, pg. 1–44, 216–260; ISBN 978-1-84569-370-1; doi: 10.1533/9781845696528
30. Katayama S (2013) Handbook of laser welding technologies, Woodhead Publishing Limited, pg. 3–120; ISBN 978-0-85709-264-9 doi: 10.1533/9780857098771
31. Kah P, Jibril A, Martikainen J, Suoranta R (2012) Process possibility of welding thin aluminum alloys. Int J Mech Mater Eng (IJMME) 7(3):232–242
32. Xiao R, Zhang X (2014) Problems and issues in laser beam welding of aluminum–lithium alloys. J Manuf Process 16(2014):166–175. doi:10.1016/j.jmapro.2013.10.005
33. Bentor Yinon: Periodic table of aluminum; URL: http://www.chemicalelements.com/elements/al.html accessed on 28th May, 2015
34. Udomphol T (2007) Aluminium and its alloys, Lecture 2 by Tapany Udomphol, Suranaree University of Technology
35. Cobden R, Banbury A: Aluminium: Physical Properties, Characteristics and Alloys, Training in aluminium application technologies (TALAT), Basic Level-Lecture 1501, prepared by Ron Cobden, Alcan, Banbury, pg. 1–60; URL: http://www.slideshare.net/corematerials/talat-lecture-1501-properties-characteristics-and-alloys-ofaluminium
36. Hatch J E (1984) Aluminium Properties and Physical Metallurgy edited by John E. Hatch, ASM International Pg. 1–57
37. Enz J, Riekehr S, Ventzke V, Kashaev N (2012) Influence of the local chemical composition on the mechanical properties of laser beam welded Al-Li alloys. Phys Procedia 39(2012):51–58. doi:10.1016/j.phpro.2012.10.013
38. Kim HR, Park YW, Lee KY (2008) Application of grey relational analysis to determine welding parameters for Nd:YAG laser GMA hybrid welding of aluminum alloy. Sci Technol Weld Join 13(4):312–317. doi:10.1179/174329307x249423
39. Vargel C: Corrosion of Aluminium translated by Dr. Martin P. Schmidt (2004) Elsevier Ltd, ISBN: 0 08 044495 4 Pg. 1–75, doi: 10.1016/b978-008044495-6/50007-0
40. Kim YP, Alam N, Bang HS, Bang HS (2006) Observation of hybrid (cw Nd:YAG laser + MIG) welding phenomenon in AA 5083 butt joints with different gap condition. Sci Technol Weld Join 11(3):295–307. doi:10.1179/174329306x107674
41. Kawahito Y, Katayama S (2006) In-process monitoring and adaptive control during pulsed yag laser spot welding of aluminum alloy thin sheets. JLMN-J Laser Micro/Nanoengineering 1(1):33–38. doi:10.2961/jlmn.2006.01.0007
42. De Bono P (2011) QCOALA- Quality Control of Aluminum Laser-welded Assemblies, PDB/gdp/068DR.11, URL: www.qcoala.eu, accessed 30th May, 2015
43. Wanjara P, Brochu M (2010) Characterization of electron beam welded AA2024. Vacuum 85:268–282. doi:10.1016/j.vacuum.2010.06.007
44. Westermann I, Pedersen KO, Furu T, Børvik T, Hopperstad OS (2014) Effects of particles and solutes on strength, work-hardening and ductile fracture of aluminum alloys. Mech Mater 79(2014):58–72. doi:10.1016/j.mechmat.2014.08.006
45. Zhao P-Z, Liu J, Chi Z-D (2014) Effect of Si content on laser welding performance of Al − Mn − Mg alloy. Trans Nonferrous Metals Soc China 24(2014):2208–2213. doi:10.1016/s1003-6326(14)63334-3
46. Von Witzendorff P, Kaierle S, Suttmann O, Overmeyer L (2015) In situ observation of solidification conditions in pulsed laser welding of AL6082 aluminum alloys to evaluate their impact on hot cracking susceptibility. Metall Mater Trans A 46A:1678–1688. doi:10.1007/s11661-015-2749-z
47. Svensson L E, Karlsson L and Soder R (2014) Welding enabling light weight design of heavy vehicle chassis, Science and Technology of Welding and Joining, (SPECIAL ISSUE ARTICLE) 2014, Vol. 000, No. 000, pp. 1–10; doi: 10.1179/1362171814y.0000000269
48. Lee CH, Kim SW, Yoon EP (2000) Electron beam welding characteristics of high strength aluminum alloys for express train applications. Sci Technol Weld Join 5(5):277–283. doi:10.1179/136217100101538326
49. Avilov VV, Gumenyuk A, Lammers M, Rethmeier M (2012) PA position full penetration high power laser beam welding of up to 30 mm thick AlMg3 plates using electromagnetic weld pool support. Sci Technol Weld Join 17(2):128–133. doi:10.1179/1362171811y.0000000085
50. Tu JF, Paleocrassas AG (2011) Fatigue crack fusion in thin-sheet aluminum alloys AA7075-T6 using low-speed fiber laser welding. J Mater Process Technol 211(2011):95–102. doi:10.1016/j.jmatprotec.2010.09.001

51. Tu J F, Paleocrassas A G (2010) Low speed laser welding of aluminum alloys using single-mode fiber lasers. In: Xiaodong N (ed) Engineering » electrical and electronic engineering » "Laser welding". North Carolina State University, USA, pp. 3–76 doi: 10.5772/9857
52. Lumley R (2011) Fundamentals of aluminium metallurgy-Production, processing and applications edited by Roger Lumley, Woodhead Publishing Limited, ISBN 978-1-84569-654-2, Pg. 1–8, doi: 10.1533/9780857090256.1
53. Mazzolani F M (2003) Aluminium Structural Design, International Centre For Mechanical Sciences, Courses and Lectures - No. 443, published by Springer-Verlag Wien New York, ISBN 978-3-211-00456-2,, Pg. 1–30, DOI: 10.1007/978-3-7091-2794-0
54. King J F (2001) The aluminium industry, Woodhead Publishing Limited, ISBN 978-1-85573-151-6, Pg. 1–5, doi: 10.1016/b978-1-85573-151-6.50008-2
55. Dwight J (1999) Aluminium Design and Construction, Taylor & Francis Group, ISBN 0 419 15710 7, Pg. 18–39, 77–103, doi: 10.4324/9780203028193
56. Jacobs M H (1999) Metallurgical Background to Alloy Selection and Specifications for Wrought, Cast and Special Applications, Training in Aluminium Application Technologies (TALAT) Lecture-1255, European Aluminium Association (EAA), Pg. 1–16
57. Muster T H, Hughes A E and Thompson G E (2009) Copper Distributions in Aluminium Alloys, Nova Science Publishers, Inc. New York, ISBN: 978-1-60741-201-4, Pg. 1–23
58. Metson J (2011) Fundamentals of aluminium metallurgy, Production, Processing and applications edited by Rodger Lumley, Production of alumina, Pg. 23–37, doi: 10.1533/9780857090256
59. Davies G (2003) Materials for Automobile Bodies, Butterworth-Heinemann, An imprint of Elsevier, ISBN 0 7506 5692 1, Pg. 87–90, 146–157, doi: 10.1016/b978-075065692-4/50021-2, 10.1016/b978-075065692-4/50022-4
60. Heinen P, Wu H, Olowinsky A, Gillner A (2014) Helium-tight laser beam welding of aluminum with brillant laser beam radiation, 8th International Conference on Photonic Technologies LANE 2014. Phys Procedia 56(2014):554–565. doi:10.1016/j.phpro.2014.08.043
61. Dittrich D, Standfuss J, Liebscher J, Brenner B, Beyer E (2011) Laser beam welding of hard to weld al alloys for a regional aircraft fuselage design—first results. Phys Procedia 12(2011):113–122. doi:10.1016/j.phpro.2011.03.015
62. Sierra G, Peyre P, Deschaux-Beaume F, Stuart D, Fras G (2007) Steel to aluminum key-hole laser welding. Mater Sci Eng A 447(2007):197–208. doi:10.1016/j.msea.2006.10.106
63. Zhu J, Lin L, Zhu L (2005) CO2 and diode laser welding of AZ31 magnesium alloy. Appl Surf Sci 247(2005):300–306. doi:10.1016/j.apsusc.2005.01.162
64. Mathieu A, Shabadi R, Deschamps A, Sueryc M, Matte S, Grevey D, Cicala E (2007) Dissimilar material joining using laser (aluminum to steel using zinc-based filler wire). Optics Laser Technol 39(2007):652–661. doi:10.1016/j.optlastec.2005.08.014
65. Scherm F, Bezold J, Glatzel U (2012) Laser welding of Mg alloy MgAl3Zn1 (AZ31) to Al alloy AlMg3 (AA5754) using ZnAl filler material. Sci Technol Weld Join 17(5):364–367. doi:10.1179/136217112x13333824902080
66. Badini C, Pavese M, Fino P, Biamino S (2009) Laser beam welding of dissimilar aluminum alloys of 2000 and 7000 series: effect of post welding thermal treatments on T joint strength. Sci Technol Weld Join 14(6):484–492. doi:10.1179/136217108x372559
67. Laukant H, Wallmann C, Muller M, Korte M, Stirn B, Haldenwanger HG, Glatzel U (2005) Fluxless laser beam joining of aluminum with zinc coated steel. Sci Technol Weld Join 10(2):219–226. doi:10.1179/174329305x37051
68. Tomashchuk I, Sallamand P, Cicala E, Peyre P, Grevey D (2015) Direct keyhole laser welding of aluminum alloy AA5754 to titaniumalloy Ti6Al4V. J Mater Process Technol 217(2015):96–104. doi:10.1016/j.jmatprotec.2014.10.025
69. Huang D, McClure JC, Nunes AC (1997) Gas contamination during plasma welding in AI-Li alloy 2195. Sci Technol Weld Join 2(5):209–211. doi:10.1179/stw.1997.2.5.209
70. The aluminium association: Product Market, URL: http://www.aluminum.org/ accessed 22nd May, 2015
71. EAI: Aluminium alloys in aviation: URL: http://www.experimentalaircraft.info/articles/aircraft-building-8.php accessed 22nd May, 2015
72. Nair BS, Phanikumar G, Rao K. P and Sinha P. P. (2007): Improvement of mechanical properties of gas tungsten arc and electron beam welded AA2219 (Al–6 wt-%Cu) alloy, Science and Technology of Welding and Joining, (ORIGINAL RESEARCH PAPER) 2007, Vol. 12, No. 7, pp.579-585; DOI: 10.1179/174329307x227210
73. Weld guru: Guide to laser welding, URL: http://www.weldguru.com/Laser-Welding.html accessed on 20th May, 2015
74. Zhao H, White DR, DebRoy T (1999) Current issues and problems in laser welding of automotive aluminum alloys. Int Mater Rev 44(6):238–266. doi:10.1179/095066099101528298
75. Duley W W (1983) Laser Processing and Analysis of Materials, PLENUM PRESS, pg. 1–44; ISBN 978-1-4757-0195-1 doi: 10.1007/978-1-4757-0193-7
76. Kocak M, dos Santos J, Riekehr S (2001) Trends in laser beam welding technology and fracture assessment of weld joints. Sci Technol Weld Join 6(6):347–350. doi:10.1179/stw.2001.6.6.347
77. Dawes C (1992) Laser welding- A practical guide, Woodhead Publishing Limited, pg. 1–28; ISBN 978–1 -85573-034-2; doi: 10.1533/9781845698843
78. Yilbas B S, Akhtar S, Shuja S Z (2013) Laser Forming and Welding Processes, Springer International Publishing, pg.1-4; ISBN 978-3-319-00980-3: doi: 10.1007/978-3-319-00981-0
79. Lin L (2000) The advances and characteristics of high-power diode laser materials processing. Opt Lasers Eng 34(2000):231–253. doi:10.1016/s0143-8166(00)00066-x
80. Olsen F O and Alting L (1995) Pulsed Laser Materials Processing, ND-YAG versus CO, Lasers, Annals of the ClRP Vol. 44/1/1995, pp. 141–145; doi: 10.1016/s0007-8506(07)62293-8
81. Walsh CA (2002) Laser welding—literature review, materials science and metallurgy department. University of Cambridge, England
82. Duley W W (1976) C02 Lasers Effects and Applications, Academic Press, pg. 1–15; ISBN 0-12-223350-6; doi: 10.1016/b978-0-12-223350-0.50007-9
83. Koechner W (2006) Solid-State Laser Engineering, Springer Science, pg. 1–10; ISBN-13: 978-0387-29094-2; doi: 10.1007/0-387-29338-8_1
84. Na X (2010) Laser Welding, Published by Sciyo, pg. 1–10, 47–60; ISBN 978-953-307-129-9; doi: 10.5772/265
85. Mrna L, Sarbort M, Rerucha S, Jedlicka P (2013) Correlation between the keyhole depth and the frequency characteristics of light emissions in laser welding, Lasers in Manufacturing Conference 2013. Phys Procedia 41(2013):469–477. doi:10.1016/j.phpro.2013.03.103
86. Ha J, Huh H (2013) Failure characterization of laser welds under combined loading conditions. Int J Mech Sci 69(2013):40–58. doi:10.1016/j.ijmecsci.2013.01.022
87. Li Z, Gobbi SL (1997) Laser welding for lightweight structures. J Mater Process Technol 70(1997):I37–144. doi:10.1016/s0924-0136(97)02906-3

88. Li S, Chen G, Zhang M, Zhou Y, Zhang Y (2014) Dynamic keyhole profile during high-power deep-penetration laser welding. J Mater Process Technol 214(2014):565–570. doi:10.1016/j.jmatprotec.2013.10.019
89. Industrial laser solutions: Laser development at Volvo published on 03/01/2013; URL: http://www.industrial-lasers.com/articles/print/volume-28/issue-2/features/laser-development-at-volvo.html accessed on 4th June, 2015
90. Industrial laser solutions: Body-in-white diode laser brazing published on 09/01/2011; URL: http://www.industrial-lasers.com/articles/print/volume-26/issue-5/features/body-in-white-diode-laser-brazing.html accessed on 4th June, 2015
91. Cui L, Li XY, He DY, Chen L, Gong SL (2013) Study on microtexture of laser welded 5A90 aluminum–lithium alloys using electron backscattered diffraction. Sci Technol Weld Join 18(3):204–209. doi:10.1179/1362171812y.0000000092
92. Tawfiq TA, Taha ZA, Hussein FI, Shehab AA (2012) Spot welding of dissimilar metals using an automated Nd:YAG laser system. Iraqi J Laser Part A 11:1–5
93. Möller F, Thomy C (2013) Interaction effects between laser beam and plasma arc in hybrid welding of aluminum, Lasers in Manufacturing Conference 2013. Phys Procedia 41(2013):81–89. doi:10.1016/j.phpro.2013.03.054
94. Masoumi M, Marashi SPH, Pouranvari M, Sabbaghzadeh J, Torkamany MJ (2009) Assessment of the effect of laser spot welding parameters on the joint quality using Taguchi Method, METAL 2009. Hradec Moravicí 5:19–21
95. Aalderink BJ, Pathiraj B, Aarts RGKM (2009) Seam gap bridging of laser based processes for the welding of aluminum sheets for industrial applications. Int J Adv Manuf Technol. doi:10.1007/s00170-009-2270-x
96. Katayama S, Kawahito Y, Mizutani M (2012) Latest progress in performance and understanding of laser Welding. Phys Procedia 39(2012):8–16. doi:10.1016/j.phpro.2012.10.008
97. Katayama S, Kawahito Y, Mizutani M (2010) Elucidation of laser welding phenomena and factors affecting weld penetration and welding defects, LANE 2010. Phys Procedia 5(2010):9–17. doi:10.1016/j.phpro.2010.08.024
98. Tao W, Li LQ, Chen YB, Wu L (2008) Joint strength and failure mechanism of laser spot weld of mild steel sheets under lap shear loading. Sci Technol Weld Join 13(8):754–759. doi:10.1179/136217108x338917
99. Kessler B (2013) Fiber laser welding in the car body shop - laser seam stepper versus remote laser welding. J KWJS 31(4):17–22. doi:10.5781/KWJS.2013.31.4.17
100. Huber S, Glasschroeder J, Zaeh MF (2011) Analysis of the metal vapour during laser beam welding. Phys Procedia 12(2011):712–719. doi:10.1016/j.phpro.2011.03.089
101. Mahrle A, Rose S, Schnick M, Beyer E, Fussel U (2013) Stabilisation of plasma welding arcs by low power laser beams. Sci Technol Weld Join 18(4):323–328. doi:10.1179/1362171813y.0000000109
102. Schweier M, Heins JF, Haubold MW, Zaeh MF (2013) Spatter formation in laser welding with beam oscillation, Lasers in Manufacturing Conference 2013. Phys Procedia 41(2013):20–30. doi:10.1016/j.phpro.2013.03.047
103. Tzeng Y-F (2000) Parametric analysis of the pulsed Nd:YAG laser seam-welding process. J Mater Process Technol 102(2000):40–47. doi:10.1016/s0924-0136(00)00447-7
104. Blecher JJ, Galbraith CM, Van Vlack C, Palmer TA, Fraser JM, Webster PJL, DebRoy T (2014) Real time monitoring of laser beam welding keyhole depth by laser interferometry. Sci Technol Weld Join 19(7):560–564. doi:10.1179/1362171814y.0000000225
105. De A, DebRoy T (2011) A perspective on residual stresses in welding. Sci Technol Weld Join 16(3):204–208. doi:10.1179/136217111x12978476537783
106. Assuncao E, Williams S, Yapp D (2012) Interaction time and beam diameter effects on the conduction mode limit. Opt Lasers Eng 50(2012):823–828. doi:10.1016/j.optlaseng.2012.02.001
107. Okon P, Dearden G, Watkins K, Sharp M, French P (2002) Laser Welding of Aluminum Alloy 5083, 21st International congress on Applications of Lasers and electro-optics, Scottsdale, October 14–17, 2002 (ICALEO 2002) ISBN: 0-912035-72-2
108. Chen YB, Lei ZL, Li LQ, Wu L (2006) Experimental study on welding characteristics of CO2 laser TIG hybrid welding process. Sci Technol Weld Joining 11(4):403–411. doi:10.1179/174329306x129535
109. Katayama S, Mizutani M, Matsunawa A (1997) Modeling of melting and solidification behavior during laser spot welding. Sci Technol Weld Join 2(1):1–9. doi:10.1179/stw.1997.2.1.1
110. Kawahito Y, Matsumoto N, Abe Y, Katayama S (2011) Relationship of laser absorption to keyhole behavior in high power fiber laser welding of stainless steel and aluminum alloy. J Mater Process Technol 211(2011):1563–1568. doi:10.1016/j.jmatprotec.2011.04.002
111. Zhang MJ, Chen GY, Zhou Y, Li SC, Deng H (2013) Observation of spatter formation mechanisms in high-power fiber laser welding of thick plate. Appl Surf Sci 280(2013):868–875. doi:10.1016/j.apsusc.2013.05.081
112. Sokolov M, Salminen A (2014) Methods for improving laser beam welding efficiency, 8th International Conference on Photonic Technologies LANE 2014. Phys Procedia 56(2014):450–457. doi:10.1016/j.phpro.2014.08.148
113. Tsukamoto S (2011) High speed imaging technique Part 2—high speed imaging of power beam welding phenomena. Sci Technol Weld Join 16(1):44–55. doi:10.1179/136217110x12785889549949
114. Zhao CX, Kwakernaak C, Pan Y, Richardson IM, Saldi Z, Kenjeres S, Kleijn CR (2010) The effect of oxygen on transitional Marangoni flow in laser spot welding. Acta Mater 58(2010):6345–6357. doi:10.1016/j.actamat.2010.07.056
115. Youhei A, Yousuke K, Hiroshi N, Koji N, Masami M, Seiji K (2014) Effect of reduced pressure atmosphere on weld geometry in partial penetration laser welding of stainless steel and aluminum alloy with high power and high brightness laser. Sci Technol Weld Join 19(4):324–332. doi:10.1179/1362171813y.0000000182
116. Karkhin VA, Plochikhine VV, Bergmann HW (2002) Solution of inverse heat conduction problem for determining heat input, weld shape, and grain structure during laser welding. Sci Technol Weld Join 7(4):224–231. doi:10.1179/136217102225004202
117. Chen YB, Miao YG, Li LQ, Wu L (2008) Arc characteristics of laser-TIG double-side welding. Sci Technol Weld Join 13(5):438–444. doi:10.1179/174329308x341861
118. Kawahito Y, Matsumoto N, Mizutani M, Katayama S (2008) Characterization of plasma induced during high power fiber laser welding of stainless steel. Sci Technol Weld Join 13(8):744–748. doi:10.1179/136217108x329313
119. Chen YB, Zhao YB, Lei ZL, Li LQ (2012) Effects of laser induced metal vapor on arc plasma during laser arc double sided welding of 5A06 aluminum alloy. Sci Technol Weld Join 17(1):69–76. doi:10.1179/1362171811y.0000000078
120. Frompo: Principes van geleidings- en dieplassen; URL: http://image.frompo.com/131a24bc1ea7664618c7f6fedfd67066 accessed on 10th June, 2015
121. He X, DebRoy T (2003) Probing temperature during laser spot welding from vapor composition and modeling. J Appl Phys 94(10):6949–6958. doi:10.1063/1.1622118
122. Mujibur Rahman ABM, Kumar S, Gerson AR (2007) Galvanic corrosion of laser weldments of AA6061 aluminum alloy. Corros Sci 49(2007):4339–4351. doi:10.1016/j.corsci.2007.04.010

123. Mattei S, Grevey D, Mathieu A, Kirchner L (2009) Using infrared thermography in order to compare laser and hybrid (laser + MIG) welding processes. Optics Laser Technol 41(2009):665–670. doi:10.1016/j.optlastec.2009.02.005
124. Haboudou A, Peyre P, Vannes AB, Peix G (2003) Reduction of porosity content generated during Nd:YAG laser welding of A356 and AA5083 aluminum alloys. Mater Sci Eng A 363(2003):40–52. doi:10.1016/s0921-5093(03)00637-3
125. Stritt P, Hagenlocher C, Kizler C, Weber R, Rüttimann C, Graf T (2014) Laser spot welding of copper-aluminum joints using a pulsed dual wavelength laser at 532 and 1064 nm, 8th International Conference on Photonic Technologies LANE 2014. Phys Procedia 56:759–767. doi:10.1016/j.phpro.2014.08.083
126. Curcio F, Daurelio G, Memola Capece Minutolo F, Caiazzo F (2006) On the welding of different materials by diode laser. J Mater Process Technol 175(2006):83–89. doi:10.1016/j.jmatprotec.2005.04.026
127. DILAS-The diode laser company: URL: http://www.dilas.com/pages/products.php accessed on 2nd June, 2015
128. Quintino L, Costa A, Miranda R, Yapp D, Kumar V, Kong CJ (2007) Welding with high power fiber lasers—a preliminary study. Mater Des 28(2007):1231–1237. doi:10.1016/j.matdes.2006.01.009
129. Wang XJ, Lu FG, Wang HP, Cui HC, Tang XH, Wu YX (2015) Experimental and numerical analysis of solidification cracking behavior in fiber laser welding of 6013 aluminum alloy. Sci Technol Weld Join 20(1):58–67. doi:10.1179/1362171814y.0000000254
130. Oliveira AC, Siqueira RHM, Riva R, Lima MSF (2015) One-sided laser beam welding of autogenous T-joints for 6013-T4 aluminum alloy. Mater Des 65(2015):726–736. doi:10.1016/j.matdes.2014.09.055
131. Fu B, Qin G, Meng X, Ji Y, Zou Y, Lei Z (2014) Materials Science & Engineering A. Mater Sci Eng 617(2014):1–11. doi:10.1016/j.msea.2014.08.038
132. Paleocrassas AG, Tu JF (2010) Inherent instability investigation for low speed laser welding of aluminum using a single-mode fiber laser. J Mater Process Technol 210(2010):1411–1418. doi:10.1016/j.jmatprotec.2010.04.002
133. Wang T, Yang Z, Chen Y, Li L, Jiang Z, Zhang Y (2013) Double-sided fiber laser beam welding process of T-joints for aluminum aircraft fuselage panels: filler wire melting behavior, process stability, and their effects on porosity defects. Optics Laser Technol 52(2013):1–9. doi:10.1016/j.optlastec.2013.04.003
134. Tusek J, Suban M (1999) Hybrid welding with arc and laser beam. Sci Technol Weld Join 4(5):308–311. doi:10.1179/136217199101537923
135. Gao M, Zeng X, Hu Q (2007) Effects of gas shielding parameters on weld penetration of CO2 laser-TIG hybrid welding. J Mater Process Technol 184(2007):177–183. doi:10.1016/j.jmatprotec.2006.11.019
136. Casalino G, Campanelli SL, Dal Maso U, Ludovico AD (2013) Arc leading versus laser leading in the hybrid welding of aluminum alloy using a fiber laser, 8th CIRP Conference on Intelligent Computation in Manufacturing Engineering. Proc CIRP 12(2013):151–156. doi:10.1016/j.procir.2013.09.027
137. Schultz V, Seefeld T, Vollertsen F (2014) Gap bridging ability in laser beam welding of thin aluminum sheets, 8th International Conference on Photonic Technologies LANE 2014. Phys Procedia 56(2014):545–553. doi:10.1016/j.phpro.2014.08.037
138. Wu S, Ri X (2015) Effect of high power CO2 and Yb:YAG laser radiation on the characteristics of TIG arc in atmospherical pressure argon and helium. Optics Laser Technol 67(2015):169–175. doi:10.1016/j.optlastec.2014.10.018
139. Le Guen E, Fabbro R, Carin M, Coste F, Le Masson P (2011) Analysis of hybrid Nd:YAG laser-MAG arc welding processes. Optics Laser Technol 43(2011):1155–1166. doi:10.1016/j.optlastec.2011.03.002
140. Ascari A, Fortunato A, Orazi L, Campana G (2012) The influence of process parameters on porosity formation in hybrid LASER-GMA welding of AA6082 aluminum alloy. Optics Laser Technol 44(2012):1485–1490. doi:10.1016/j.optlastec.2011.12.014
141. Zhang C, Gao M, Li G, Chen C, Zeng XY (2013) Strength improving mechanism of laser arc hybrid welding of wrought AA 2219 aluminum alloy using AlMg5 wire. Sci Technol Weld Join 18(8):703–710. doi:10.1179/1362171813y.0000000153
142. Liu LM, Yuan ST, Li CB (2012) Effect of relative location of laser beam and TIG arc in different hybrid welding modes. Sci Technol Weld Join 17(6):441–446. doi:10.1179/1362171812y.0000000033
143. Yan J, Zeng X, Gao M, Lai J, Lin T (2009) Effect of welding wires on microstructure and mechanical properties of 2A12 aluminum alloy in CO2 laser-MIG hybrid welding. Appl Surf Sci 255(2009):7307–7313. doi:10.1016/j.apsusc.2009.03.088
144. Casalino G (2007) Statistical analysis of MIG-laser CO2 hybrid welding of Al–Mg alloy. J Mater Process Technol 191(2007):106–110. doi:10.1016/j.jmatprotec.2007.03.065
145. Zhang D-Q, Li J, Joo HG, Lee KY (2009) Corrosion properties of Nd:YAG laser–GMA hybrid welded AA6061 Al alloy and its microstructure. Corros Sci 51(2009):1399–1404. doi:10.1016/j.corsci.2009.03.030
146. He C, Huang C, Liu Y, Li J, Wang Q (2015) Effects of mechanical heterogeneity on the tensile and fatigue behaviors in a laser-arc hybrid welded aluminum alloy joint. Mater Des 65(2015):289–296. doi:10.1016/j.matdes.2014.08.050
147. Ola OT, Doern FE (2015) Fusion weldability studies in aerospace AA7075-T651 using high-power continuous wave laser beam techniques. Mater Des 77(2015):50–58. doi:10.1016/j.matdes.2015.03.064
148. Tong H, Ueyama T, Nakata K, Ushio M (2003) High speed welding of aluminum alloy sheets using laser assisted alternating current pulsed metal inert gas process. Sci Technol Weld Join 8(3):229–234. doi:10.1179/136217103225010853
149. Yan-Bin C, Miao Y-G, Li-Qun L, Wu L (2009) Joint performance of laser-TIG double-side welded 5A06 aluminum alloy. Trans Nonferrous Metal Soc China 19(2009):26–31. doi:10.1016/s1003-6326(08)60223-x
150. Wu SC, Yu C, Zhang WH, Fu YN, Helfen L (2015) Porosity induced fatigue damage of laser welded 7075-T6 joints investigated via synchrotron X-ray microtomography. Sci Technol Weld Join 20(1):11–19. doi:10.1179/1362171814y.0000000249
151. Yang ZB, Tao W, Li LQ, Chen YB, Li FZ, Zhang YL (2012) Double-sided laser beam welded T-joints for aluminum aircraft fuselage panels: Process, microstructure, and mechanical properties. Mater Des 33(2012):652–658. doi:10.1016/j.matdes.2011.07.059
152. Schneider A, Avilov V, Gumenyuk A, Rethmeier M (2013) Laser beam welding of aluminum alloys under the influence of an electromagnetic field, Lasers in Manufacturing Conference 2013. Phys Procedia 41(2013):4–11. doi:10.1016/j.phpro.2013.03.045
153. Gatzen M, Tang Z, Vollertsen F (2011) Effect of electromagnetic Stirring on the Element Distribution in Laser Beam Welding of Aluminum with Filler Wire, LiM 2011. Phys Procedia 12(2011):56–65. doi:10.1016/j.phpro.2011.03.008
154. Ancona A, Sibillano T, Tricarico L, Spina R, Lugara PM, Basile G, Schiavone S (2005) Comparison of two different nozzles for laser beam welding of AA5083 aluminum alloy. J Mater Process Technol 164–165(2005):971–977. doi:10.1016/j.jmatprotec.2005.02.048
155. Ancona A, Lugara PM, Sorgente D, Tricarico L (2007) Mechanical characterization of CO2 laser beam butt welds of

AA5083. J Mater Process Technol 191(2007):381–384. doi:10.1016/j.jmatprotec.2007.03.048
156. Cui L, Li X, He D, Chen L, Gong S (2012) Effect of Nd:YAG laser welding on microstructure and hardness of an Al–Li based alloy. Mater Character 71(2012):95–102. doi:10.1016/j.matchar.2012.06.011
157. Pastor M, Zhao H, Debroy T (2009) Pore formation during continuous wave Nd:YAG laser welding of aluminum for automotive applications. Weld Int 15(4):275–281. doi:10.1080/09507110109549355
158. Malek Ghaini F, Sheikhi M, Torkamany MJ, Sabbaghzadeh J (2009) The relation between liquation and solidification cracks in pulsed laser welding of 2024 aluminum alloy. Mater Sci Eng A 519(2009):167–171. doi:10.1016/j.msea.2009.04.056
159. de Mota Siqueira RH, de Capella Oliveira A, Riva R, Abdalla AJ, Baptista CARP, de Fernandes Lima MS (2014) J Braz Soc Mech Sci Eng. doi:10.1007/s40430-014-0175-6, Technical paper
160. Sanchez-Amaya JM, Delgado T, Gonzalez-Rovira L, Botana FJ (2009) Laser welding of aluminum alloys 5083 and 6082 under conduction regime. Appl Surf Sci 255(2009):9512–9521. doi:10.1016/j.apsusc.2009.07.081
161. Zain-ul-abdein M, Nelias D, Jullien J-F, Deloison D (2010) Experimental investigation and finite element simulation of laser beam welding induced residual stresses and distortions in thin sheets of AA 6056-T4. Mater Sci Eng A 527(2010):3025–3039. doi:10.1016/j.msea.2010.01.054
162. Liu H, Shang DG, Guo Z-K, Zhao YG, Liu JZ (2014) Fatigue crack growth property of laser beam welded 6156 aluminum alloy. Fatigue Fract Eng Mater Struct 37:937–944. doi:10.1111/ffe.12176
163. Hu B, Richardson IM (2007) Microstructure and mechanical properties of AA7075(T6) hybrid laser/GMA welds. Mater Sci Eng A 459(2007):94–100. doi:10.1016/j.msea.2006.12.094
164. Sibillano T, Ancona A, Berardi V, Schingaro E, Basile G, Lugara PM (2006) A study of the shielding gas influence on the laser beam welding of AA5083 aluminum alloys by in-process spectroscopic investigation. Opt Lasers Eng 44(2006):1039–1051. doi:10.1016/j.optlaseng.2005.09.002
165. Zhao YB, Lei ZL, Chen YB, Tao W (2011) A comparative study of laser-arc double-sided welding and double-sided arc welding of 6 mm 5A06 aluminum alloy. Mater Des 32(2011):2165–2171. doi:10.1016/j.matdes.2010.11.041
166. Eibl M, Sonsino CM, Kaufmann H, Zhang G (2003) Fatigue assessment of laser welded thin sheet aluminum. Int J Fatigue 25(2003):719–731. doi:10.1016/s0142-1123(03)00053-7
167. Guo-liang Q, Wang G-G, Zeng-da Z (2012) Effects of activating flux on CO2 laser welding process of 6013 Al alloy. Trans Nonferrous Metals Soc China 22(2012):23–29. doi:10.1016/s1003-6326(11)61134-5
168. KahP, Hiltunen E. and Martikainen J (2010) Investigation of Hot Cracking in the Welding of Aluminum Alloys (6005 & 6082), 63rd Annual Assembly & International Conference of the International Institute of Welding 11–17 July 2010, Istanbul, Turkey, pp. 373–380
169. Chen XL, Yan HG, Chen JH, Su B, Yu ZH (2013) Effects of grain size and precipitation on liquation cracking of AZ61 magnesium alloy laser welding joints. Sci Technol Weld Join 18(6):458–465. doi:10.1179/1362171813y.0000000117
170. Marya M, Edwards GR (2002) Influence of laser beam variables on AZ91D weld fusion zone microstructure. Sci Technol Weld Join 7(5):286–293
171. Reddy GM, Gokhale AA, Prasad KS, Prasad Rao K (1998) Chill zone formation in Al-Li alloy welds. Sci Technol Weld Join 3(4):208–212. doi:10.1179/stw.1998.3.4.208
172. Avilov V, Schneider A, Gumenyuk A, Rethmeier M (2012) Electromagnetic Control of the Weld Pool Dynamics in Partial Penetration Laser Beam Welding of Aluminum Alloys, Federal Institute for Materials Research and Testing (BAM), 12205 Berlin, Germany, p 233–236
173. Cicala E, Duffet G, Grevey D (2008) Optimization Of The Laser Welding of Aluminum Alloys used in Aeronautics, Nonconventional Technologies Review – no. 2/2008, pp. 9–16
174. Taban E, Kaluc E (2011) Welding behavior of Duplex and Superduplex stainless steels using Laser and Plasma Arc Welding processes. Welding World 55(7–8):48–57. doi:10.1007/bf03321307
175. El T, Deleu E, Dhooge A, Kaluc E (2009) Laser welding of modified 12% Cr stainless steel: Strength, fatigue, toughness, microstructure and corrosion properties. Mater Des 30(2009):1193–1200. doi:10.1016/j.matdes.2008.06.030